2000

ISAS - INTERNATIONAL SCHOOL FOR ADVANCED STUDIES

"Distributed processing underlying whole-body shortening in the leech central nervous system"

Thesis submitted for the degree of "Doctor Philosophiae"

CANDIDATE
Ivan Arisi

SUPERVISOR
Prof. Vincent Torre

SISSA - SCUOLA INTERNAZIONALE SUPERIORE DI STUDI AVANZATI

TRIESTE
Via Beirut 2-4

TRIESTE

To Maria Pia

Table of contents

Acknowledgements

I wish to express my gratitude to Prof. Vincent Torre for carefully supervising my Ph.D. work.

I thank Prof. John Nicholls for inspiring our work on the leech nervous system, for all he taught me and for many stimulating discussions.

The production of this thesis would have not been possible without the help of many colleagues and friends: Giulietta Pinato who was my first colleague, Alessandro Bisso who wrote most of the software for the data analysis, Davide Zoccolan who worked with me for the experiments on the whole-body shortening, Laura Giovanelli who did the most of the artwork.

I'm very grateful to my friend Gerry Cargnelutti for revising the text and for feeding hundreds of articles into the Harchirudo leech database, together with Emanuela Cazzaniga.

I also thank the other members of the Harchirudo leech database group: Fabio Venuti and Riccardo Brancaleon.

I also thank my father for his suggestions and for the revision of the text.

Finally, I thank Mr. Claudio Becciani for his invaluable technical support.

Note

The work described in this dissertation was carried out at the International School for Advanced Studies, Trieste, between November 1996 and June 2000. All work reported has not been submitted, as in whole or in part, to any other University or Institute.

Ivan Arisi

Abbreviations used in the text

σ: standard deviation

AA: anterior anterior branch of the anterior root

AE: annulus erector motor neuron

AFR: average firing rate

AP: anterior pagoda cell

CNS: central nervous system

CPG: central pattern generator

CV: coefficient of variation

C.V.: ventrolateral circular excitatory motoneuron

DE: dorsal excitatory motor neuron

DP: dorsal posterior branch of the posterior root

DP1: main trunk of the DP branch

FMRFamide: phe-met-arg-phe-amide

GABA: gamma-aminobutyric acid

Gn: segmental ganglion number n

h2: amplitude of extracellular spikes

HE: heart excitatory motoneuron

L: large longitudinal excitatory motoneuron

MA: medial anterior branch of the anterior root

N_l: lateral nociceptive mechanosensory neuron

N_m: medial nociceptive mechanosensory neuron

P_d: dorsal pressure mechanosensory neuron

P_v: ventral pressure mechanosensory neuron

PP: posterior posterior branch of the posterior root

T_d: dorsal touch mechanosensory neuron

T_l: lateral touch mechanosensory neuron

T_v: ventral touch mechanosensory neuron

Abstract

The CNS of the leech *Hirudo Medicinalis* has often been used as an animal model for neurobiology, due to its simple structure and the ease of obtaining electrical recordings. The main purpose of my Ph.D. thesis was to study the statistical properties of the firing of neurons in distributed processes. In this context, two main problems were addressed while studying the simple nervous system of the leech:

i) the identification of action potentials produced by specific motoneurons from parallel extracellular recordings obtained with pipettes sucking fine branches of leech roots;

ii) the analysis of the firing pattern of motoneurons involved in the whole-body shortening reaction.

The realization of an amplifier for recording extracellular signals and the development of software for data analysis were also part of my work.

During the first part of the project I developed a procedure to identify the shape of action potentials of specific neurons. My work focused on motoneurons, which can produce the largest extracellular signals on the roots, together with the T and P mechanosensory neurons. Single or short chains of segmental ganglia were isolated and the roots carefully cleaned and cut to enable recordings by suction pipettes. For each motoneuron, action potentials were evoked by passing a depolarizing current with an intracellular microelectrode or by injury discharge. With this procedure it was possible to have a clear signature of extracellular voltage signals of many motoneurons in each preparation. The mean amplitudes of all signals of each known motoneuron were compared. Software was developed in Matlab language to extract all extracellular action

potentials from the recordings and to cluster them on the base of their shape. A well isolated cluster was considered as belonging to a single neuron. Additional software was developed to compute first and second order statistics of identified action potentials.

The second part of my thesis concerned whole-body shortening, a vital escape reaction, which was studied by a combination of videomicroscopy and multielectrode recordings. Video microscopy was used to monitor animal behaviour and muscle contraction. Eight suction pipettes were used to obtain simultaneous electrical recordings from nerve branches arising from the ganglia. The behavioural response was rather reproducible and the coefficient of variation of the animal contraction during whole body shortening was between 0.2 and 0.3. The great majority of longitudinal motoneurons were activated during this escape reaction, in particular motoneurons 3, 4, 5, 8, 107, 108, and motoneuron L. Therefore the whole-body shortening is a distributed process.

The motoneuron firing pattern during whole-body shortening was poorly reproducible from trial to trial and the coefficient of variation of single motoneurons firing was always larger than 0.5 and usually about 1. During whole-body shortening the electrical activity of coactivated motoneurons was not pairwise correlated on a time window of 100 ms, except for the left and right L motoneurons, well known to be electrically coupled. Because of the lack of correlation, the global electrical activity of coactivated motoneurons became reproducible with a coefficient of variation below 0.3 during maximal activation. These results indicate that whole-body shortening is mediated by the coactivation of a large fraction of all leech motoneurons and that coactivated motoneurons exhibit a significant statistical independence. Because of this statistical independence this vital escape reaction becomes smooth and reproducible.

Introduction

A major issue of neuroscience is to understand sensory-motor reactions and in particular to identify the neuronal circuits underlying these behaviours and to understand their firing patterns. This task is likely to be addressed in simpler nervous systems such as those of invertebrates, where these reactions are mediated by a limited number of neurons, from a few hundreds in the worm *C. elegans* to some thousands as in the leech and in the *Aplysia*.

The leech central nervous system is rather simple, thus it is possible to study in detail behavioural reactions at a single cell level, because most of the neurons have been identified and show stereotyped positions in all the preparations.

The major aim of my thesis was to investigate firing properties of leech neurons during evoked motor behaviours.

Three main models of neural architectures have been described in the literature for the generation of behavioural responses: dedicated, distributed and reorganizing circuitry (Morton & Chiel, 1994). In dedicated circuitry, each behavioural response is generated by a distinct neural circuit. In response to a particular input, only one of the dedicated circuits exerts control over the periphery, producing a specific response, while the other circuits are not activated. Since only one circuit can control the periphery at any time, no conflicts between different behaviours can arise.

In distributed circuitry, the response to any input is distributed over a large population of neurons, with each neuron contributing a small amount to the final

behavioural response. In these circuits, the same neurons may be involved in different behaviours.

In reorganizing architecture, different responses are produced by altering the circuit connectivity. This may be caused by the addition or removal of specific neurons, changes in the intrinsic properties of neurons or in the effective synaptic connections, interaction between different dedicated circuits.

Examples belonging to one or more of the three models may be found in nature. The mollusk *Clione* shows two different dedicated circuits for wing retraction and swimming, but this might also be a case of reorganizing circuit; *Locusta migratoria* has dedicated circuits mediating flying and walking (Morton & Chiel, 1994).

Tritonia can contract alternatively muscles to swim or together to withdraw from a stimuli (as the shortening in the leech), reorganizing the circuit also at the level of motoneurons (Morton & Chiel, 1994). Different levels of circuitry reorganization may take place: for example in the lobster (Clemens et al., 1998a & 1998b) two separate oscillating circuits, the pyloric and gastric pattern generators, are interacting; in the leech some multifunctional interneurons are active both during swimming and shortening (Wittenberg & Kristan, 1992).

The leech distributes the neural computation for the bending response over a population of interneurons and motoneurons (Lockery and Kristan, 1990), the same distributed processing is observed in the *Aplysia* when retracting the syphon (Tsau et al., 1994)

In order to understand the parallel processing underlying sensory-motor reactions, and to distinguish between distributed, dedicated and reorganizing processing, it is necessary to have a suitable technique for multi-channel recordings and a method for the simultaneous identification of a large amount of action potentials from different

neurons. The first part of my work was devoted to the development of a procedure to identify action potentials produced by different neurons from extracellular recordings.

Having solved this problem, it is possible to compute statistics of firing sequences of identified neurons. In particular the following questions arose:

i) which preparation provides recordings suitable to identify the firing neurons?

ii) starting from a single extracellular action potential, is it possible to identify the neuron generating it?

iii) are extracellular signals of different neurons clearly distinguishable?

iv) is it possible to have a semi-automatic procedure to cluster and separate them?

v) to which extent are different experimental preparations comparable?

vi) can we deduce general criteria to recognize particular neurons from recordings without any further information?

This procedure was tested and successfully used to study the firing properties of neuronal circuits responsible for the whole-body shortening escape reaction of the leech. The electrode configuration used to record extracellular signals with suction pipettes has a remarkable mechanical stability, is suitable for studying motor reactions, and allows long recordings, necessary to obtain a statistical significant amount of data. The purpose of the second part of my work was to determine the pattern of action potentials of motoneurons activated during whole-body shortening, and to investigate the statistical properties of the evoked activity. I wanted to answer these questions:

i) how many motoneurons are activated during the shortening in the leech?

ii) is the electrical activity of these motoneurons correlated?

iii) does the pattern of neuronal evoked activity show a given temporal structure?

iv) is sufficient information provided to outline either a dedicated, a reorganizing or a distributed structure for the shortening circuit?

v) is the underlying computation a distributed process?

vi) how can we explain the reproducibility and smoothness of this vital behaviour?

Recent reports have shown that the mechanism of action potential generation is very reliable (Mainen and Sejnowski, 1995), however an intrinsic property of the nervous system seems to be that the discharge patterns of action potentials in neurons receiving an almost constant input are affected by a large variability. This has been observed both in mammals and in lower animals (Allen & Stevens, 1994; Tsau et al., 1994). It is possible that neuronal variability represents a functional property, which could be exploited to statistically reduce the noise of the behavioural output, rather than an obstacle to reliability. The question arises of how single neuron response unreliability is compatible with the capability of neuronal networks to process information or perform behavioural tasks in a reproducible manner across different trials.

****

In the first Chapter reasons will be given for the choice of the leech CNS as a good model for neuroscientists. Then, some basic information will be provided about the anatomy and the neurobiology of the leech, including a detailed description of sensory cells, motoneurons and motor behaviours. The main results concerning the circuits controlling motion will be then reviewed.

In Chapter 2 the preparations and the experimental set-up will be presented. A brief description of the software for data analysis will be provided, since it was realized during my Ph.D. work.

In Chapter 3 the main experimental methods to obtain multi-site recordings from leech ganglia will be reviewed in order to explain the choice of parallel recordings by suction pipettes. Extracellular signals of all motoneurons will be analyzed to obtain a table of spike amplitudes on the main root branches; the table will be used to recognize action potentials of identified neurons from extracellular voltage recordings. The semi-automatic algorithm for clustering extracellular action potentials will be described.

In Chapter 4 the whole-body shortening escape reaction will be analyzed: characterization of the body contraction; investigation of the underlying neuronal circuits controlling motion, by means of the identification procedure explained in Chapter 3. An explanation will be then proposed for the smoothness and reliability of this vital reaction.

Chapter 1

Background

The leech has been used for centuries for medical treatments, but the novel interest in the leech for neuroscience dates only very recently, as shown by the published literature. The leech nervous system turned out to be useful for most of the basic research issues in neurobiology. A detailed description of the leech CNS will justify this choice.

1.1 Why the leech?

The medicinal use of leeches goes back into the past, when they were exploited to remove blood from patients (Payton, 1981a). The practice of bloodletting by leeches reached a peak during the 18th and 19th centuries, together with a flourishing of literature on this subject, and it continued with a declining trend even in the 20th century. The discovery of the protein hirudin by Haycraft (1884) enabled the exploitation of this anticoagulant factor as a drug. Today there is a novel interest in the therapeutic use of leeches in microsurgery: the animals are left attached in the injured area to avoid venous congestion in replanted limbs (Golden et al., 1995). It was only at the end of the 19th century, with the fundamental work by Retzius (1891) that the nervous system of the leech became for the first time an object of scientific research.

Leeches are segmented worms belonging to the class Hirudinea and they are related to the earthworms (Class Oligochaeta). Most of the about 650 leech species are aquatic or

terrestrial parasitic bloodsucking animals (classes Gnathobdellida and Rhynchobdellida) though some ingest their small preys (class Pharyngobdellida). The animal used in all my Ph.D. work is *Hirudo medicinalis*, an aquatic leech belonging to the family Hirudinidae, which feeds on mammals and frogs. A major feature of leeches compared to other worms, is the presence of a caudal sucker, which is developmentally incompatible with a posterior growth region: leeches do not add new segments to the body during their mature life and each species has the same number of body segments. This constancy allows a specialization of the different parts of the body, and as a consequence of the nervous system; this specialization is remarkably identical from one individual to the other, making the leeches organisms suitable for neurobiology.

The leech CNS presents other experimental advantages compared to different animals species: high similarity between segmental nervous ganglia, a small number of cells in each ganglion of the nervous chain, easy extracellular recordings from motoneurons, high accessibility to intracellular recording both of neurons and glial cells, long duration of experimental preparations, a limited repertoire of stereotyped motor behaviours.

Several fundamental issues of neuroscience have been addressed in the last 35 years using the leech nervous system: physiology of glial cells (Kuffler & Potter, 1964; Kuffler & Nicholls, 1966; Deitmer & Kristan, 1999), action potential generation and conduction block (Gu, 1991; Mar & Drapeau, 1996; Melinek & Muller, 1996), motor system coordination (Kristan, 1982; Wittenberg & Kristan, 1992a & 1992b; Baader & Bächtold, 1997), oscillatory circuits (Calabrese et al, 1977; Stent et al., 1978; Pearce & Friesen, 1985a & 1985b; Brodfuehrer et al., 1995b; Calabrese, 1995), neurotransmitters (Willard, 1981; Gardner & Walker, 1982; Thorogood & Brodfuehrer, 1995; Szczupak & Kristan, 1995; O'Gara et al., 1999), neuromodulation (Hashemzadeh-Gargari &, 1989, Gascoigne & McVean, 1991), sensory cells and signal transduction (Nicholls & Baylor, 1968; Blackshaw, 1981b, 1993; Friesen, 1981; Blackshaw et al., 1982, Peterson 1985a & 1985b),

neural basis of learning (Boulis & Sahley, 1988; Sahley et al., 1994a & 1994b; Modney et al., 1997), development (Martindale & Shankland, 1990; Shain et al., 1998), axon growth and regeneration (Jansen & Nicholls, 1972; Jellies et al., 1995), test for new experimental techniques (Wilson et al., 1994; Cacciatore et al., 1999; Canepari et al., 1996), models of complete real networks (Lewis and Kristan, 1998b).

1.2 Anatomy of the leech

The adult leech *Hirudo medicinalis* consists of 4 partially fused segments in the head region, 21 segments along the body and 7 modified segments in the posterior region forming the tail sucker (Payton, 1981b); exactly 5 annuli correspond to each segment, except for the head and tail regions (**Fig. 1.1A**). The sensilla, small sense organs, are distributed around the central annulus of the segment. The front sucker contains three teeth used to bite the preys. Internally, the intestines containing the ingested blood run all along the body (**Fig. 1.1B**). The leeches own blood circulates in four main vessels: the dorsal sinus, the ventral sinus also containing the CNS and two lateral sinuses which form the beating heart system driven by a neuronal oscillating circuit (Calabrese et al., 1995). The sexual organs lie in segments 5 and 6 but there are 9 pairs of connected testes in segments 7 to 15. The excretory system is made up of 17 pairs nephridia in segments 1-17 and it is open to the outside through two nephridiophores per ganglion.

The leech has five main types of muscles (**Fig. 1.1B**): three layers of muscles (longitudinal, oblique, and circular) form the main part of the body wall and are therefore distributed uniformly around the perimeter of the body; another type of muscles (dorsoventral) connect internally the dorsal and ventral sides of the animal. A further kind of muscles, the annulus erectors (not shown in Fig. 1.1), are located immediately under the

skin and are responsible for erecting annuli in ridges. The longitudinal muscles, the thickest and deepest layer, shorten the leech in the longitudinal direction when contracting; the oblique muscles, an outer thin layer, twist the body; the circular muscles lie just under the skin and are able to elongate the animal when they contract; the dorsoventral muscles flatten the body, for example during the swimming.

1.3 The leech CNS

1.3.1 General properties

The segmentation is reflected in the CNS, where a nervous ganglion corresponds to each segment. The CNS is a chain of ganglia (Fig. 1.1A) all linked by the connectives. The connectives are the largest bundle of axons of the body and they are composed by a couple of thick nerves and the thin Faivre's nerve, running centrally between them. The 21 segmental ganglia (G1-G21) are numbered sequentially from the anterior to the posterior region and are almost identical, except for G5 and G6 which innervate the sexual organs. The first 4 ganglia in the head region (H1-H4) are fused and modified to form the head brain, which is composed by a specialized supraesophageal unit and a different subesophageal unit where the structure of 4 segmental ganglia is still recognizable. The last 7 ganglia (T1-T7) are fused in the specialized tail brain. Each of the segmental ganglia innervates a well defined segment of the body wall by two pairs of nerves (roots) arising symmetrically from the left and right sides (**Fig. 1.1B**). The four roots are defined as anterior and posterior, left and right. The two posterior roots bifurcate near the ganglion, each one originating two branches called posterior-posterior nerves (PP) and dorsal posterior nerve (DP). Through these nerves the ganglion innervates the whole segment.

The anterior and PP nerves innervate the territory corresponding to the lateral and ventral part of the animal, while the DP nerves innervate the dorsal part of the animal.

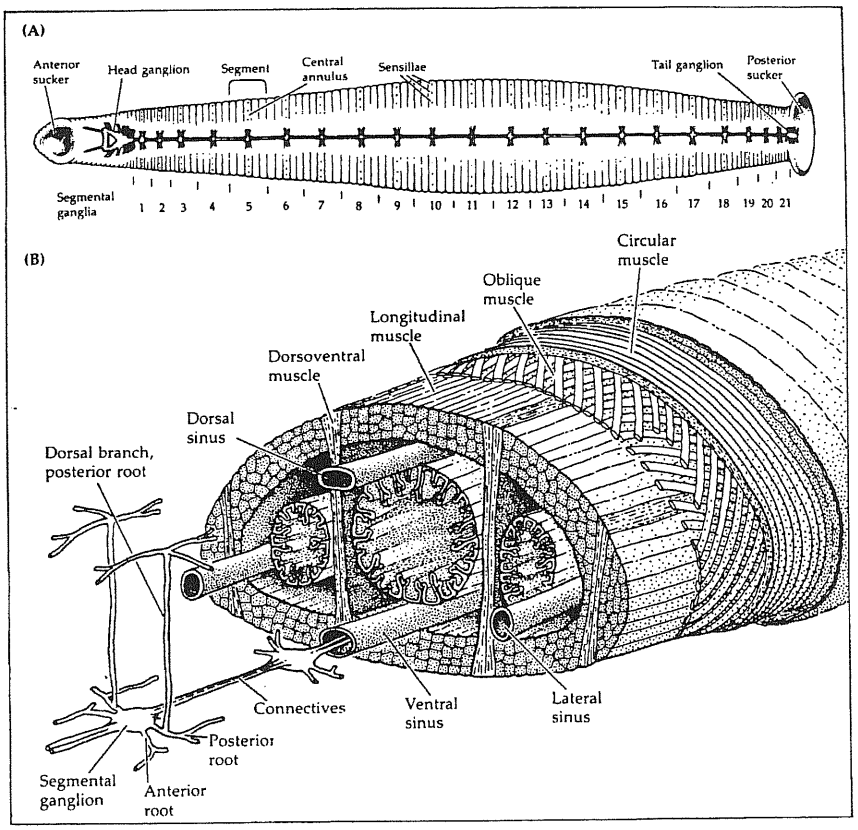

Fig. 1.1. The leech central nervous system. (A): Schematic diagram of the leech showing the segmentation and the two specialized regions of anterior and posterior suckers. The CNS consists of a ventral nerve cord composed of a chain of 21 segmental ganglia and two more specialized head and tail ganglia, linked one to the other by bundles of axons (connectives). Segments are indicated, composed of five annuli, the central one of which contains sensilla, specific sensory organs. (B): Cross-section of the leech showing its anatomy. The body wall is made-up of three layers of muscles (circular, oblique and longitudinal), dorso-ventral muscle fibers run from the dorsal to the ventral side of the animal. Annulus erector muscles (not shown here), are located immediately under the skin. The nerve cord lies in the ventral part of the body and it is surrounded by the ventral blood sinus. Ganglia innervate the body wall through the anterior and posterior roots. The posterior root bifurcates near the ganglion and the dorsal branch crosses ventro-dorsally the body to innervate the dorsal region. The other roots innervate lateral and ventral regions. *(From: Nicholls et al., 1992)*

1.3.2 The segmental ganglion

The leech segmental ganglion contains the cell bodies of about 400 neurons, with the exception of ganglia 5 and 6, which innervate the sexual organs and contain over 700 cells. Its aspect and structure are conserved from segment to segment and from animal to animal; indeed the same neurons are recurrent in each ganglion for their positions, dimensions and functions. All neurons in the leech ganglion are monopolar; the cell bodies are contained in six separated regions (packets), each enveloped by a glial cell, while their innervations take place in the central neuropil, a specialized region in which synapses are arranged, surrounded by two giant glial cells (Schmidt & Deitmer, 1996); two other glial cells form the nuclei of the connective nerves. The glial cells show membrane potential variations during evoked behaviours and may play a role in computation (Deitmer & Kristan, 1999).

The neurons in the CNS can be roughly divided into three categories on the basis of their function: interneurons, sensory neurons and motoneurons. The category of interneurons broadly contains all neurons whose entire arborization does not exit from the CNS, but often exits the ganglion through the connectives: they are involved in a variety of functions such as heartbeat, motor control, reproduction, learning. An example of interneurons is the network of S cells, involved also in the shortening reaction. There is one S cell per ganglion which projects a very large axon, maybe the largest in the nerve chord, through the Faivre's nerve in the connectives; they are all strongly electrically coupled and represent probably the fastest electrical pathway connecting the two ends of the animal (Baader & Bächtold, 1997).

Sensory cells are neurons that directly translate a physical input coming from the environment into membrane potentials, or more generally are specialized to transform a physical quantity like, pressure, heat, salt concentration. into a change of their electrical

properties. Motoneurons are responsible for the excitation or inhibition of muscles (Stuart, 1970; Ort et al., 1974; Sawada et al., 1976; Stent et al., 1978). Motoneurons and sensory neurons project outside the ganglion to the periphery through the roots, sensory neurons also project in the connectives. Other excitable cells project their branches outside the CNS, for example Retzius cells whose firing is related to serotonin release (Willard, 1981; Gardner and Walker, 1982; Mar and Drapeau, 1996) and AP cells (Gu, 1991; Melinek and Muller, 1996) of still unknown function.

1.3.3 Properties of mechanosensory neurons

In the CNS there are sensory neurons responsible for three different mechanosensory modalities (**Fig. 1.2**) (Nicholls and Baylor, 1968; Yau, 1976a; Yau, 1976b; Blackshaw, 1981a & 1981b; Blackshaw et al., 1982): T (touch) cells are three for each hemiganglion and respond to a light mechanical stimulus applied to the skin, P (pressure) cells are two for each hemiganglion and respond to stronger stimuli, N (noxious) cells are two for each hemiganglion and respond to a damaging stimulation of the skin, with a threshold more than three times higher than the P cells (Carlton & McVean, 1995). Recent studies have demonstrated that N cells exhibit also functional properties similar to those of polymodal nociceptive neurons in mammals (Pastor et al., 1996), i.e. they are not simple mechanosensitive cells but respond to different sensory modalities of noxious stimulus like temperature rise and irritant chemical substances.

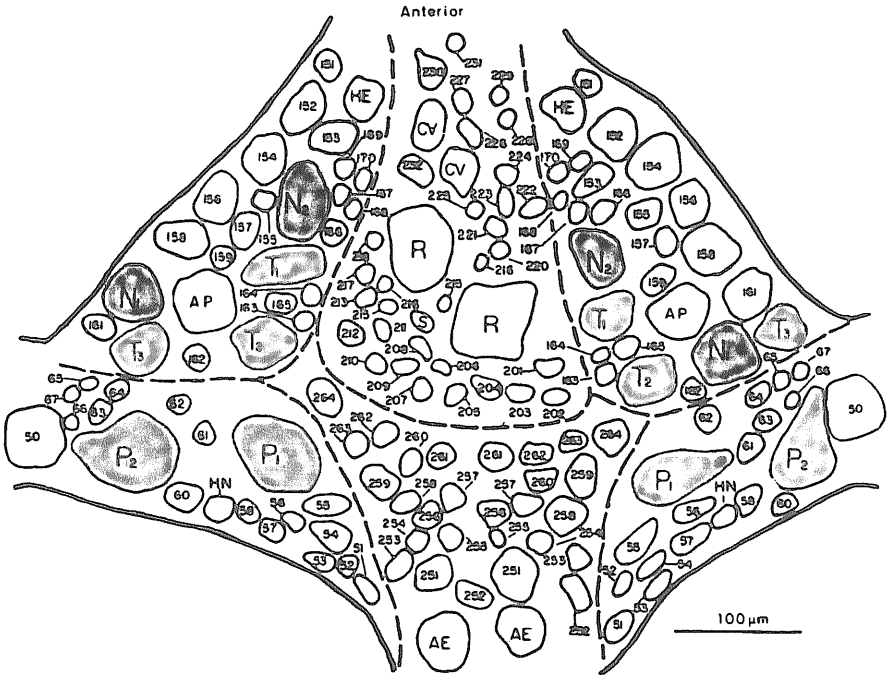

Fig. 1.2. Map of leech ganglion from the ventral aspect, showing the recurrent positions of the different kinds of mechanosensory cells. In green are indicated the six Touch (T) cells, in red the four Pressure (P) cells and in blue the four Nociceptive (N) cells. *(From: Nicholls et al., 1992)*

The mechanosensory cells in each ganglion innervate a well defined territory of the skin in the corresponding segment (Nicholls and Baylor, 1968), for example the three T cells respond respectively to the stimulation of the ventral (T_v), lateral (T_l) and dorsal (T_d) region of the segment. Analogously, P cells respond one to ventral (P_v) and the other to dorsal (P_d) touch stimuli. For the two ipsilateral N cells (N_m , N_l) the receptive fields in the same ganglion are approximately coincident and span the entire hemisegment from dorsal to ventral midline (Blackshaw et al., 1982).

Mechanosensory neurons are characterized by a main process arising from the cell body that gives rise to several branches projecting through the ipsilateral roots and the connectives to innervate the roots of adjacent ganglia. The receptive fields span 12-13 annuli over the central and the two adjacent segments; they appear to be composed of several non overlapping sub-fields (**Fig. 1.3**) innervated by separate branches of the same cell (Nicholls and Baylor, 1968; Yau, 1976). T cells have the simplest branching pattern in the ganglion, while N cells have the most complex projecting also though contralateral

neuropile. T cells branch extensively close to the surface in the epithelial layer of the skin, with a high density of terminals each one able to transduce independently a mechanical stimulus; the highest density of sensory terminals is in the central segment. The P cells branch less extensively and make far less terminals than the touch cells (Blackshaw, 1981a). The nociceptive neurons are different in that their branches end farther from the surface, below the epithelial layer, unlike the T cells, and also make distinct coil shaped terminals associated with large neurons (Hoovers cells) of the peripheral system: a feature that may be compatible with their polymodal function (Pastor et al., 1996), as previously explained.

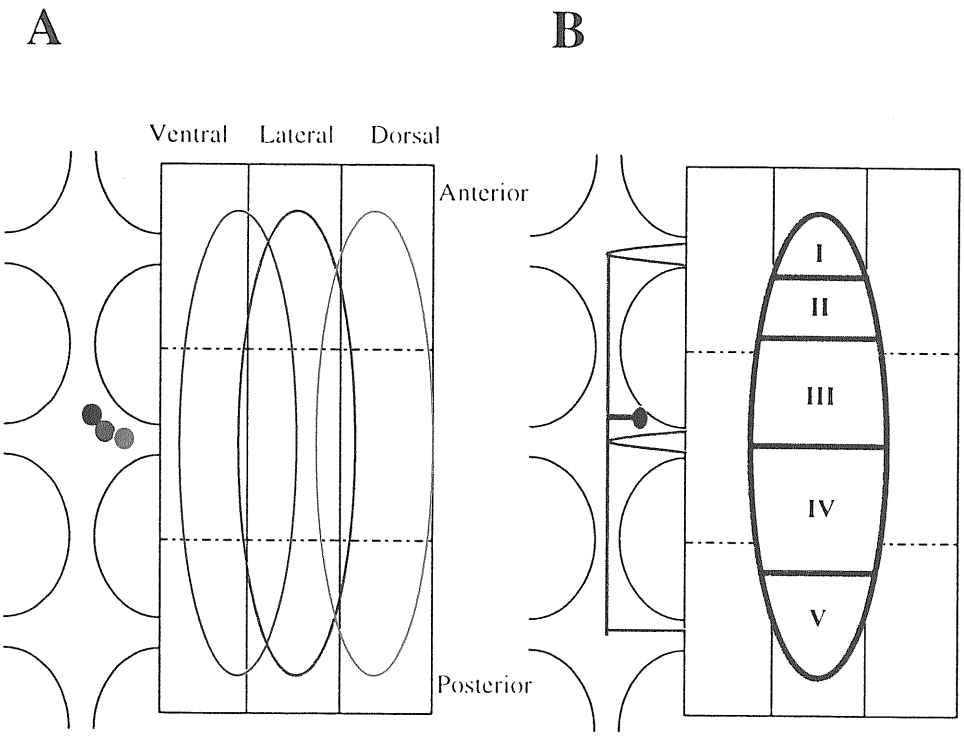

Fig. 1.3 Organization of the receptive fields. (**A**): the boundaries of the receptive fields of three T cells in the same ganglion overlap. The cells are drawn in the same color as their receptive fields. T_v is represented in red, T_l in blue, T_d in green. (**B**): adjacent subfields (I II III IV V) of a T_l cell, innervated by separated branches, do not overlap (Yau, 1976b).

By comparing the extension of receptive fields of cells responsible for the same sensory modality in the central segment or in the two adjacent ones, a considerable overlapping between receptive fields has been observed, as shown in **Fig. 1.3A** (Nicholls & Baylor, 1968).

1.3.4 Properties of motoneurons

In each hemiganglion there are 21 excitatory and 7 inhibitory identified motoneurons (see **Table 3.2**) (Stuart, 1970; Ort et al., 1974; Sawada et al., 1976; Stent et al., 1978; Muller et al., 1981; Norris & Calabrese, 1987; Baader, 1997). When the ganglion is observed in transmitted light, 25 are visible on the dorsal side and 3 are visible on the ventral side (**Fig. 1.4**). All motoneurons are in pairs, one lies in the left hemiganglion and the other in the right hemiganglion, with a corresponding location.

With the exception of the Annulus Erector (AE) which erects the skin at the centre of annuli and the heart excitor (HE) which supplies the lateral heart tubes, they are all responsible for the leech locomotion and movement. They can be divided into four groups, according to the muscle fibres they innervate: longitudinal, circular, oblique, dorsoventral. With the only exception of cell 4, a ventral longitudinal excitor, and cell 117, a dorsoventral excitor, all motoneurons exit the ganglion via the contralateral roots to innervate the corresponding body wall (Ort et al., 1974). Their fields of innervation extend longitudinally into adjacent body segments (Blackshaw, 1981a) and frequently overlap with those of neurons supplying the same muscles group. The motoneurons probably innervate muscle fibres by many terminals along their length, as it happens in crustacean (Stuart, 1970).

Excitatory motoneurons induce a smooth contraction of muscle fibres when increasing the firing frequency above a certain threshold level and over a functional range: each motoneuron in the ganglion shows a characteristic kinetics of the contraction. Rising the

firing frequency over the characteristic active range of the neuron, increases the contraction rate and its peak amplitude (Mason and Kristan, 1982; Blackshaw & Nicholls, 1995).

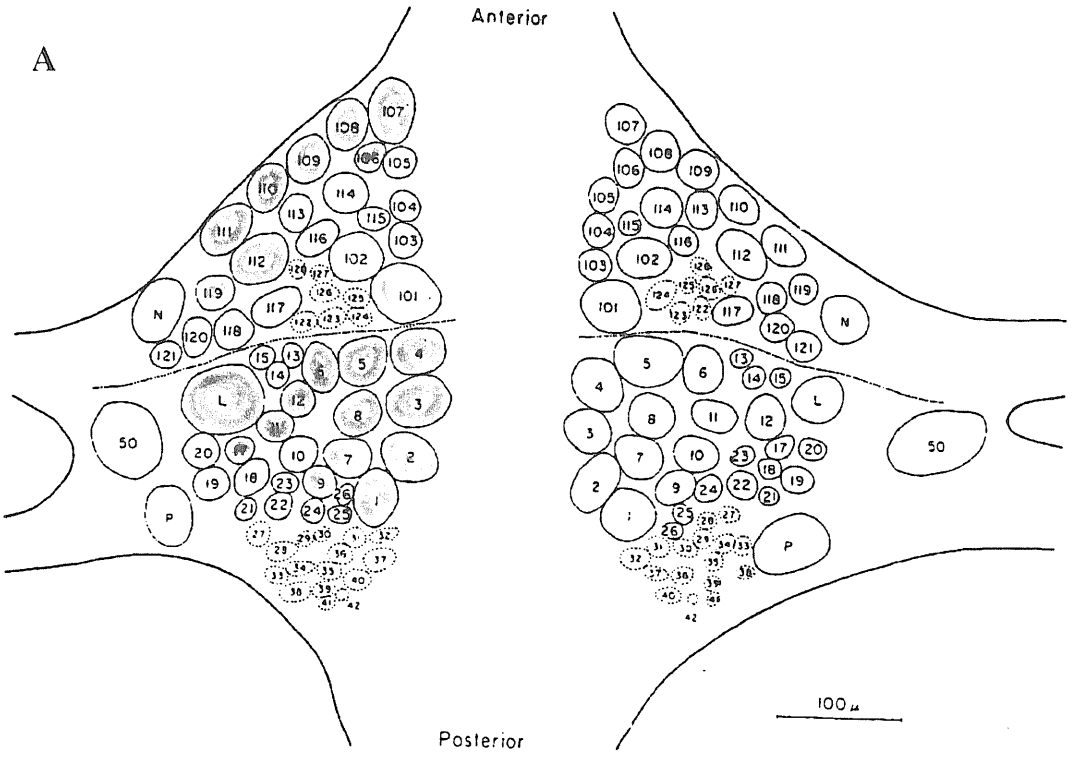

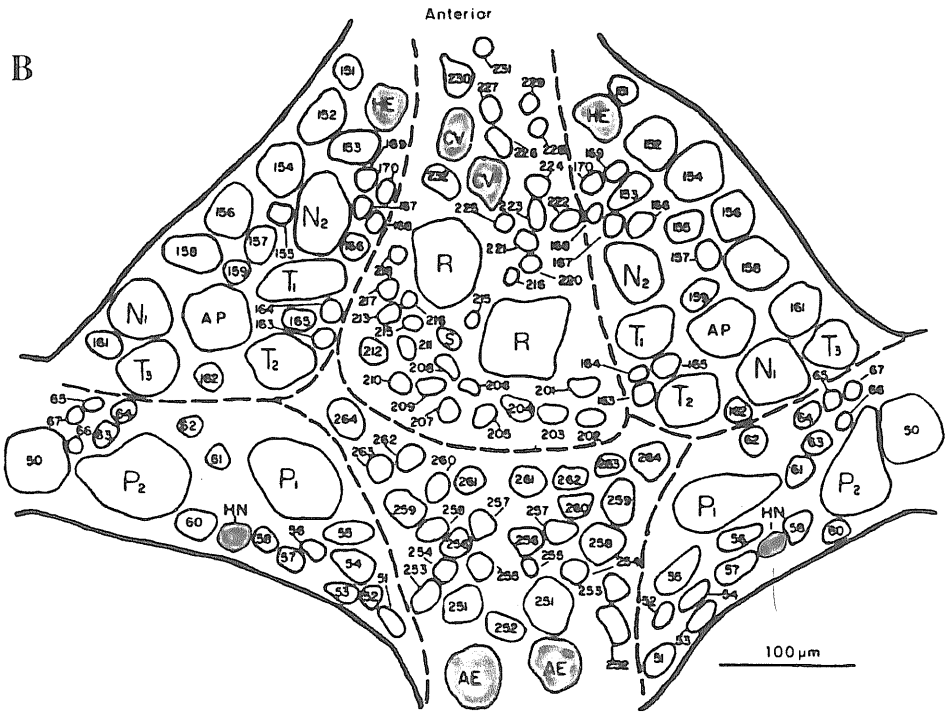

Fig. 1.4 Recurrent positions of the inhibitory (green) and excitatory (red) motoneurons in the leech ganglion. (**A**): map of the ganglion from the dorsal aspect; only left side motoneurons are colored. (**B**): map of the ganglion from the ventral aspect; all visible ventral motoneurons are colored. *(From: Nicholls et al., 1992)*

Inhibitory motoneurons counteract the effect of excitors. Since inhibitor activity does not reduce basal tension, it is necessary for the excitors to be active in order for the inhibitors to exert a peripheral effect. The ability of inhibitors to oppose strongly the effects of excitors suggest they contact most of the fibers contacted by the excitors (Mason and Kristan, 1982). In addition to their direct action on body wall, they also inhibit centrally the excitatory cells which innervate the same muscle (Granzow et al., 1985). Unlike the contraction, the relaxation of muscles is much slower, but the leech provides a modulation system. Stimulation of Retzius cells evokes slow reduction of tone in the longitudinal muscle and increases the rate of the slow phase of relaxation following a contraction; these effects have a long latency and duration and are mimicked by direct application of serotonin. There are 7 to 9 serotonin-containing cells in the leech ganglion (Gascoigne and McVean, 1991) but among them only the Retzius cells send processes to the periphery. There is some evidence for serotonin as an inhibitory neuromuscular transmitter in the leech *Haementeria ghilianii*, and also as a central inhibitory transmitter, since it is present in the blood and probably in the neuropil (Gardner and Walker, 1982; Mason and Kristan, 1982).

When impaled by intracellular electrodes, motoneurons appear to be non-spiking (Stuart, 1970), as the soma and the proximal axonal region are inexcitable; the action potentials arise at a site distant from the soma, near the primary bifurcation of the axon (Gu et al., 1991; Blackshaw & Nicholls, 1995). There is consistent evidence that the leech longitudinal nerve muscle junction is cholinergic (Gardner and Walker, 1982) and more generally that excitatory motoneurons synthesize, accumulate and release acetylcholine (Norris & Calabrese, 1987). FMRFamide appears to play a significant role in controlling

the heartbeat: FMRFamide-like immunoreactivity has been localized in heart excitators and heart interneurons (Norris & Calabrese, 1987). Leech inhibitory motoneurons are thought to be GABAergic (Blackshaw & Nicholls, 1995), since the longitudinal motoneurons take up and synthesise GABA from the precursor glutamate and further, central and peripheral inhibitory synaptic effects are mimicked by GABA.

1.4 Peripheral nervous system

Though no circuits lie in the periphery, the peripheral nervous system of the leech is well developed, mostly in its sensory part, including various kind of mechanosensors, chemosensors, photosensors; all these sensory neurons project centrally as witnessed by the hundreds of axons running in the lateral roots (Wilkinson & Coggeshall, 1975).

Two families of peripheral mechanosensors are known: the stretch receptors, whose cells bodies are located in the body wall, and the ciliated cells located in the sensilla. The stretch receptors bodies lie between two bands of longitudinal muscles and project centrally a large axon (10 to 15 μm in diameter), the largest in the leech nervous system, through the roots; large specialized fan-shaped dendrites are associated with the longitudinal muscles of the body wall (**Fig. 1.5**). The axons are nonspiking, with a large length constant between 2 and 5 mm, suitable to passively conduct impulses from the periphery to the centre. These receptors detect both the rate of change of stretch and release of longitudinal muscles and the amplitude of the deformation (Blackshaw, 1993; Blackshaw & Nicholls, 1995).

A second type of mechanosensor is located in the sensillum, polymodal sensory organ contaning photoreceptors (Tai et al., 1996) and three types of ciliated cells: among them the cells with a single long cilium (S hair cells) are probably involved in the water movement detection (Friesen, 1981; Blackshaw & Nicholls, 1995). The anterior sensilla

around the lip are both mechanosensitive and chemosensitive, responding to the presence of plasma, blood and other substances (Blackshaw & Nicholls, 1995).

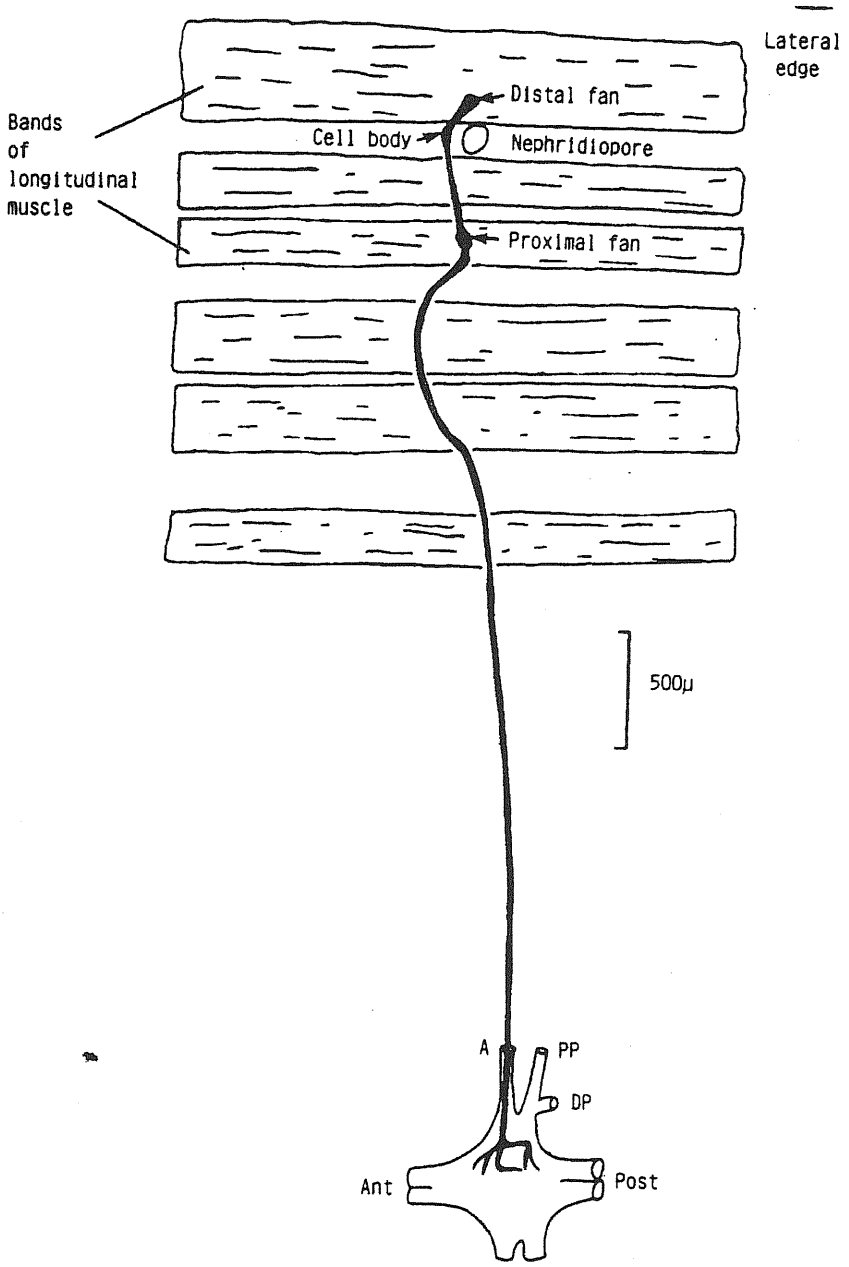

Fig. 1.5. Structure of a stretch receptor neuron innervating body wall muscle in the leech. The cell has two fan-shaped sensory terminals (labelled as distal fan and proximal fan). Both distal and proximal dendrites are associated with ventral longitudinal body wall muscle but with separate bands of fibres. The 10 μm diameter axon runs over a distance of approximately 4 mm into the segmental ganglion in the anterior nerve root (A). The cell body is located between the two sensory terminals and adjacent to the nephridiopore (opening of the excretory duct). (*From: Blackshaw, 1993*)

Another example of chemosensory neurons are the nephridial nerve (NNC) cells which innervate the escretory system, one per nephridium, and are involved in salt regulation. The cell body is located close to the sphincter, where it projects centrally through the roots; the receptive terminals are sensitive to chloride concentration and lie between urine-forming cells and blood capillaries (Wenning et al., 1982).

The leech visual system is formed by 5 pairs of primitive eyes, located on the dorsal part of the head region: each eye is composed by about 50 photoreceptors, each sending directly an axon to the CNS through nerves coming from the supraesophageal and subesophageal ganglia, where interneurons involved in the photoreception are located (Peterson, 1985a & 1985b).

1.5 Typical adult motor behaviours and underlying circuits

1.5.1 Overview

The leech exhibits a limited repertoire of basic adult motor behaviours, already present in the embryonic phase (Sawyer, 1981; Baader & Kristan, 1992; Reynolds et al., 1998): local bending and the associated local shortening, whole-body shortening, crawling, swimming. Bending and shortening are essentially escape reactions, crawling is a locomotory movement and swimming can be both. The way in which the leech responds to a stimulation depends upon the intensity and the location of the stimulus, roughly: a gentle mechanical stimulus on the skin produces a local bending in the touched segment, a stronger electrical or mechanical stimulus elicits also local shortening of the nearby segments if delivered in the midbody region, whole-body shortening if delivered to the rostral part, whole-body shortening or swimming if delivered in the posterior region. In

experiments with semi-intact preparations, these behaviours can also be evoked by direct intracellular excitation of mechanosensory neurons or particular interneurons. These behaviours are rather stereotyped, making this animal a good experimental model to study sensory-motor reactions (Kristan, 1982; Baader & Kristan, 1992). The underlying neural circuits have been only partially elucidated, especially for the case of crawling.

Even in the simplest case of local bending the computation is distributed among several interneurons (Lockery and Kristan, 1990), which leads to say that, as a general rule, motor behaviours in the leech are controlled by distributed processes, even if some dedicated circuits may exist. The swimming, crawling and shortening circuits are partially superimposed, since some interneurons and motoneurons are active during different motor behaviours: cells 204 and 208 during swimming and crawling, S cell during shortening and crawling, dorsal and ventral excitatory motoneurons probably during swimming, crawling and shortening. The data reported until now by different authors, all favour a partially distributed organization of leech motor circuits, with some dedicated interneurons, most of motoneurons and some multifunctional interneurons taking part in different behaviours. This corresponds to a reorganizing model of neural architecture (see Introduction), where different motor responses can be produced by altering the same circuit.

1.5.2 Local Bending

Local bending consists of a contraction of longitudinal muscles on the stimulated side of the segment and a relaxation on the opposite side, leading the segment away from the stimulus in the opposite direction (Kristan, 1982). The stimulus direction is encoded almost completely by the P cells, with the T cells playing an accessory role (Lewis & Kristan, 1998a & 1998b & 1998c). Several interneurons are involved in the bending circuit, all of them also recruited during the shortening (Lewis & Kristan, 1998b). Local shortening is

strictly associated with bending; around the stimulus site an number of segments increasing with the stimulus intensity are involved, but the stimulated segment only bends and does not shorten. It is generally believed (Wittenberg & Kristan, 1992a & 1992b) that mostly motoneurons 3 (dorsal excitor), 4 (ventral excitor), with a weak contribution of the L cell (longitudinal excitor), could account for the local body shortening. All described shortening interneurons are also part of the bending circuit, no exclusively shortening dedicated interneuron was found; on the contrary some interneurons appear to be multifunctional, such as cells 159 and S also involved in crawling and cell 115 already known as a swim interneuron (Wittenberg & Kristan, 1992b; Baader, 1997).

1.5.3 Whole-body shortening

Whole-body shortening is a withdrawal response to a strong mechanical or electrical stimuli delivered to the anterior of the animal (see **Fig 2.2B** and **C**), a similar reflex can be seen also when the posterior is stimulated. Compared to local shortening, it is a distinct behaviour, though being apparently similar: it is not associated with local bending, the sensory thresholds, the motor patterns and partially the circuitries are different. At the sensory level local shortening can be produced by stimulating one single P cell, whereas whole-body shortening requires activation of multiple P and T sensory neurons; the motor pattern for local shortening involves a graded activation of dorsal and ventral excitors, with a weak activation of the L cell, in contrast whole-body shortening requires the symmetrical activation of several motoneurons throughout the body (see Chapter 4) and involves all the segments of the animal. Fast interneuronal pathways together with the S cell network (Magni and Pellegrino, 1978) are responsible for whole-body shortening and they appear not to be activated during local shortening (Shaw and Kristan, 1995 & 1997 & 1999).

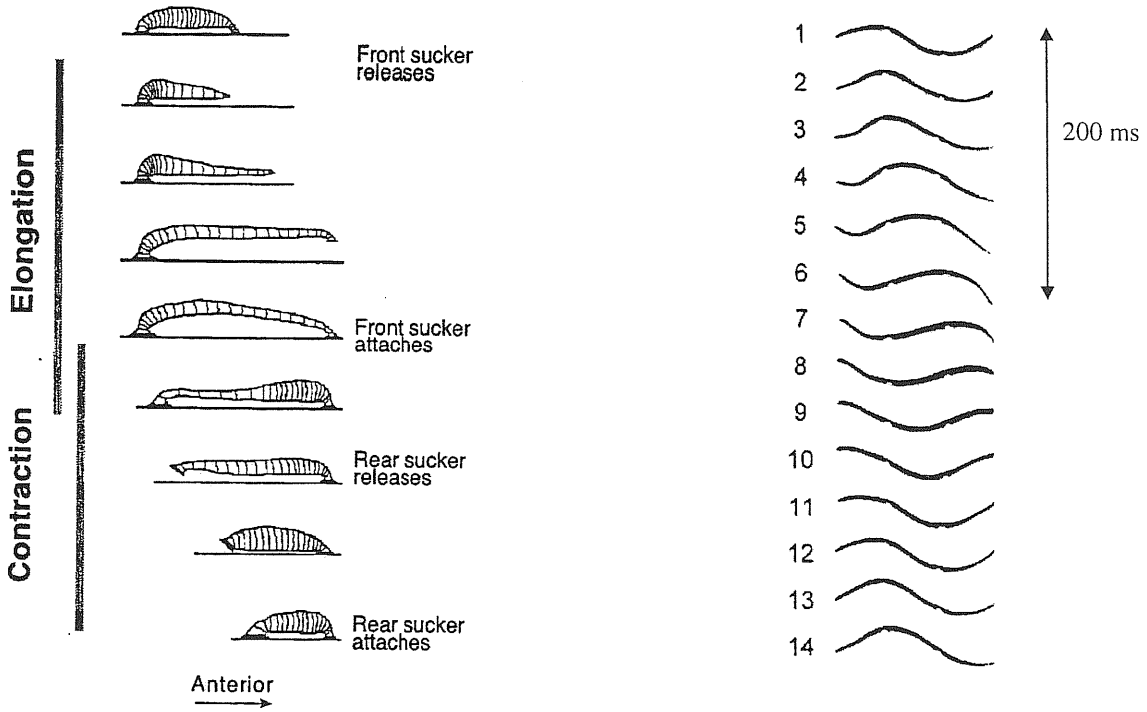

Fig. 1.6. Swimming and crawling. (**A**): Sequence of events in a vermiform crawling step of the leech. The step begins with the front sucker release and the commencement of a front-to-back wave of segmental elongations (indicated by the top grey bar). Some time later, the front sucker attaches and a front-to-back wave of contraction ensues (bottom bar). Note that in the step shown there is overlap between contraction of anterior segments and elongation of posterior segments, as indicated by the overlap of the bars. During the contraction wave the rear sucker releases and later it attaches after the animal has fully shortened, completing the step. (**B**): Sequential video frames of a freely swimming leech. A full sinusoid-like swim wave is developed along the leech body, with a crest and a trough passing backward while the leech is swimming forward (anterior is to the left). Frames 1 and 12 show identical profiles, with a cycle period of 0.37 sec. (*From: Yu et al., 1999; Cacciatore et al., 2000*)

1.5.4 Swimming

In the aquatic environment the leech is able to swim. The swimming rhythm consists of a periodical continuous antero-posterior undulation of the whole body, produced by an antiphasic contraction of dorsal and ventral longitudinal muscles. The delay between segments is function of the position along the animal and of the swim period. The body is kept flattened by the activation of dorsoventral muscles (**Fig. 1.6B**). The neural correlate of swimming occurs in the isolated nerve chord, and even in isolated ganglia if serotonin is

provided (Willard, 1981), which proves that the intersegmental coordination is maintained by a CPG present in all segmental ganglia. From a biochemical point of view, the glutamate is involved, as an excitatory neurotransmitter, in the activation of oscillating circuits by the leading trigger interneuron, cell 204 (Thorogood & Brodfuehrer, 1995). Serotonin is well known as a modulator of locomotion in a variety of animals and it is present in the leech blood; intracellular stimulation of the serotonergic system, whose main members are the large Retzius neurons, facilitates swimming, as well as a direct application of the substance to the isolated nerve chord. Serotonin is recognized as the major modulator both centrally, on the CPG where serotonin-containing interneurons synapse on oscillator cells, and peripherally, acting on the muscle tension (Willard, 1981; Brodfuehrer et al., 1995a).

The local swimming network in each ganglion is composed of at least 21 neurons: 7 paired and 1 unpaired interneuron, 3 pairs of motoneurons, mostly connected by inhibitory synapses (Brodfuehrer et al., 1995a). The mechanism that generates the swimlike oscillations is based on reciprocal inhibition between several pairs of oscillating interneurons, the same occurs for the leech heartbeat CPG (Calabrese et al., 1995) and other invertebrate circuits (Clemens et al., 1998a & 1998b). The whole swimming circuit can be considered as a chain of coupled oscillators (Pearce & Friesen, 1985a & 1985b), one per ganglion: the interganglionic connections, some spanning even 6 ganglia in length, are essentially repeats of the intraganglionic ones, most of them being also inhibitory. A leading role is played by the subesophageal ganglion in the head brain, as suggested by the fact that a leech is much more likely to swim if the head is removed, as if it exerted an inactivating action on the CPG. In the head some key interneurons, not present in the segmental ganglia, are located: cells Tr1, Tr2, Tr3 (swim trigger interneurons), SIN1 (swim inhibitory interneuron), SE1 (swim excitatory interneuron). These neurons are at the highest level in the hierarchy of the circuit, indeed above the CPG, and project caudally

probably along the entire nerve chord, exciting swim oscillatory cells in every ganglion: Tr1, Tr2, Tr3 can trigger swimming when stimulated, though Tr2 is more efficient in stopping the rhythm and with SIN1 is part of the swim inactivating system, while SE1, together with Tr1 and Tr3, is part of the swim activating system. Though previously neglected, the mechanical feedback has recently been shown to play a primary role (Yu et al., 1999): intersegmental coordination during swimming is entirely achieved in leeches with severed nerve chord, that is with electrically uncoupled swim oscillators.

1.5.5 Crawling

Crawling is the normal locomotory behaviour of the leech in the terrestrial environment. A vermiform crawling locomotion cycle in the medicinal leech consists of an elongation and a contraction phases: the leech is initially attached to the substrate both by the front and the rear suckers, then it releases the front sucker and a head-to-tail wave of elongation leads the leech to attach farther the front sucker; this last event triggers the release of the rear sucker, then the leech shortens completely, while the front sucker remains attached, and attaches again with the rear one.(**Fig. 1.6A**). The entire movement lasts between 3 and 10 sec. Several motoneurons are recruited both in the shortening (contraction of longitudinal muscles) and elongation phase (contraction of circular muscles); moreover during the elongation phase the anterior part of the animal starts shortening while the posterior part still elongates, superimposing two patterns of motoneurons activity. The crawling circuit, rather complex, is a Central Pattern Generator (CPG), as the animal is able to produce several successive crawling cycles, and a neural correlate of crawling occurs in the isolated nerve chord. The crawling CPG differs from the swimming one in that precise intersegmental coordination is not essential and much more flexibility is needed to make variable exploratory movements on the solid substrate before

deciding where to attach and continuing the cycle, unlike the swimming which takes place in an aqueous uniform environment (Cacciatore et al., 2000). Therefore a crucial role is played by sensory feedback to modulate the CPG activity. The CPG is certainly located part in the head and tail brains and part in the midbody ganglia, since leeches with either or even both brains removed are still able to crawl, though slowly, but a prominent role seems to be played by the head brain (Cacciatore et al., 2000). In midbody ganglia several interneurons active during crawling were identified, such as cells 151, 213, 258, in particular some multifunctional cells were found: the swim-initiating neuron 204 and the swim oscillator neuron 208, well known to be part of the swim-generating circuit, are also active during crawling. The S cell is also active during shortening, but whose role in the crawling circuit is still unknown. The head and tail brains contain both elongation and contraction driver circuits, which are connected by fast interneuronal pathways; these pathways run mainly through the lateral large connectives, since disruption of Faivre's nerve and of S cell network has only a minor effect (Baader & Kristan, 1995). Some candidate interneurons with soma lying in the tail brain and projecting rostrally have been characterized (Baader & Bächtold, 1997).

Chapter 2

Materials and methods

All the experiments shown in this thesis were always performed in the leech CNS using different kinds of preparations and experimental protocols. In this chapter all the experimental procedures are explained with attention to technical questions and data analysis. The procedure for neuron identification is only outlined here, since it is part of my Ph.D. project and it will be the main subject of the next chapter.

2.1 Animals and preparations

Specimens of *Hirudo medicinalis* were obtained from a commercial supplier (Ricarimpex, Eysines, France) and kept at 5° C in tap water dechlorinated by aeration for at least 24 hours. The leeches were dissected under a stereomicroscope. Two kinds of preparation were arranged for the experiments: isolated ganglia and semi-intact leeches.

For the study of neuron identification or local bending single or couple of midbody ganglia (chosen between the 7^{th} and the 16^{th}) were isolated from the CNS, roots were carefully cleaned and cut in order to draw them into suction pipettes (**Fig. 2.1**). The ganglia were then pinned through the connectives with the ventral or dorsal side up. Since mechanosensory neurons are visible from the ventral side of the ganglion, ventral side up configuration is suitable for impaling mechanosensory cells. On the other hand, since most

motoneurons are contained in the dorsal side of the ganglion, dorsal side up configuration is useful when motoneurons have to be impaled.

For the study of whole-body shortening, a semi-intact preparation was used, consisting of a whole leech with three ganglia (usually the 10^{th}, 11^{th} and 12^{th}) exposed and isolated from the corresponding body wall (**Fig. 2.2A**). The central part of the animal was held fixed and pinned down, but the head and tail were left free to move. In other experiments, a different preparation was used to monitor simultaneously whole-body shortening and deformations of a piece of skin innervated by only one ganglion: a piece of skin corresponding to a whole body segment (**Fig. 2.2B** and **C**) or a half segment was isolated from the rest of the body but kept innervated by one ganglion. This piece of skin was fixed to the bottom of the recording chamber at the edges only, so as to allow it to deform during muscle contraction. The roots emerging from ganglia were cleaned and cut for recording with suction pipettes. The tail and head of the leech were left intact and free to move; both suckers were sutured with a surgical thread to avoid sticking to the Sylgard gel.

Preparations were pinned in a Sylgard-coated dish and micromanipulators (Narishige, Japan) used to position the extracellular electrodes. All the experiments were done at room temperature (20-24°C).

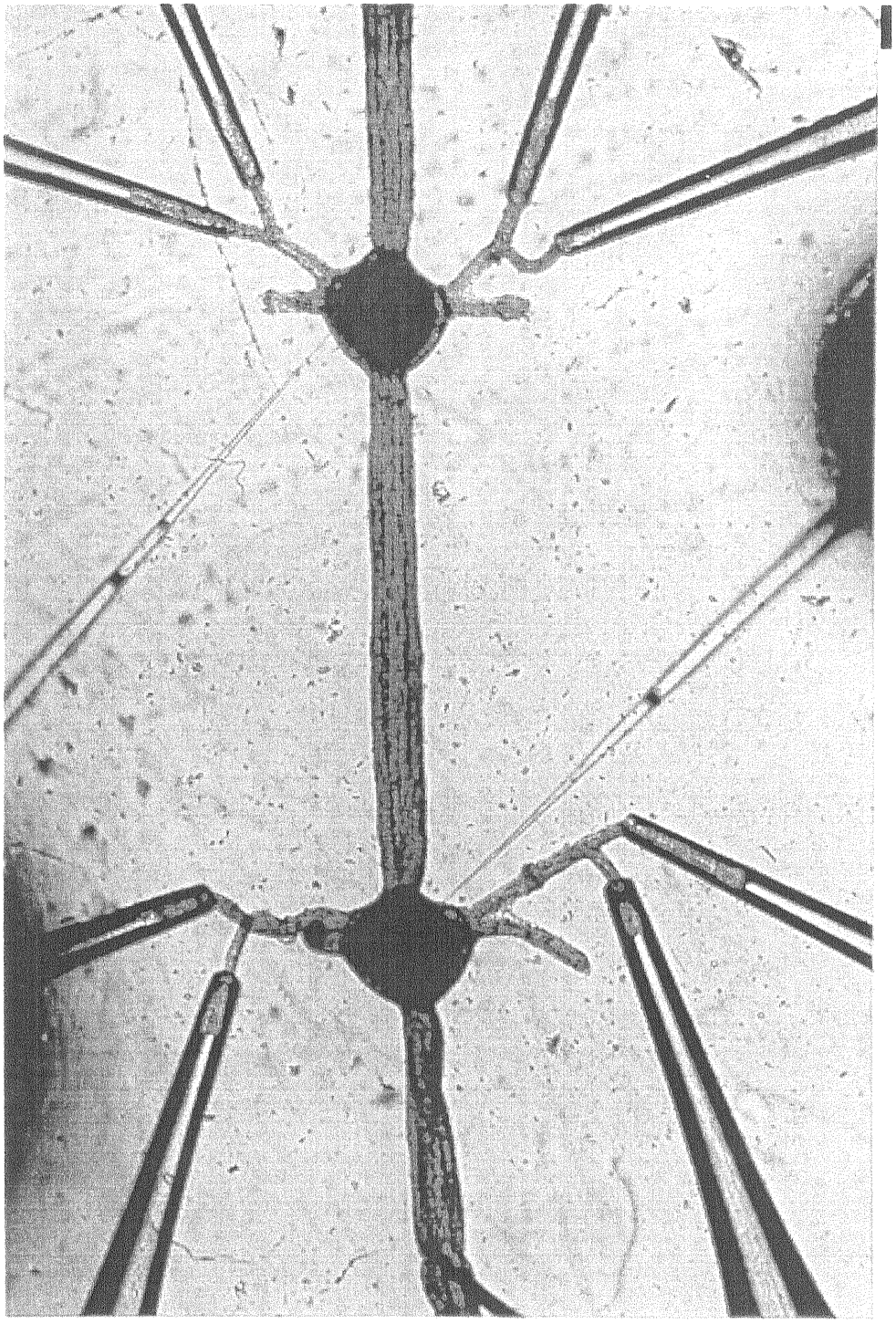

Fig. 2.1. Photograph with a preparation of two isolated leech segmental ganglia. In each ganglion right and left DP and PP nerves are drawn into suction pipettes. Two intracellular sharp electrodes are visible. The ganglia are pinned to the Sylgard substrate through the connectives, a pin is visible at the bottom.

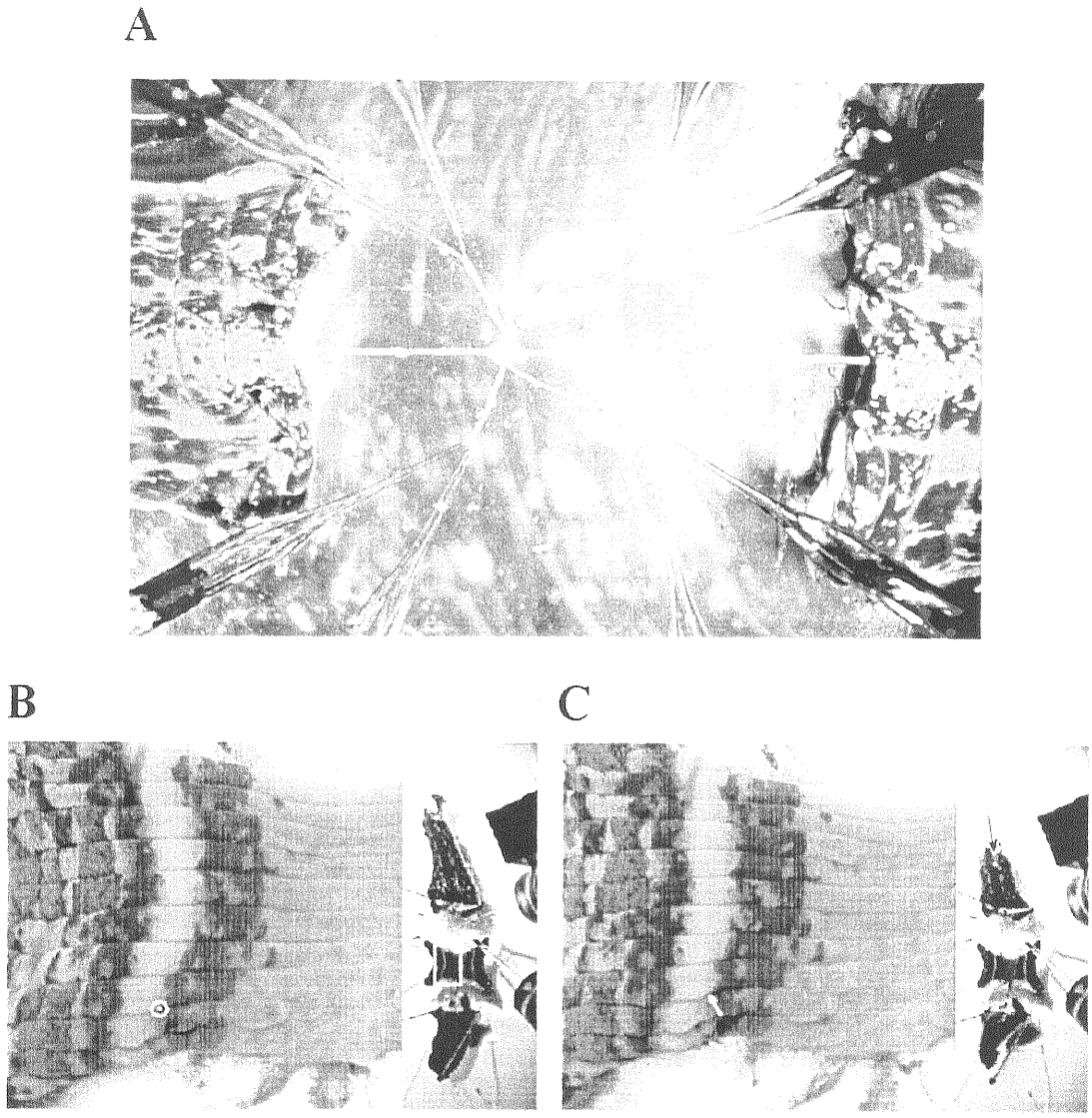

Fig. 2.2. The semi-intact preparation and the recording electrodes. (**A**): Eight suction pipettes surrounding the 10th ganglion of a semi-intact leech were used to record the electrical activity from eight fine branches emerging from the ganglion. (**B**) and (**C**): Combined images of a semi-intact leech (on the right) and of a piece of skin (on the left) before and during whole-body shortening (see Chapter 4). The leech was imaged with a miniaturized CCD camera viewing the recording apparatus. The head and tail of leech were kept intact and the 8th and 10th ganglia were isolated, while the skin of the 9th body segment was flattened so as to be monitored by another CCD camera mounted on a dissecting microscope viewing the skin. The two CCD cameras were synchronized and their images combined in a single image, as shown in (**B**) and (**C**). The two white wires connected to the head are used to provide the noxious stimulation. The yellow rectangle indicates the isolated segment shown on the left of panels **B** and **C**. The yellow and red arrows in (**C**) indicate the observed displacement of the head and a point mark on the skin (yellow dot in **B**) during whole-body shortening (see Chapter 4).

2.2 Electrophysiology

2.2.1 Extracellular recordings

Four to eight suction pipettes were used for extracellular recordings as shown in **Fig. 2.1** and **2.2**. The electrodes were obtained pulling (P-97 puller, Sutter Instruments) thick walled glass capillaries (GC100-10, Clark Electromedical Instruments); the pipettes were then cut on the tip and shaped by a microforge. In some experiments eight pipettes were used to record the electrical activity from the left and right anterior anterior (AA) and medial anterior (MA) nerves and from the left and right bifurcations (DP:B1 and DP:B2) of the dorsal posterior nerves (Ort et al., 1974; Baader, 1997) of the same ganglion; in some cases only four pipettes were used to record the electrical activity from ipsilateral AA, MA, DP:B1 and DP:B2 nerves. In other experiments eight suction pipettes were used to record the electrical activity of the left and right AA and MA nerves (or the DP:B1 and DP:B2 nerves). Often one suction pipette was used for recording en passant from the anterior connective entering into the ganglion under investigation. In other experiments only the left and right posterior posterior (PP) nerves of two adjacent ganglia were sucked into four suction pipettes and their electrical activity recorded.

The design and realization of an 8-channel standard amplifier was part of my Ph.D. project. This amplifier is made up of two amplification stages. The head-stage contains an 8-channel amplifier with a bandwidth of 200-2500 Hz (2-pole filter) and a fixed gain of 10^3. The second stage of amplification is a rack mounted instrument and has a gain ranging from 0.2 to 200 (**Fig. 2.3**). This amplifier was used to record the extracellular signals. The signals produced by the action potentials, recorded by the suction electrodes from the connectives and roots, ranged about between 15 and 500 μV. The standard deviation of the noise was about 10 μV.

2.2.2 Intracellular recordings

The electrical activity of neurons was also monitored by one or two intracellular recordings, obtained by impaling neurons with sharp electrodes. The electrodes were pulled (P-97 puller, Sutter Instruments) using thin walled glass capillaries (TW100F-4, WPI). The input resistance was in the range 20-40 MΩ. Potassium acetate 4.0 M solution was used to fill the electrodes (Muller et al., 1981b). The intracellular recordings were performed using either a double Axoclamp-2b amplifier (Axon Instruments) or a 4-pole filter (VBF8 variable filter, Kemo) and two amplifiers (Cyto 721, WPI) (**Fig. 2.3**). The electrode holders, including head stage, were mounted on micromanipulators (Narishige, Japan).

2.2.3 Electrical stimulation

The sensory input on a single segment, inducing local bending, was mimicked by evoking action potentials in central mechanosensory neurons by the injection of current in P cells with sharp intracellular electrodes: one to four action potentials were elicited, according to the stimulation protocol.

Noxious stimulation to induce whole-body shortening consisted of an electrical pulse of 0.8-1.2 mA (Isolator-10, Axon Instruments), delivered to a platinum wire sutured tightly on the skin of the animal near the third segment as described in (Shaw & Kristan, 1995). The pulse lasted 1 second and it was delivered at intervals of at least 3 minutes. We took care to use the lowest possible stimulus amplitude able to elicit the shortening contraction (**Fig. 2.2B** and **C**). In experiments on leeches with intact head and tail, the animal occasionally attached to the bottom of the perfusing chamber with its head sucker and in

these cases electric stimulation often failed to elicit whole-body shortening. The behavioural response was more reproducible when the head sucker was sealed with a surgical thread.

2.2.4 Data collection and storage

Voltage recordings, either extracellular or intracellular, were digitized at 10 kHz; extracellular signals were recorded with a bandwidth of 200-2500 Hz and a standard gain of 2 $x10^4$. Voltage signals were collected through Digidata 1200B board (Axon Instruments) and stored on a personal computer using Clampex8 or Axoscope8 programs and also on an 8-channel digital audio recorder (DA-88 TASCAM). During the first phase of my Ph.D. work I used also a programmable Digital Signal Processing (DSP) board (Fulcrum, Data Translation), whose software I entirely wrote, as explained below (**Fig. 2.3**).

2.3 Video recordings

With the semi-intact preparation also two black and white CCD cameras were used for monitoring whole-body shortening (see Chapter 4). One standard CCD camera mounted on a dissecting microscope was used to measure deformations of a piece of skin induced by muscle contraction during whole body shortening (**Fig. 2.2B** & **C**) or by direct stimulation of motoneurons impaled with a sharp intracellular microelectrode. The second miniaturized camera (CS3500C, Teli) was mounted on a micromanipulator at a distance of about 10 cm from the entire leech. This camera was used to quantify whole-body shortening. Images from the two cameras were synchronized and combined in a single image by a Video

Screen Splitter (Model 613, Colorado Video, Inc.). Images were acquired at 8.3 Hz and stored on a Personal Computer using a frame grabber (DT3155, Data Translation) and the Imaging Workbench 2.2 acquisition software (Axon Instruments). Displacements (arrows in **Fig. 2.2C**) of selected features (dotted circle in **Fig. 2.2B**) in images were obtained by correlation based algorithms (Aggarwal and Nandhakumar, 1988; Zoccolan & Torre, in preparation).

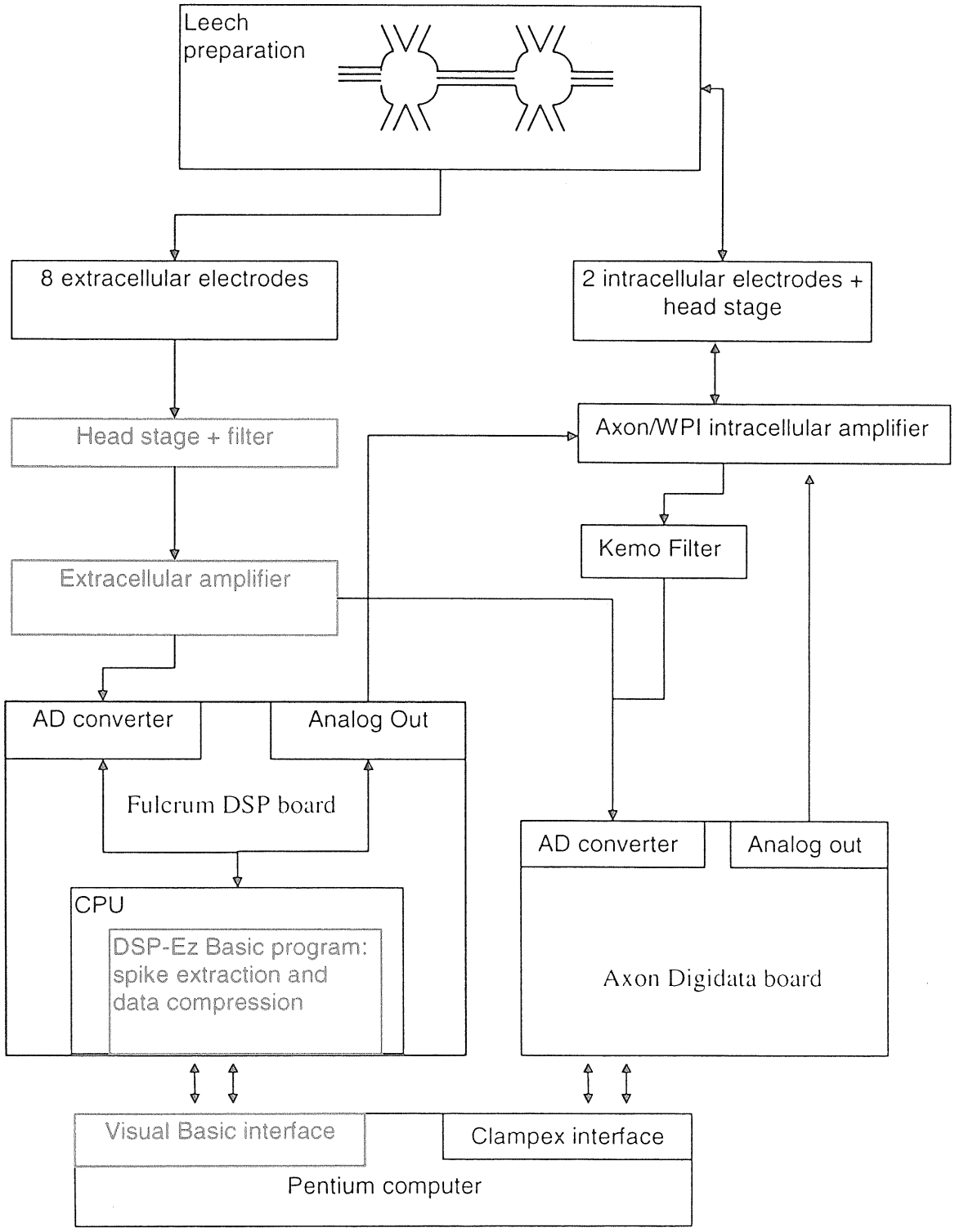

Fig. 2.3. Scheme of the electrophysiological data acquisition system. Eight extracellular pipettes and two intracellular sharp electrodes are used to record from the leech ganglia. Signals are conveyed to the computer after a filtering and amplification stage and through two different acquisition boards which work in parallel. The Digidata board is controlled by a commercially available software while the Fulcrum DSP board must be programmed by the user. The green boxes indicate hardware and software whose realization was part of my Ph.D. work.

2.4 Optics

A stereomicroscope (SMZ-2B, Nikon) was used during the dissection. The preparation was then transferred on the stage of a larger microscope (IX70 Inverted Microscope, Olympus), where a second stereomicroscope (SZ-11, Olympus) was mounted to impale neurons under visual control in bright field transmitted light.

2.5 Data analysis

2.5.1 Spike clustering and statistics

Preliminary data display and analysis were performed with Clampex8 and Axoscope8 software (Axon Instruments). Since the problems addressed in all my experiments concerned the parallel processing in the leech CNS, it was necessary to develop a suitable method for further analysis of the multi-electrode recordings. The possibility of discriminating in parallel signals produced by different neurons is based on the assumption that action potentials produced by the same neuron have almost identical extracellular signals. Hence a crucial problem was the classification of the shapes of action potentials. In

most experiments this task was accomplished in a semi-automatic way. The development of software to face this problem was part of my Ph.D. work, carried out in collaboration with other people in my laboratory. Programs for semi-automatic spike extraction, spike sorting (see 3.4.3 for details), statistical analysis and results display (**Fig. 2.4**) were realized in Matlab language (Math Works Inc.). Routinely computed first order statistics of clustered neuron included: AFR of identified neurons, coefficient of variation, histograms of the time occurrences of the 1^{st}, 2^{nd}, ...,n^{th} spikes in each trial. Second order statistics included time crosscorrelations and joint firing probabilities. I personally wrote an additional program for on-line spike event detection and extraction in DSP-EZ Basic language (Data Translation) and ran it directly on the Fulcrum Board (**Fig. 2.3**); I also wrote the Personal Computer user interface in Visual Basic language (Microsoft Corp.) to control the Fulcrum board.

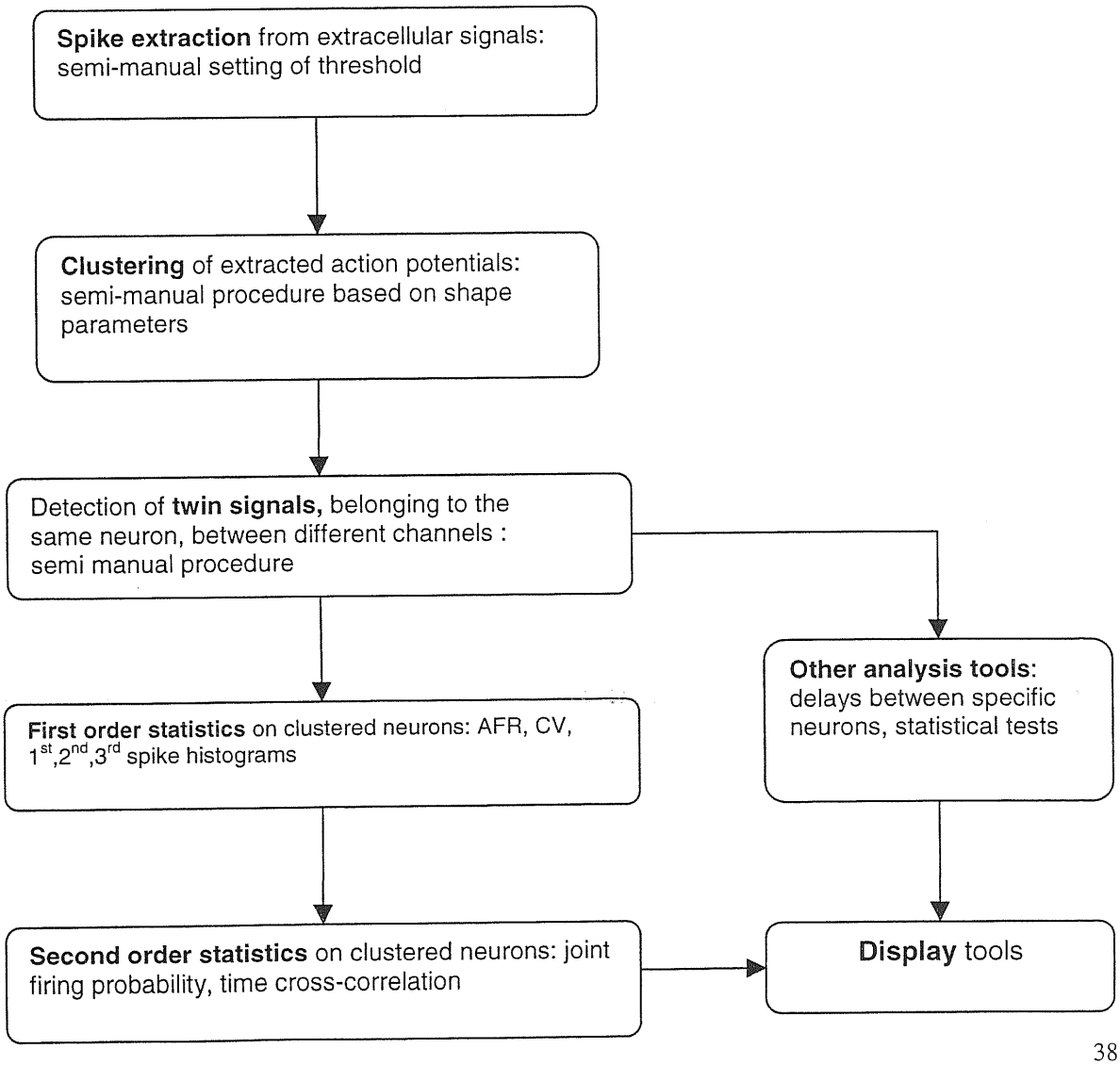

Fig. 2.4. Scheme of the basic operations for the analysis of multi-channel extracellular recordings; all the suitable software was written in Matlab language (Math Works Inc.) in our lab. Action potentials are extracted from recordings, spikes are clustered so as to isolate the contribution of different neurons in the recordings. Twin signals of the same neuron on separate channels are detected. First and second order statistics are performed on the activity of clustered neurons; any step of the analysis can be displayed

2.5.2 Analysis of variability

The variability of action potentials identified as originating from the same neuron N was characterized by computing the coefficient of variation CV of the firing rate of the neuron. It is defined as CV = σ/AFR, where σ is the standard deviation of the firing rate and AFR is the average firing rate of the neuron, over the number of trials of a given stimulation, in a given time window Δt. When the electrical activity of several neurons i=1, ... , n was analyzed, the CV of the random vector $X = (x_1, x_2, ..., x_n)$, with x_i being the firing rate of neuron N_i, was considered. The CV of the ensemble of motoneurons in **Fig. 4.7** was computed by averaging (see Appendix), i.e. as the CV of the random variable $X = (x_1 + x_2 + ... + x_n)$:

$CV_X(t) = \sigma_X(t) / \sum_i AFR_i(t)$, where $AFR_X(t) = \sum_i AFR_i(t)$ is the mean firing rate of X and $\sigma_X(t) = \sqrt{\frac{1}{R}\sum_{r=1}^{R}(X(r,t) - AFR_X(t))^2}$ is its standard deviation, R is the number of trials (see Appendix).

In order to quantify the degree of correlation of two neurons the crosscorrelogram was computed, histogramming the differences between their spiking times, as described in (Brivanlou et al., 1998).

Whole-body shortening was quantified by computing the relative shortening S, defined as the ratio between the shortening of the anterior part of the leech and its initial length, both measured on the image plane (see **Fig. 4.1**). The variability of the evoked behavioural

response was characterized by computing the coefficient of variation CV_S of the relative shortening S. It is defined as $CV_S(t) = \sigma_S(t)/ M_S (t)$, where σ_S is the standard deviation and M_S is the average value of S over the number of trials of a given stimulation, in a time window Δt, equal to the sampling period of image acquisition (see 2.3).

A similar approach was used to quantify the deformation of a piece of the leech skin and its reproducibility over the series of trials. In this case the total displacement D of a selected landmark on the leech skin was measured on the image plane and its coefficient of variation $CV_D(t) = \sigma_D(t)/M_D (t)$ was evaluated (see **Fig. 4.1**). Here σ_D is the standard deviation and M_D is the average value of D over the number of trials of a given stimulation, in a given time window Δt, equal to the sampling period of the image acquisition (0.12 sec, see 2.3).

Chapter 3

Identification of extracellular signals

3.1 Introduction

The nervous system of mammals and even of more developed invertebrates is too complex to allow a detailed description of the network, therefore it is not usually possible to obtain an atlas of identified neurons. In most cases only a description of brain anatomy and of tissue histology is available. Compiling an atlas of the neural connections would be even more difficult.

In the mammalian cortex (Quirk et al., 1990; Wilson & McNaughton, 1993; Gothard et al., 1996; O'Keefe and Burgess, 1996, Csicsvari et al., 1998) or even in complex invertebrates such as bees and locusts (Laurent et al., 1996; MacLeod & Laurent, 1996; Stopfer et al., 1996; Wehr & Laurent, 1997) whose CNS contains hundreds of thousands of neurons, it is not possible to identify each single cells which produces recordable extracellular signals. What is in fact possible is to characterize their histological class on the basis of their morphological, anatomical and electrophysiological features.

Unfortunately this neuron identification problem can be and actually has been addressed only in simple invertebrates, such as the leech, the mollusc *Aplysia* and the worm *C. elegans*.

Leeches offer invaluable advantages to the neuroscientist: the CNS is organized in stereotyped ganglia containing few hundreds cells each (see 1.3.2); the total number, locations and synaptic connections of the neurons are rather constant among specimens

belonging to the same species; the transparency of a ganglion enables the visual inspection and electrode penetration of almost all its neurons; the entire neural output from a ganglion can in principle be monitored with extracellular electrodes.

The aim of the work presented in this chapter was to develop a method to analyze extracellular signals recorded with pipettes sucking fine branches of leech roots, in order to isolate action potentials belonging to different cells and to label them with the standard names of neurons producing them. When extracellular action potentials have been labelled, first and second order statistics can be computed.

3.2 Features of extracellular signals from a suction electrode

No simple relationship exists between the transmembrane voltage of action potentials recorded with intracellular electrodes or patch pipettes and the corresponding extracellular signals, first of all because the latter are strictly dependent on how and where they are recorded. Generally speaking, the extracellular signal describes the time course of currents flowing between the extracellular space in contact with the measuring electrode and a reference terminal; of course the higher the impedance between the two, the larger the signal. I will qualitatively justify the dependence of the extracellular recorded voltage upon the axon diameter, which is the main limiting step in the application of this experimental technique.

Pipettes sucking leech nerves record from a bundle containing hundreds of axons, each contributing with its own current to the global signal; since these currents add up linearly, we can suppose for simplicity that we are recording from just one single axon.

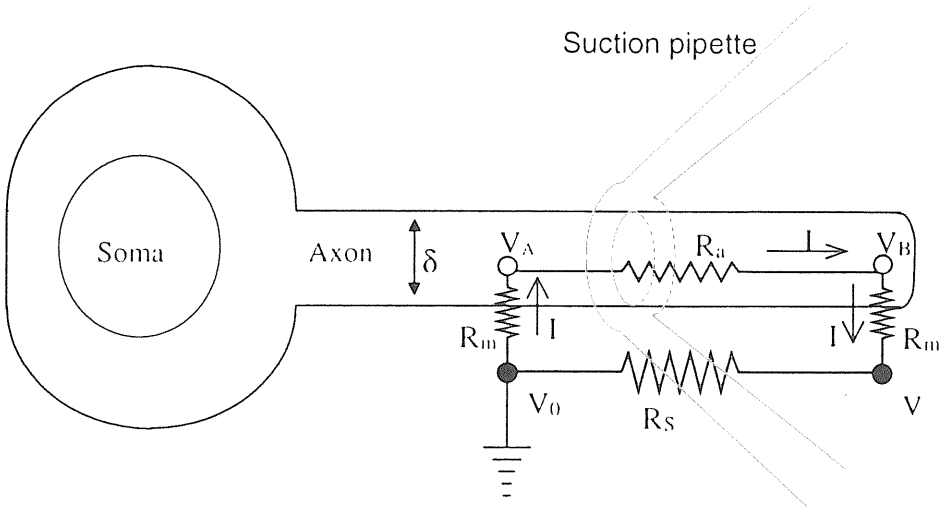

Fig. 3.1. Approximate equivalent circuit for extracellular signals measured by glass pipettes sucking a leech nerve. For simplicity, only one neuron and one single axon inside the pipette are shown here. δ is the axon diameter, V is the potential inside the suction pipette, V_0 the reference potential, V_A and V_B are the potentials in two points A and B along the axon; $(V-V_0)$ is then the recorded signal. R_S is the seal resistance, R_m the membrane resistance and R_a the internal axon resistance. Capacitance and inductance effects are neglected.

Let δ be the axon diameter, V the potential inside the suction pipette, V_0 the reference potential, V_A and V_B the potentials in two points A and B along the axon; $(V-V_0)$ is then the recorded signal. Suppose also that we can neglect the capacitance of the membrane and the pipette-axon seal, and we can consider only the resistive part of the impedance: in this case R_m is the transmembrane resistance, R_a the internal resistance of the axon and R_S the seal resistance (**Fig. 3.1**). If the seal is good enough, R_S remains high during the experiment and the current flows mostly through the membrane and the axon bulk, on the other hand, if R_S is low, V approaches V_0 and the electrode will record low amplitude signals. For our purpose assume that $R_S >> R_m$ and $R_S >> R_a$. R_m depends on the membrane area, namely on the diameter, while R_a

depends on the section area, namely on the square of the diameter. All the variables depend on the time t . Calling $\alpha(t)$ and $\beta(t)$ two quantities independent on δ ,

$R_a \cong \frac{\alpha}{\delta}$ and $R_m \cong \frac{\beta}{\delta^2}$. The recorded signal is then:

$$V-V_0 = (V-V_B) + (V_B-V_A) + (V_A-V_0) \cong (\frac{\alpha}{\delta} + 2\frac{\beta}{\delta^2})I \xrightarrow[\delta\to\infty]{} \frac{\alpha}{\delta} I = I R_m \cong (V_A-V_0)$$

that is, for δ large the recorded potential drops mainly across the membrane because the axon internal resistance becomes negligible compared to the membrane resistance. Besides, the current is $I \cong (V_A-V_B)/ R_m = \frac{\delta^2}{\beta} (V_A-V_B)$ which implies that the recorded potential equals:

$$V-V_0 \cong 2 (\frac{\alpha}{\delta} + 2\frac{\beta}{\delta^2}) \frac{\delta^2}{\beta} (V_A-V_B) = 2(\frac{\alpha}{\beta}\delta + 2) (V_A-V_B)$$

This result is valid at any time t . V_A and V_B are not function of δ because they are intracellular potentials which depend mainly on the active and passive properties of membrane ionic channels and not on the geometry of the system, as a consequence we can conclude that the measured potential $(V-V_0)$ increases with the axon diameter δ .

3.3 Techniques for parallel recordings from the leech ganglion

There are different techniques that can be used to record electrical signals in parallel or to derive information about functional associations between neurons. All the extracellular recording techniques share the common feature that they cannot measure the absolute amplitude of action potentials, because there is no linear correspondence between the

detected signal and the real membrane potential. Each experimental method shows different limitations and advantages.

One of the main techniques is the application of fluorescent dies and the following detection of emitted optical signals by photodiodes arrays and CCD cameras (Tsau et al., 1994; Canepari et al., 1996; Cacciatore et al., 1999). This method is suitable for following extracellularly the parallel time course of a large amount of cells with a good spatial resolution and no physical damage to the network, except for the toxicity of the dyes, but it shows low temporal resolution and it is very sensitive to mechanical artifacts, which is a problem in the leech: the leech ganglion is surrounded by muscle fibers, which very often contract when the nervous system is excited. Mechanical artifacts are usually not a problem with suction pipettes, which leave the ganglion free to move within a wide range. CCDs are specially suitable to study circuit interneurons, the overwhelming majority of them being not accessible from the lateral roots and the connectives; previously unknown neurons involved in specific behaviours could be found in optical recordings (Cacciatore et al., 1999).

Arrays such as fakir beds or planar extracellular electrodes present a high temporal resolution, typical feature of electrophysiological techniques, but a spatial resolution worse than video recordings. They are very useful for neurons in culture grown directly on the electrodes (Pinato et al., 1999), where they show a very high signal to noise ratio, and to map processes of isolated single neurons (Wilson et al., 1994; Breckenridge et al., 1995), but they are hard to apply to the intact leech CNS: the ganglion should be accurately desheathed in order to enable the electric contact between the matrix of electrodes and the cells, letting the cells almost free to move away from their original location, which would mean loosing further spatial information.

A reduced parallel recording methods is obtained associating one or two standard intracellular recordings with a further microelectrode or a tension transducer to detect the

muscle activation in a semi-intact preparation (Stuart, 1970). Invaluable advantages are the precise measure of the membrane potential and the possibility to recognize a motoneuron on the basis of its direct action on muscles. Unfortunately there is a limited spatial sampling of the neurons belonging to the network, not more than two in parallel, the stability of recordings is low and there can be consistent damage when impaling or patching the cells.

An additional method must be cited here, because it can be integrated with all the others: less invasive than sharp intracellular electrodes and fakir beds, antibodies against specific peptides (Zipser & McKay, 1981; Norris & Calabrese, 1987) offer the advantage to verify at first which neurotransmitters are contained and where in the CNS, and as a second step allows to find groups of neurons associated in sub-networks, which can then be studied with standard electrophysiological techniques (Norris & Calabrese, 1987).

A preparation with leech nerves inserted into extracellular suction pipettes provides a high mechanical stability and long duration of electrophysiological recordings, compared to intracellular electrodes; this allows to collect large amounts of data and to have a good statistical sampling. The technique is relatively low cost and easy to implement, though it requires some care in home manufacturing the glass pipettes. Tens of neurons per ganglion can be detected in parallel with this technique: on fine roots most of the detected signals are motoneurons, with the exceptions of Anterior Pagoda (AP), Retzius and mechanosensory cells; only interneurons and mechanosensory cells run in the connectives, as far as it is known, but the largest and the only one clearly detectable signal belongs to the S cell. As a consequence, recordings from arbitrary interneurons are generally not available by suction pipettes, but there is an absolutely non invasive access to motoneurons, with a good signal to noise ratio especially for the thinnest nerves.

3.4 Development of a procedure to identify extracellular action potentials

3.4.1 Introduction

A technique was developed to identify the motoneurons that produce the extracellular signals recorded sucking fine root branches of the leech ganglion by glass pipettes. Thousands of axons run in the leech nerves (Wilkinson & Coggeshall, 1975), but the great majority of them conduct undetectable signals, well below the noise level, since they are too thin (see above). I will consider only the few tens of neurons whose action potentials are visible in extracellular recordings by suction pipettes: among these neurons, my work will focus on motoneurons. As a consequence, mechanosensory cells and the few detectable interneurons must be distinguished from the motoneurons, of course on the basis of their signal properties.

The first phase of this work consisted of measuring, from the root branches, the mean amplitudes of extracellular action potentials of all the known motoneurons in the ganglion. This enabled me to obtain approximate relations between the amplitudes of all motoneuron signals, and also to update the information, previously known from the literature, about the neuronal branching, using electrophysiology. This phase was integrated by an accurate screening of the literature, to investigate in detail all the identified axonal projections of cells in the ganglion, in order to know in which root branches the signals corresponding to the different neurons might be detected, and how large signal amplitudes should be expected.

The second phase of this work concerned the tuning of a general procedure to characterize and identify the firing of motoneurons from extracellular recordings of evoked activity.

3.4.2 Classification of extracellular signals produced by known leech motoneurons

All the motoneurons in the leech CNS were impaled in order to measure the mean amplitude of their extracellular action potentials. I performed my experiments recording from the following root branches of the ganglion, designated according to (Ort et al., 1974): AA1, MA1, PP1, DP1, DP:B1, DP:B2. AA1 and MA1 are the first bifurcations of the anterior root, PP1 and DP1 are the first bifurcations of the posterior root, DP:B1 and DP:B2 are the first bifurcations of DP1 nerve (**Fig. 3.2**). The usual names for AA1, MA1, PP1 and DP1 nerves are respectively AA, MA, PP, DP.

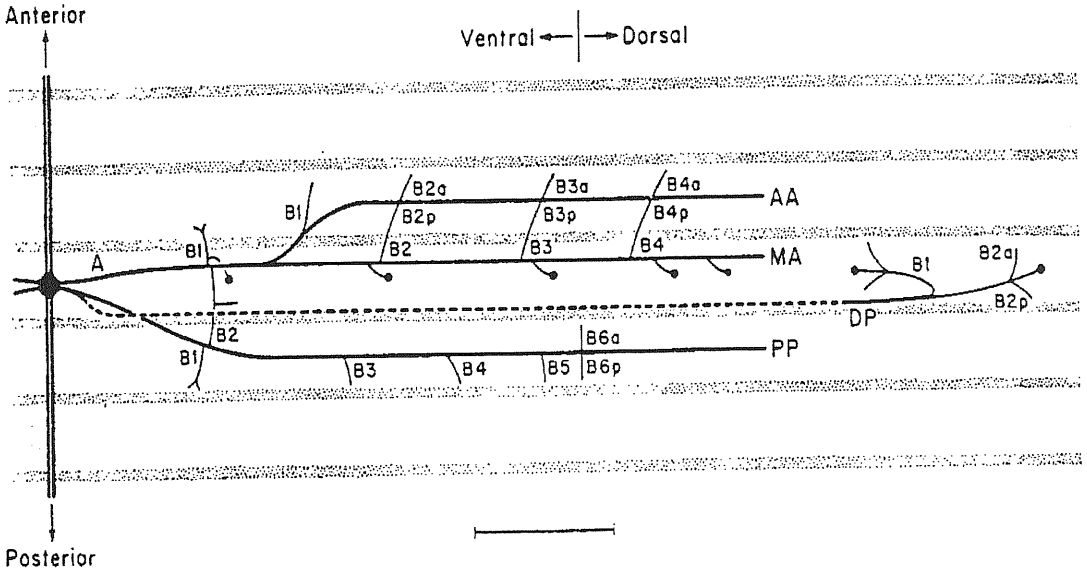

Fig. 3.2. The main trunks and major branches of the nerves of the right side in a midbody leech ganglion. Horizontal bands indicate the borders of the five annuli comprising the segment. The ganglion and its paired connectives are at the left edge of the drawing. One anterior (A) and one posterior root emerge from each side of the ganglion. The anterior root bifurcates into an anterior (AA) and a medial (MA) nerve, and the posterior root bifurcates into a posterior (PP) and dorsal (DP) nerve. The dashed portion of the DP nerve is above the plane of the drawing and actually much shorter in length than drawn here. The method of designating nerve segments and branches is described in (Ort et al., 1974). The dark spots at intervals along the middle of the central annulus indicate the location of sensillae on the body wall. *(From: Ort et al., 1974).*

In the connectives there are projections of the central mechanosensory cells (T, P, N), as far as we know only one motoneuron, the L cell (Norris & Calabrese, 1987), and mostly interneurons, including the S cell. The lateral roots contain projections from mechanosensory cells (T, P, N), all the motoneurons, and from peripheral neurons.

Interneurons and mechanosensory neurons produce clearly recognizable signals. Among the interneurons running in the connectives, the largest and the only two clearly identifiable signals belongs to the S cell and a still unidentified interneuron involved in shortening with an even larger action potential (Shaw & Kristan, 1999). AP and Retzius neurons produce extracellular signals visible from the root branches by suction pipettes. The AP cell project in many root branches, sharing this properties with the L and AE motoneurons, but can be distinguished because of the smaller signal amplitude. The two Retzius cells in each ganglion are strongly electrically coupled and very often fire together with a very small delay between them mutually reexciting one another, therefore their twin signals can be easily tagged. T and P mechanosensory cells produce large and easily recognizable signals on the roots ipsilaterally to their locations, while signals from N cells are small but they fire rarely and have a high threshold. All central mechanosensors fire only in response to direct intracellular depolarization or mechanical stimuli on the corresponding or neighbouring segments, therefore their extracellular signals can be easily recognized. All the previous features enabled me to easily isolate from the recordings the contribution of mechanosensory cells and interneurons.

The ideal method to identify the neurons whose action potentials generate the signals, would be a template matching between the signal shapes recorded during the experimental trials and those obtained during a complete survey of all motoneurons by intracellular stimulation. Unfortunately different experimental problems arise that need to find alternative and more general criteria. First of all, spike templates valid for every

preparation do not exist, the template matching can be accomplished only in preparations where identified neurons are also impaled intracellularly; secondly a perfect template matching is compromised by the variability of the signal shape, including a gradual decline of the amplitude with time. Moreover it is not usually possible to impale intracellularly all the motoneurons, because some of them are not visible or can be damaged during this operation becoming silent.

Action potentials were evoked in each motoneuron with an intracellular microelectrode by passing a depolarizing current pulse or by the injury discharge caused by cell penetration. With this procedure it was possible to obtain a clear signature of extracellular voltage signals evoked by action potentials of many motoneurons (**Fig. 3.3**). All motoneurons project into the contralateral nerves, except cells 4, which project ipsilaterally into the PP nerve (see **Table 3.2**). Therefore to monitor the signals produced by all the motoneurons located on one side of the ganglion, it is necessary to suck DP:B1, DP:B2, MA, AA, PP nerves contralaterally to the motoneurons and also the ipsilateral PP nerve. There is always a propagation delay between the intracellular and the corresponding extracellular signals of a motoneuron. The delay is variable from cell to cell; each motoneuron shows, in each preparation, a typical range of values, which depends on the site of spike generation (Melinek & Muller, 1996) and amounts to about 0.3-10 ms.

For example an action potential in motoneuron L is associated with large extracellular voltage signals on both the DP:B1 and DP:B2 nerves, but often on PP, AA, MA too, since it projects in all these root branches (**Fig. 3.4**). An action potential of motoneuron 3 causes one large extracellular signal on the DP:B2 nerve, but occasionally also a smaller signal on the DP:B1 (Shaw and Kristan, 1995; Ort et al., 1974). An action potential of motoneuron 109 is associated with a large extracellular voltage signal on the MA nerve with a much smaller signal on the AA nerve (**Fig. 3.4**) (Ort et al., 1974; Baader, 1997).

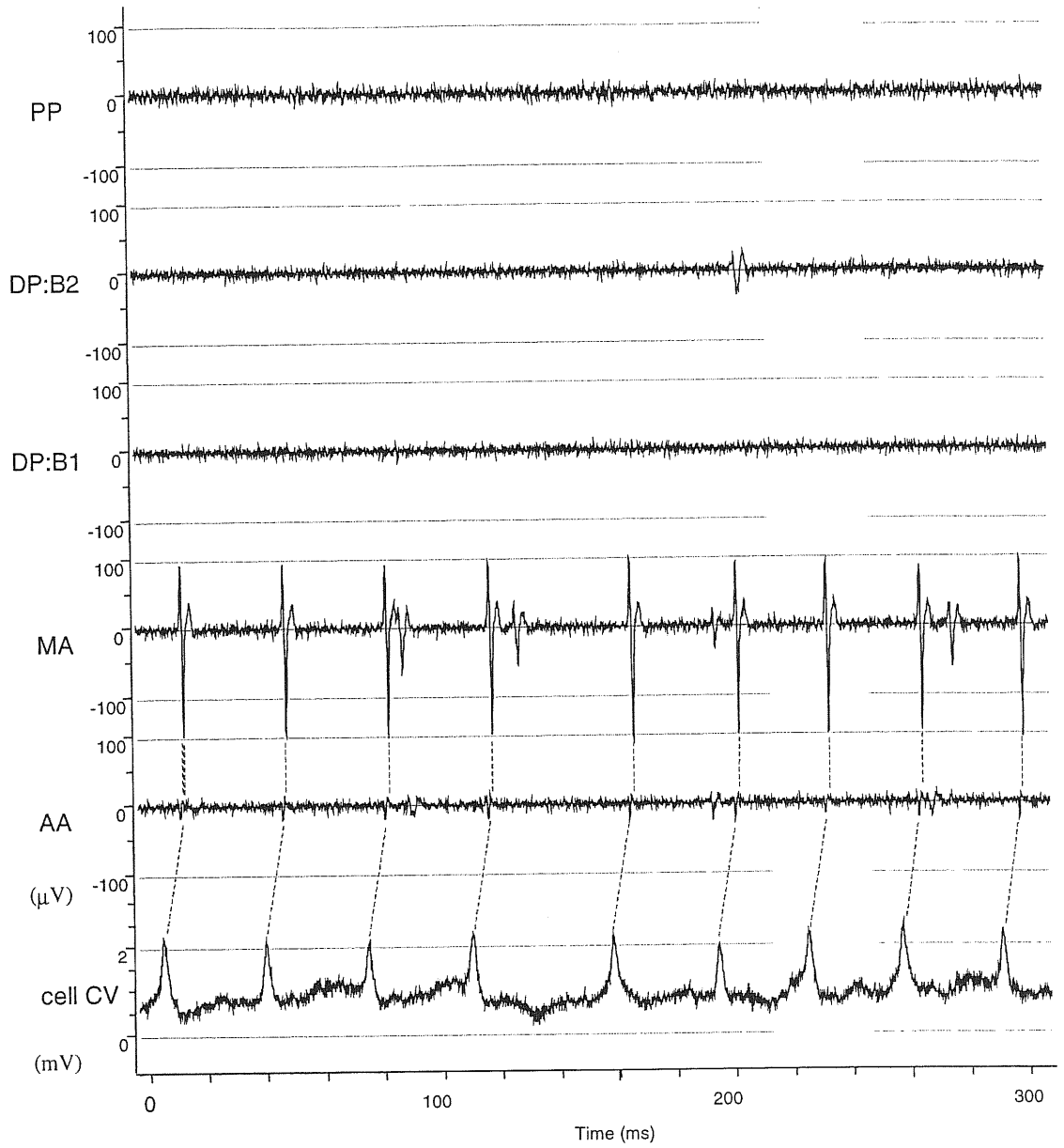

Fig. 3.3. Injury discharge activity of a C.V. motoneuron. The five main root branches of the ganglion, contralateral to the C.V. cell, are recorded extracellularly: PP, DP:B1, DP:B2, MA, AA (first upper traces from top). The bottom trace is the intracellular recording, where somatic activation potentials are clearly visible; the corresponding extracellular signals are slightly delayed and visible on MA (large) and AA (small) nerves.

The firing of motoneurons 107 and 108 can be recognized by large voltage signals on the AA nerve (Ort et al., 1974; Baader, 1997). Assignment of the largest extracellular voltage signal on the AA nerve to motoneurons 107 or 108 (**Fig. 3.4**) was achieved by intracellular recording. Action potentials from motoneurons 4, 5 and 8 were identified in

extracellular recordings from the PP nerves (Ort et al., 1974). Action potentials of motoneuron 8 always had the largest extracellular voltage signals, followed by motoneurons 5 and 4.

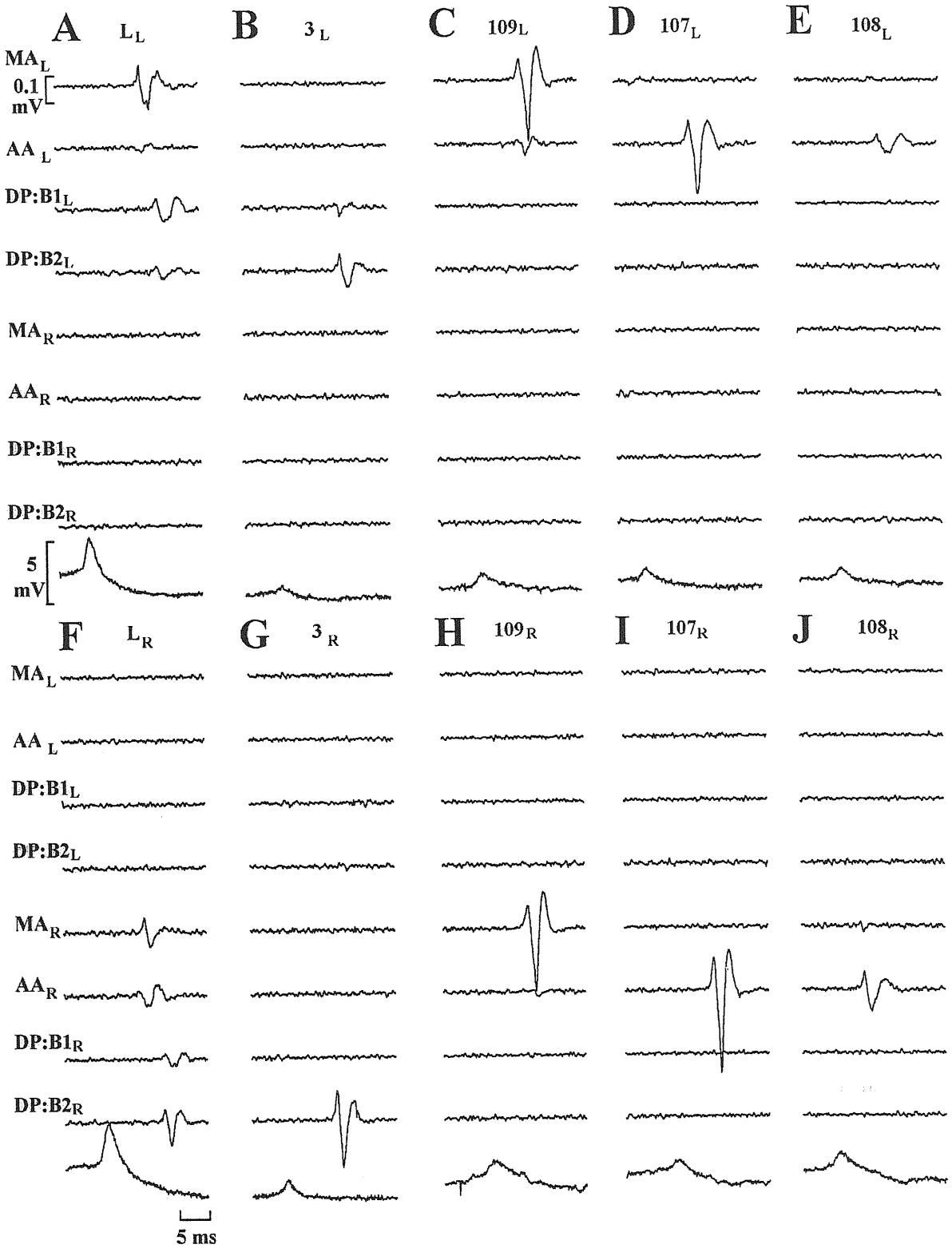

Fig. 3.4. Motoneuron identification. Each panel shows eight extracellular recordings (eight upper traces) and one intracellular recording (bottom trace). Extracellular recordings from the medial anterior (MA), anterior anterior (AA), the B1 branch of the dorsal posterior (DP:B1), the B2 branch of the dorsal posterior (DP:B2) left (L) and right (R) nerve of the 10^{th} ganglion of a semi-intact leech preparation as that shown in **Fig 2.2A**. Intracellular recordings from the left L motoneuron (**A**), left motoneuron 3 (**B**), left motoneuron 109 (**C**), left motoneuron 107 (**D**), left motoneuron 108 (**E**), right L motoneuron (**F**), right motoneuron 3 (**G**), right motoneuron 109 (**H**), right motoneuron 107 (**I**) and right motoneuron 108 (**J**) from the same ganglion.

All these collected results were summarized for the different root branches in **Table 3.1**: it was sometimes impossible to find exact relations for all the neurons, so I enclosed in parenthesis the neurons showing usually very similar amplitudes of extracellular action potentials.

Root Branch	Amplitude relations
DP:B1	L > (AE ,3) > (6, 110)
DP:B2	3 > (L, AE) > (6, 110)
PP	8 > (5, 4) > (L, AE, 1, 2, 7, 10, 11, 12) > (6, 9, 102, 110)
MA	C.V. > 109 > (L, AE, 102) > (101, 110, 111, 119)
AA	107 > 108 > (L, 119) > (C.V., AE, 106, 109, 112)

Table 3.1. Relations between the amplitude of extracellular action potentials produced by motoneurons stimulated intracellularly, as measured by glass pipettes sucking the root branches listed on the left. Motoneurons showing usually action potentials of very similar amplitudes are enclosed in parenthesis.

Extracellular spike amplitudes varies sometimes drastically from one preparation to the other, but if preparations with a good pipette-nerve seal are selected, this variability decreases: in this condition a reliable comparison could be done among the amplitudes (parameter h2 of the spike, see 3.4.3) of identified spikes, and an approximate scale was built for each nerve. Even if the signal amplitudes decreases during the experiment, the

relations in **Table 3.1** do not change, because all the amplitudes decline in time by the same amount.

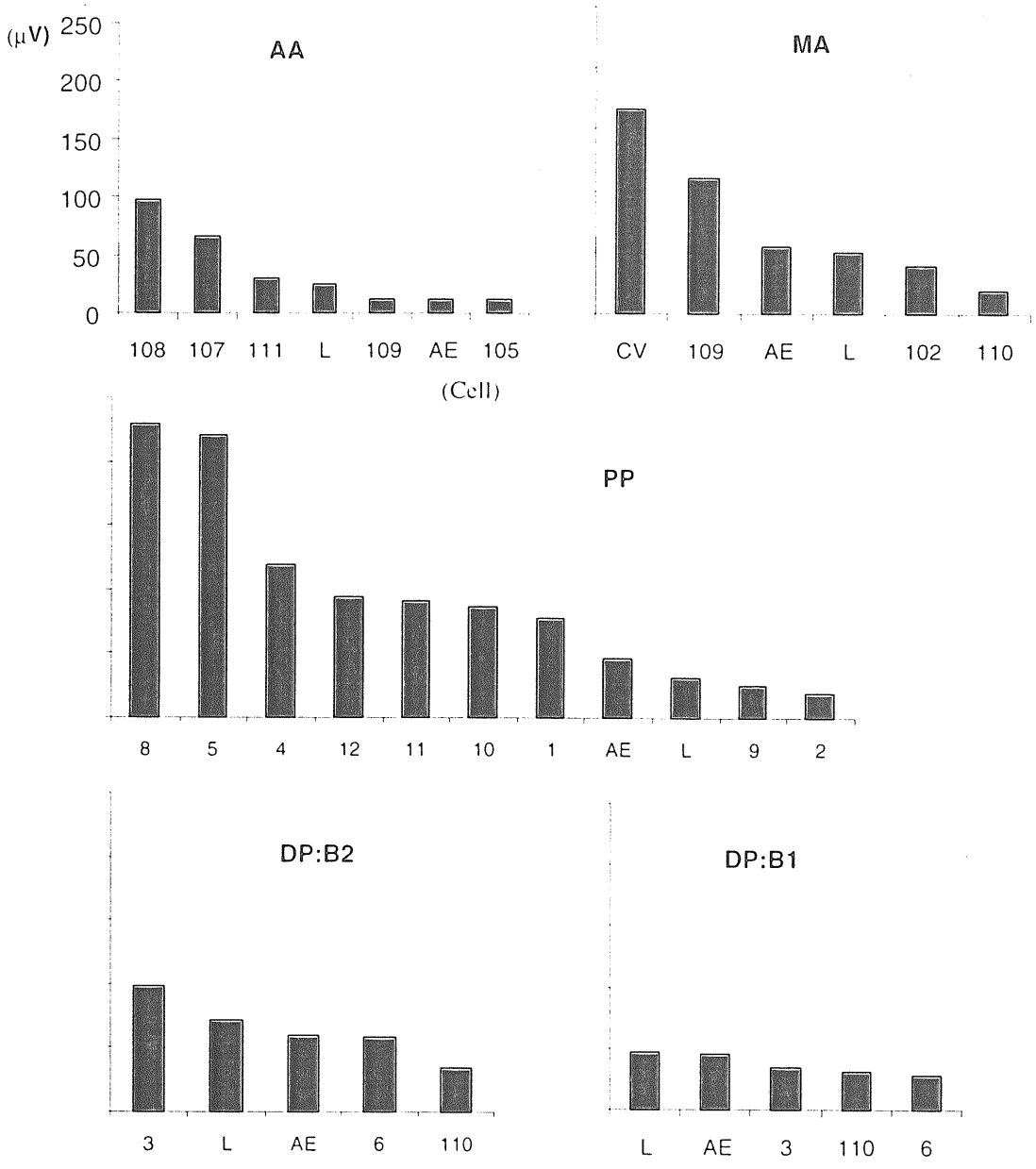

Fig. 3.5. Amplitude of action potentials. Absolute amplitude of extracellular signals of many motoneurons on the five main root branches: AA, MA, PP, DP:B1, DP:B2. Data are averaged over one single experiment; they are obtained from recordings similar to those shown in **Fig. 3.3**. These examples are in agreement with **Table 3.2**.

These relations were used as the first tool to interpret any arbitrary recording, but were always integrated with further information, especially template matching with extracellular

action potentials obtained stimulating intracellularly some identified neurons, whenever this was possible. Examples of typical amplitudes histograms from various experiments and for the different root branches are shown in **Fig. 3.5**. It is clear that a discrimination based on the spike amplitude is maximally reliable among the largest signals.

When impaling motoneurons, care was taken to correctly designate them on the basis of their position in the ganglion from a visual inspection (see **Fig. 1.4A** and **B**) and on the basis of information on axonal projections and mean spike size from the literature (Stuart, 1970; Ort et al., 1974; Muller et al., 1981; Norris & Calabrese, 1987; Baader, 1997). The locations of neuron somas can differ slightly from one ganglion to the other, very often neighbouring cells exchange their positions, therefore multiple comparisons between potentially recognized neurons can help to correct a wrong visual identification.

Alternative information, and an integration of **Table 3.1**, was provided by monitoring exactly all the projections of motoneurons along the analyzed root branches and comparing my experimental data with the literature. **Table 3.2** is a rough classification of what should be expected from signals recorded by pipettes with a tight seal. The condition of a high impedance seal should be considered as the standard level for a classification based on the spike amplitude. To obtain this table I chose four ranges of absolute amplitudes, classified as large (L/l), medium (M/m), small (S/s), following (Ort et al., 1974), except the very large ones, classified as enormous (E): due to the variability of extracellular signals a more precise classification would have been unuseful. Some cells were previously identified as motoneurons with precise muscle target, but no information was available about their precise branching in the roots. I added the mean results of my experiments (capital letters in **Table 3.2**) to the information derived from previous reports (lower case letters in **Table 3.2**). This map of axonal projections in the main root branches may be used to discriminate between neurons with similar signal shape but different projections. The DP:B1 and DP:B2 nerves contain the lowest number of projections, therefore the identification of

extracellular signals is very easy, at least for cells 3, L, AE, the last two also signalling in all the other branches. On the other hand the PP nerve contains the highest number of motoneurons projections, from all the motoneurons in the posterior glial packet (see Chapter 1) except cell 3, and from some neurons in the anterior packet, such as cells 102, 108, 109, 110: the identification is more difficult than in the previous case, at least for the smallest spikes.

Neuron	DP1	DP:B1	DP:B2	PP1	MA	AA	Function of motoneuron	Original references
1				s , M			dorsal longitudinal inhibitor	1, 2
2				s , M			ventral longitudinal inhibitor	1, 2
3	l	S	l , E				dorsomedial longitudinal excitor	2
4*				m , L			ventromedial longitudinal excitor	2
5				l , L			dorsal longitudinal excitor	1, 2
6		S	S	S			dorsal longitudinal excitor	6
7				m , M			ventral longitudinal inhibitor	2, 6
8				l , E			ventral longitudinal excitor	1, 2
9				S			ventral and dorsal longitudinal inhibitor	6
10	s			M			unknown	2
11				M			ventral circular excitor	1, 2
12				M			ventrolateral circular excitor	1, 2
17	-	-	-	-	-	-	dorsolateral longitudinal excitor	5
101					S		dorsoventral longitudinal inhibitor	1, 2
102				[s**] , S	M	s	dorsal longitudinal inhibitor	2
106						S	lateral longitudinal excitor	1, 2
107						l , E	dorsomedial longitudinal excitor	1, 2
108				[l*]		m , M	ventromedial longitudinal excitor	1, 2
109				[m/s**]	l , L	S	lateral dorsoventral excitor	1, 2, 6
110		S	S	S	S		oblique excitor	1, 2
111					S		oblique excitor	1, 2
112						S	dorsal circular excitor	1, 2
117*	-	-	-	-	-	-	medial dorsoventral excitor	5
119					S	M	ventral longitudinal inhibitor	3, 4
L	l , M	l , L	s , S	s , M	s , M	s , M	ventral and dorsal longitudinal excitor	1, 2
152***	-	-	-	-	-	-	dorsolateral circular excitor	7
166***					m		ventrolateral circular inhibitor	7
CV					l , E	S	ventrolateral circular excitor	1, 7
AE	M	L	L	M	M	S	subcutaneous excitor	1
HE	-	-	-	-	-	-	lateral heart tubes excitor	5

Table 3.2. Approximate amplitude of extracellular action potentials, produced by identified motoneurons (left column) excited intracellularly. Column 7 provides a brief functional description of each motoneuron. Columns 2-6 contain the spike amplitudes: spikes were classified as large (L/l), medium (M/m), small (S/s), following (Ort et al., 1974), except the very large ones, classified as enormous (E). The mean results of my experiments are in capital letters (E/L/M/S) and are added to the information derived from the listed reports (lower case letters, l/m/s). Spikes were recorded by glass pipettes sucking the following root branches: medial anterior (MA), anterior anterior (AA), the entire dorsal posterior (DP1), the B1 branch of the dorsal posterior (DP:B1), the B2 branch of the dorsal posterior (DP:B2), the posterior posterior (PP). All nerves are contralateral to the neurons, except for cells 4 and 117. In the last column the original references are listed. The references are the following: 1) Stuart, 1970; 2) Ort et al., 1974; 3) Sawada et al., 1976; 4) Stent et al., 1978; 5) Muller et al., 1981; 6) Norris & Calabrese, 1987; 7) Baader, 1997. Footnotes: (*) = ipsilateral projections; (**) = in PP fine branches PP:B1 and PP:B2; (***) = candidate motoneurons, not fully verified.

The anterior MA and AA nerves contain also a large number of axons originating from neurons in the anterior packet. Signals produced by the same neurons but appearing in parallel (with some delay) on different nerves are called "twins" and can be detected by a dedicated software developed in our laboratory (see below).

3.4.3 Analysis of arbitrary extracellular recordings: clustering and neuron labelling

When this survey of projections and signal amplitudes of all motoneurons was completed, enough preliminary information was available to start the second phase of this part of my work (see above): the development of a general procedure to analyze extracellular recorded activity of motoneurons during evoked behaviours, like shortening and bending. Comparing these recordings with those obtained impaling motoneurons, I assessed that every recorded event is actually a single action potential and not a summation of several signals: the recorded traces are therefore sequences of unitary action potentials.

A preliminary visual inspection of recorded traces was always the first step of the analysis, in order to evaluate how many different neuron shapes were clearly distinguishable on each channel. In the example shown here (**Fig. 3.6**) three main units are visible, each one with a different shape and peak amplitude.

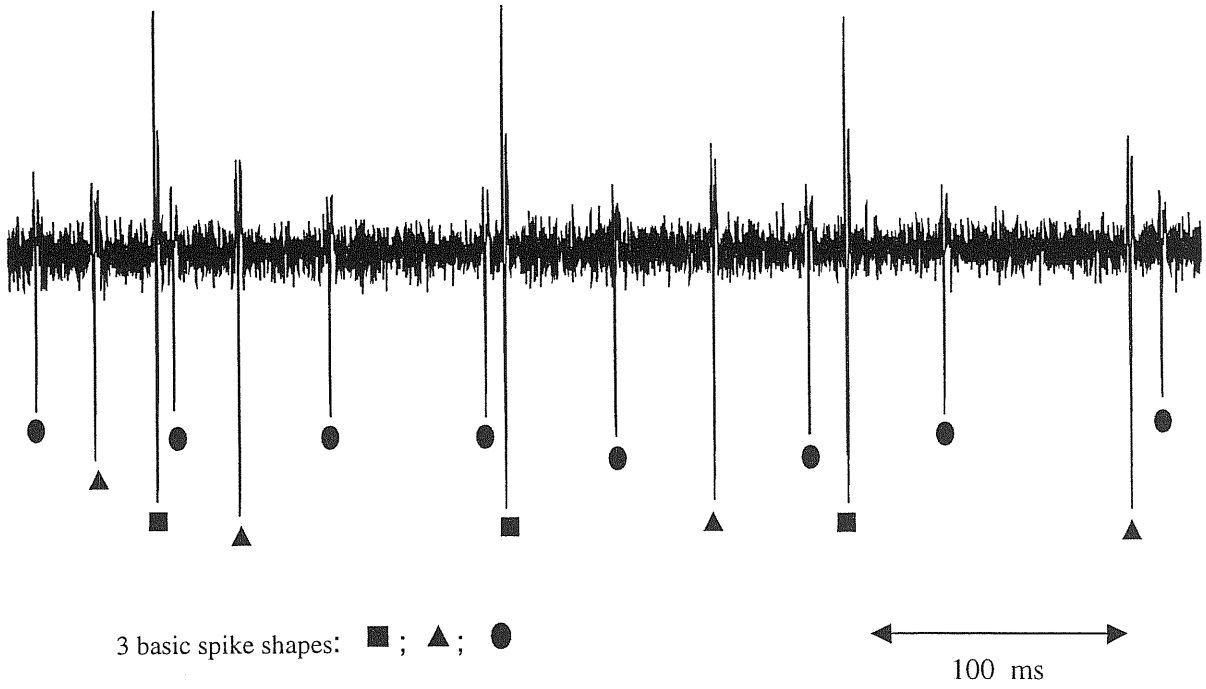

Fig. 3.6. Example of preliminary visual inspection on extracellular traces. Three spike shapes can be recognized as clearly different. A further analysis is necessary to verify that the three units correspond to three separate neurons.

The key assumption, on which the validity of spike clustering is based, is that every neuron generates an action potential with a peculiar extracellular shape, and this shape remains fairly constant during all the experiment, though being different in each preparation. The aim of the clustering procedure is to separate all the extracellular signals into groups (clusters) each one belonging to only one neuron. A dedicated software was developed entirely in our laboratory, in order to perform the entire data analysis: display of raw data, spike extraction and clustering, first and second order statistics on the activity of identified neurons (see Chapter 2).

After the visual inspection of digitized traces, the following step is the extraction of all events crossing a threshold, that can be set manually or semi-manually above to the noise level (red line in **Fig. 3.7A**). The threshold was usually set as 4 times the standard deviation of the background noise, in such a way that all the real events, but the noise fluctuations, could be detected. All the peaks of detected events are defined as the times of occurrence of pulses, a fixed range of samples around each peak are extracted and all these small intervals are considered to be the extracellular action potentials.

The typical spike shape is divided into three phases, each one described by two geometrical parameters (**Fig. 3.7B**), the amplitude h and the integral I: the six parameters h1, I1, h2, I2, h3, I3, the time T and the width W are used to obtain 28 two-dimensional plots of the detected spikes in the parameters space considering all the possible combinations, such as (h1, h2), (h2, I2), (h3, T) and so on. The parameters are used to separate the signals on the basis of their shape: as a general rule, if sets of points appear in one plot the corresponding spike shapes have some similarity and might belong to the same cell; if the same spikes cluster in all the diagrams, the shapes are very similar and the probability that they are originated by the same neuron is very high. The software allows to chose 4 plots out of 28 where the clouds of points are more evident: potential clusters belonging each one to a different neuron can then be drawn manually (**Fig. 3.7C**). The spikes belonging to each cluster are plotted superimposed (**Fig. 3.7D**) to compare their shapes.

Histograms of parameters (h1, I1, h2, I2, h3, I3, T, W) and Average Firing Rate (AFR) plots are also available as an additional tool to discriminate between very similar clusters. For example, a typical doubtful case often occurs if a long time interval (hours) elapses between two recordings from the same preparation by the same suction electrodes: the mean amplitude of signals may decrease (see above) and two separate clusters may appear.

In this case AFR histograms of the two preliminarily identified neurons will identically show that the two clusters are collections of signals of the same cell.

This clustering procedure can be performed only channel by channel but, as shown before, several neurons project in different root branches (see **Table 3.2**) giving visible twin signals in multiple channels (see Chapter 2). The delay between corresponding twin signals falls in the range 0.5-10 ms.

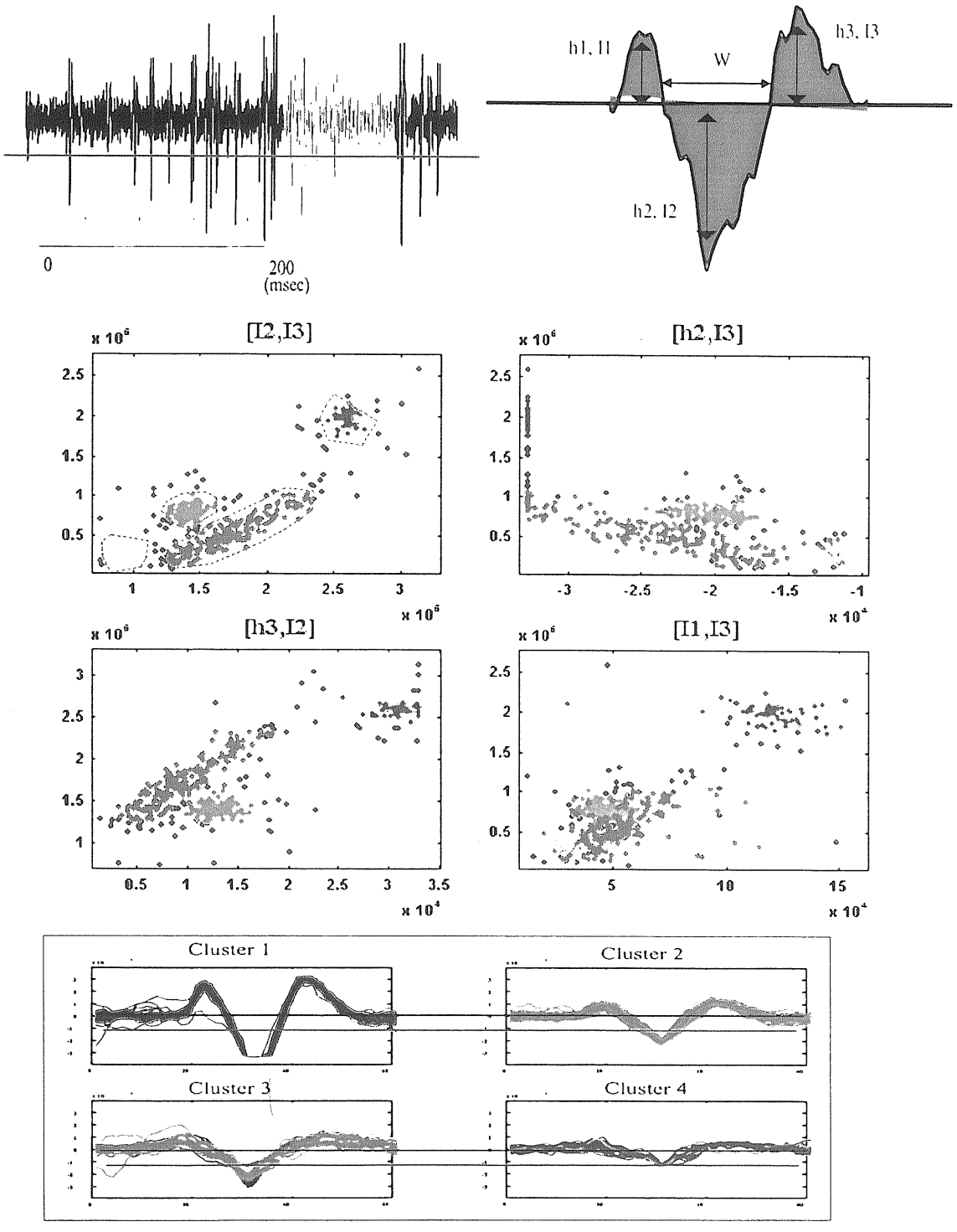

Fig. 3.7. Clustering procedure. (**A**): All events which overcome a threshold (red line) are extracted from raw extracellular recordings. (**B**): Typical shape of one extracellular action potential recorded from a suction pipette. All detected events have a similar shape, which can be divided into three phases, each one characterized by the geometrical parameters amplitude h and integral I. W represents the time duration of phase 2. The parameter h2 is the spike amplitude. (**C**): Spikes are plotted in the parameters space. Four diagrams are chosen, out of all the possible combinations of two parameters, where the spikes appear divided into small clouds of dots. Cluster outlines are drawn manually on a selected plot. If the dots appear to cluster also in the other plots, as it is the case shown here, they may correspond to different neurons. (**D**): Clustered spikes are plotted superimposed; the black line is the zero amplitude, while the red line is the original threshold.

Though the twins produced by the same neuron show fairly constant delays between them, they are sometimes difficult to find out by visual inspection, but they can be detected if the occurrence times of spikes belonging to clusters in different channels are all compared. Given couples of clusters on separate channels, our dedicated software performs an automatic screening to detect and extract all the twin signals (see Chapter 2) and associate them to the same neuron. This is a necessary step to avoid computing a wrong second order statistical analysis between identical neurons as if they were distinct cells. The twin-detecting software requires an approximate value for the mean delay and standard deviation between the twin spikes (**Fig. 3.8A**) belonging to separate channels, thus all the couples of signals falling inside the chosen time window can be labelled.

The times of occurrence of the labelled spikes in the first cluster are plotted versus the times of occurrence of the labelled spikes in the second cluster: if most of the original spikes are selected and lie on a straight line, it means that they are perfectly timed (**Fig. 3.8B**) therefore they are twins; on the contrary, if only few spikes out of the total amount are detected as twins and they are spread over the plane, they can be discarded (**Fig. 3.8C**).

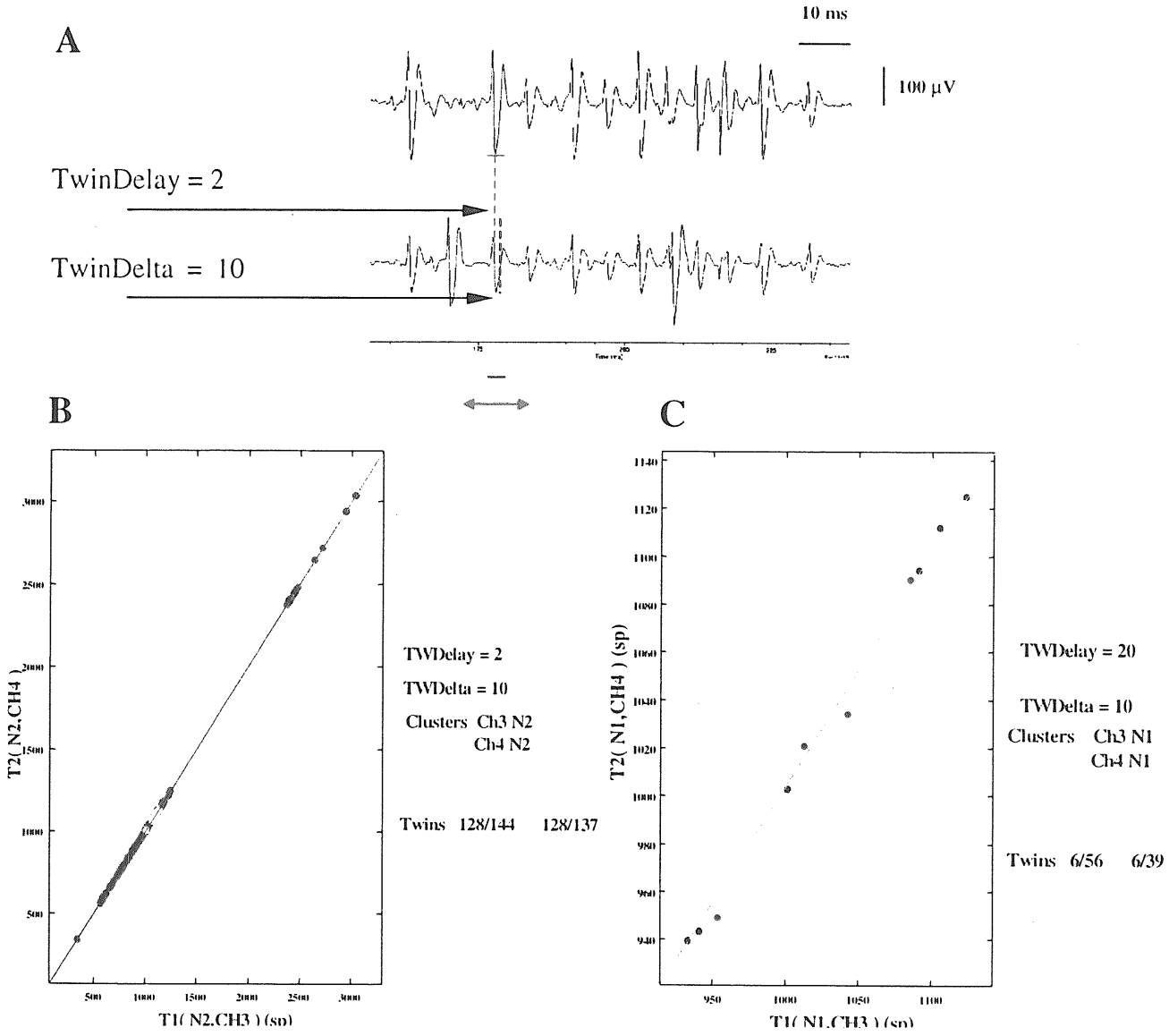

Fig. 3.8. Twin signals detection. Some neurons project in different nerves and therefore signal on different recorded channels: the result may be that there are two clusters produced by the same cell on separate channels. (A): From visual inspection of the parallel traces, the user can evaluate an approximate value for the delay and delay range between the corresponding spikes. All the couples of signals falling inside the chosen time window are selected. The times of occurrence of the labelled spikes in the first cluster are plot versus the times of occurrences of the labelled spikes in the second cluster. (B): When most of the spikes are automatically selected and lie on a straight line, this implies that they are perfectly timed and that they are almost certainly twins. (C): When only few couples of spikes are selected as twins and they are not aligned, either the values for delay and delta are wrong or the two clusters are not associated at all.

When completed, the clustering and the twin detection provide the firing times of all the action potentials for each motoneuron recorded extracellularly: that is required to perform any statistical analysis. In every experiment, direct template matching was always used as a validation whenever intracellular and the corresponding extracellular recordings of visually identified neurons were available. Additional information comes from the expected pattern of activation of the motoneurons following the delivered stimulus. For example, in the case of local bending, intracellular stimulation of ventral P cells should activate mostly ventral excitatory motoneurons, the reverse should happen when exciting dorsal P cells, as shown below.

3.5 An example of application of the spike identification procedure

An example of identification of motoneurons is shown in **Fig. 3.9**, where all the criteria explained before were used. The recordings show evoked activity when exciting a ventral P cell (panels **A** and **C**) and a dorsal P cell (panels **B** and **D**), both cells ipsilateral to the recorded nerves, which explains why extracellular action potentials of P cells are visible. The activity shown here can be considered a neural correlate of local bending.

When the leech is not crawling, the C.V. neuron is not active (Baader, 1997) and the largest signal on MA nerve is therefore the neuron 109 (see **Table 3.1**). Cell 107 (dorsal excitor) generates usually the largest signal on AA nerve and is rarely activated when a ventral P is stimulated, whilst cell 108 is excited, which justifies the identification. On DP:B1 and DP:B2 nerves the identification is made easier by the large amplitude of cell 3 spike and the visible twin signals of L cell on DP:B1, DP:B2 and PP nerves; L cell signals cannot be mixed up with the AE cell twin signals of smaller amplitude (see **Tables 3.1** and **3.2**). The PP nerve shows in this case the larger variety of signals: the largest belongs to

cell 8, cells 4 and 5 spike are smaller and have generally similar amplitudes (see **Table 3.1**) but cell 4, a ventral excitor, is very unlikely to be activated by a dorsal P, which on the other hand probably excites cell 5. The identification received an additional confirmation by the matching with the extracellular templates of some motoneurons impaled during the experiment.

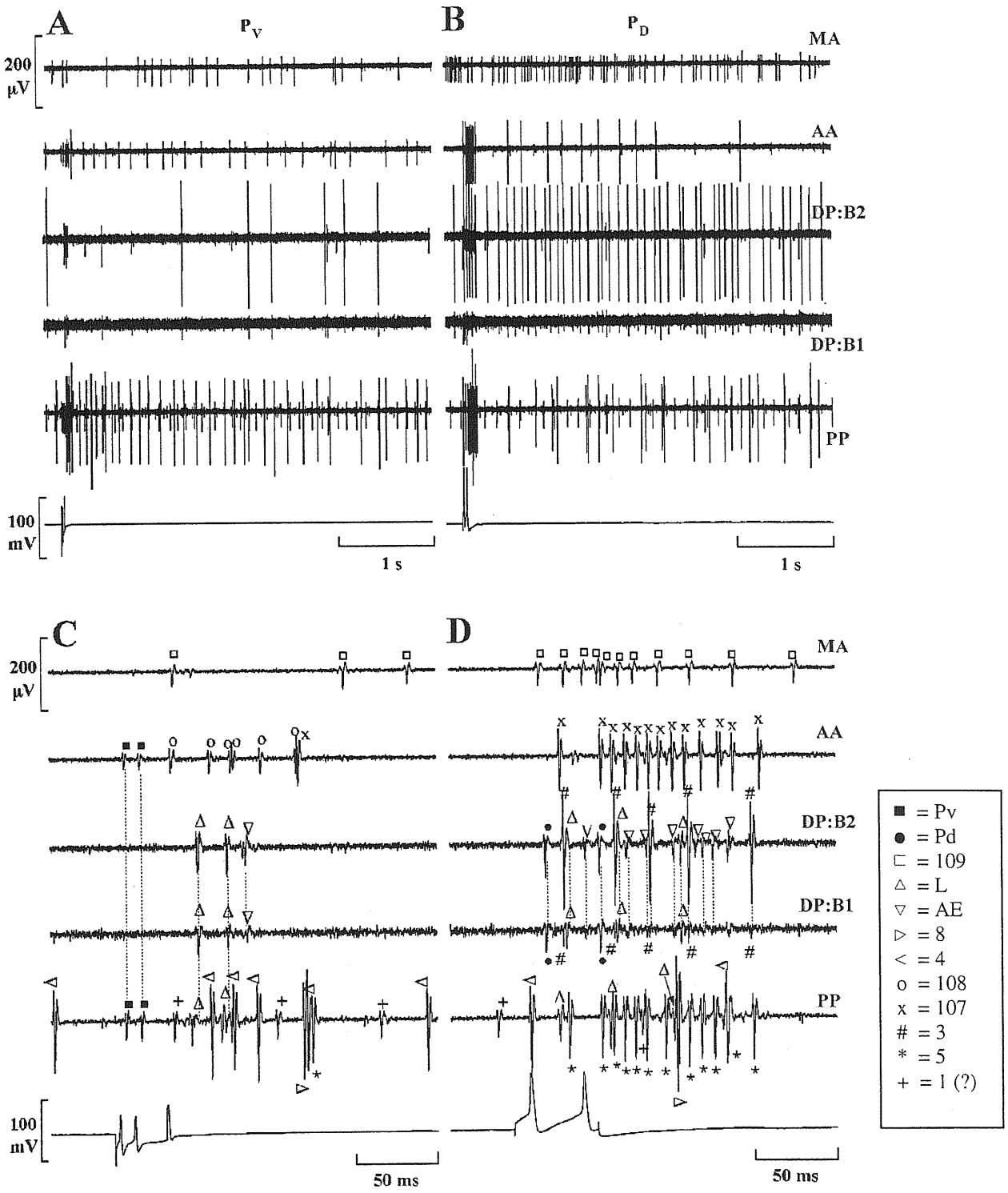

Fig. 3.9. Extracellular electrical recordings during local bending. Extracellular recordings were obtained from an isolated midbody ganglion by five suction pipettes on the medial anterior (MA) and anterior anterior (AA) nerves, the B1 branch of the dorsal posterior (DP:B1), the B2 branch of the dorsal posterior (DP:B2), the posterior posterior (PP) nerve. The stimulus was a brief current pulse delivered intracellularly to ventral P cell (left panels) or dorsal P cell (right panels), both ipsilateral to the recorded nerves; the current pulse always elicited two spikes (bottom trace in each panel). (**A**) and (**B**): Recordings at low sweep speed, spikes of different amplitudes are clearly visible. (**C**) and (**D**): Recordings at higher sweep speed with identified neurons, labeled as described in this Chapter. The labeling legend is on the bottom right. The identification of spikes labelled as (+) in not certain.

3.6 Discussion

In this chapter I showed that in the leech CNS it is possible to label extracellular action potentials recorded by pipettes sucking nerve branches, as produced by specific motoneurons and interneurons. The identification is based on the shape of action potentials. Due to the limited variety of large signals visible from ganglion roots, correct identification can be often achieved with a small error. Most of the axons in the roots arise from the peripheral nervous system and are unable to generate action potentials, such as the stretch receptor (see 1.4), or conduct undetectable signals. Other techniques are required to record the activity of interneurons, such as voltage sensitive dyes or intracellular electrodes (see 3.3).

The absolute amplitudes of signals originated by the same neuron in different experiments are generally not comparable, because they depend heavily on some experimental variables, both biological and instrumental. Extracellular spike shapes are only marginally influenced by stimulation artifacts and electronic noise, on the contrary the baseline noise is originated by the ionic currents in the Ringer solution: the noise amplitude decreases when the pipette diameter increases, as a consequence of the smaller impedance.

Axon diameter is one of the main factors determining the spike amplitude: almost three thousands axons run in each one of the two paired connectives and slightly less in the anterior and posterior roots, the large majority (98%) of them are less than 1 μm in diameter (Wilkinson & Coggeshall, 1975). As a consequence very few neurons exhibit large signals; the overwhelming majority of them are too small to be detected extracellularly, well below the baseline noise level. A confirmation may be the fact that when the signals are extracted from the recordings, the total number of smallest visible spikes amount to tens of times the number of the largest. Another major factor shaping the signal amplitude is the pipette-nerve seal impedance, since the nerves diameter is sometimes different from ganglion to ganglion, especially for the thinnest branches whose dimensions can vary as much as 100%; in these cases the seal depends on the availability of appropriate size pipettes.

The shape of extracellular action potentials is both time and space dependent. As time passes, the pipette-nerve seal resistance generally decreases and the ionic concentrations inside the pipette changes because there is no refresh. Non-stationarity of recorded signals can be taken into account when designing clustering algorithms, with the assumption that the rate of change is a continuous function of time (Snider & Bonds, 1998). The shape may depend also on previous neuronal activity (Quirk & Wilson, 1999), particularly during high frequency discharges, and on action potential initiation site (Melinek & Muller, 1996), since currents are differently modulated at soma, axons and dendrites (Lopez-Aguado et al., 2000; Varona et al., 2000).

Sometimes, when action potentials are evoked intracellularly in some neurons and there are no extracellular spikes visible from nerves, where they are supposed to be according to their arborization, the reasons may be: a conduction block (Yau, 1976b; Gu, 1991; Mar & Drapeau, 1996) or too small an amplitude to be detected, since it is unlikely that the pulse is not propagating along the axon. Therefore extracellular action potentials,

usually visible, produced by some neurons may be missing from recordings though being activated.

I chose to record from fine branches of the roots and not from the roots themselves, since there are some experimental advantages. As less axons are contained in thinner nerves, there is a smaller variety of distinct signals to be separated by spike clustering. We observed that the signal-to-noise ratio is usually better and signals are larger when nerves are thin, probably because the thinner the pipette the higher the seal resistance. Intracellular recordings show that different neurons may have very similar amplitude and shape, which makes sometimes impossible to separate their clusters; therefore a large signal-to-noise ratio is always advisable in order to discriminate and refine clusters which appear very close in the parameter space.

The chance to make mistakes on the identification remains when spike amplitudes are too small, close to the noise level, because the spike shapes are very similar, thus rendering difficult the separation of signals with different neuronal origin, except those with twins in other channels, which can be easily isolated through software analysis. In this case an help in identification comes from the knowledge of the anatomical projections of some particular neurons, which can be further distinguished taking into account the presence of twin signals on specific root branches: for example cell 3 projects in branches B1 and B2 of the DP nerve but never into PP nerve, on the other hand cells 8, 5, 4 project in PP but never in DP nerve, and so on (see **Table 3.2**). At this level recording directly from the main trunk of anterior or posterior root would result only in a large amount of smaller signals with no further spatial information on the axonal branching.

I focused my work on the identification of signals originating from motoneurons, because they produce the largest extracellular signals recordable from the roots, together with the T and P mechanosensory cells and the Retzius and AP neurons. Besides

motoneurons are activated all along the chain of ganglia during evoked behaviours such as whole-body shortening or swimming.

The recording procedure by pipettes sucking root branches is non-invasive for the network connectivity in the CNS, which remains intact during all the experiment. This means that the neural computation is partially altered only in its sensory feedback part, since the sensory terminals of cells in the recorded ganglion are removed.

The long duration of these recordings allows a good statistical analysis. Therefore, starting from multi-channel extracellular recordings, the average activity of motoneurons during specific behaviours can be analyzed in parallel, allowing an almost full access to the last step of the underlying distributed computation, the behavioural output.

Chapter 4

Whole body shortening

4.1 Introduction

The leech exhibits a limited set of repeatable behaviours: in particular, when a very strong mechanical or noxious stimulus is delivered to its head, it withdraws and rapidly shortens to escape from the potential danger (Magni and Pellegrino, 1978; Kristan and Nusbaum, 1982; Wittemberg and Kristan, 1992a & 1992b; Shaw and Kristan, 1995 & 1997 & 1999). The shortening reaction causes the simultaneous contraction of all or most of its body, involving the entire CNS. The shortening reaction is mediated by the simultaneous activation of excitatory motoneurons innervating longitudinal muscles. Several motoneurons involved in whole-body shortening have been identified, including the dorsal excitatory motoneuron 3 and the ventral excitatory motoneurons 4 and 108 that supply restricted groups of longitudinal muscle fibers and the longitudinal motoneuron L which supplies all of them. These motoneurons are activated through the S cell network and other parallel interneuronal pathways running through the connective fibers (Shaw and Kristan, 1999). The S cell network consists of a chain of electrically coupled neurons, providing a fast signalling pathway; this network, however, is neither sufficient nor necessary for the activation of whole-body shortening (Shaw and Kristan, 1999) which is triggered by chemical polysynaptic pathways.

From each leech ganglion two pairs – on the right and on the left - of nerve bundle fibers emerge, usually referred to as the anterior and posterior roots. Axons of

mechanosensory neurons and of motoneurons run along these roots and it is possible to obtain clear extracellular recordings of their action potentials from bifurcations of these roots. As a consequence, by using simultaneous extracellular recordings from root bifurcations it is possible to monitor the motoneurons firing pattern underlying different leech behaviour, such as the whole-body shortening (see Chapter 3).

The purpose of this part of my work was to determine the pattern of firing of action potentials of motoneurons activated during this behaviour. In particular some questions arose: i) how many motoneurons are recruited during whole-body shortening ii) how concerted is the electrical activity of these motoneurons? iii) has the underlying pattern or sequence of neuronal activity a given structure? iv) what is the origin of the reliability of this essential and vital behaviour?

The results reported in this manuscript indicate that during whole-body shortening the great majority of coactivated motoneurons fire action potentials with a very poor pairwise correlation. Indeed they fire action potentials in a statistical independent way. As a consequence of statistical independence the behavioural response becomes smooth and reproducible.

4.2 Results

Whole-body shortening was studied in a semi-intact preparation where the behavioural response was monitored with a CCD camera and the electrical activity measured with either suction or sharp intracellular electrodes (see **Fig. 2.2A**). In order to monitor also the local muscle contraction, a piece of the central body segment was isolated, flattened and kept innervated by a single ganglion (see **Fig. 2.2B** and **C**) and its skin deformation was observed with another CCD camera.

4.2.1 Video recordings of whole body shortening

Whole-body shortening in a semi-intact leech (see **Fig. 2.2B** and **C**) was elicited with a current pulse of 0.8-1 mA delivered to the head, lasting 1 s. As a consequence of the electric shock, the leech shortened its whole body. Whole-body shortening disappeared within one or two minutes after the cessation of the noxious stimulation and the animal returned to its normal length. Maximal shortening was achieved with voltage pulses lasting at least 0.5 s. The reproducibility of this escape behaviour was quantified by analyzing in different trials the relative shortening S of the anterior part of the leech (**Fig. 4.1A**) and the total displacement D (**Fig. 4.1B**) of a piece of the skin, indicated in **Fig. 2.2C** by a red and a yellow arrow, respectively. Shortening started within approximately 100 ms from the onset of the voltage pulse and within 1 or 2 seconds the head and tail reached their final position, rather reproducibly. The average shortening was about 35% (continuous line in **Fig. 4.1C**) and the average contraction of the analyzed piece of skin was 13%, corresponding to about 30 pixels (continuous line in **Fig. 4.1D**). The head, tail and the central piece of skin moved simultaneously within 120 ms, i.e. the image acquisition time (see 2.3). The skin of the isolated central body segment contracted longitudinally in an almost uniform way. After an initial increase, the coefficient of variation CV (see 2.5.2) of whole-body shortening and of skin displacement became less than 0.3 at maximal whole body shortening. The low values of the CV indicate that this escape reaction is significantly reproducible.

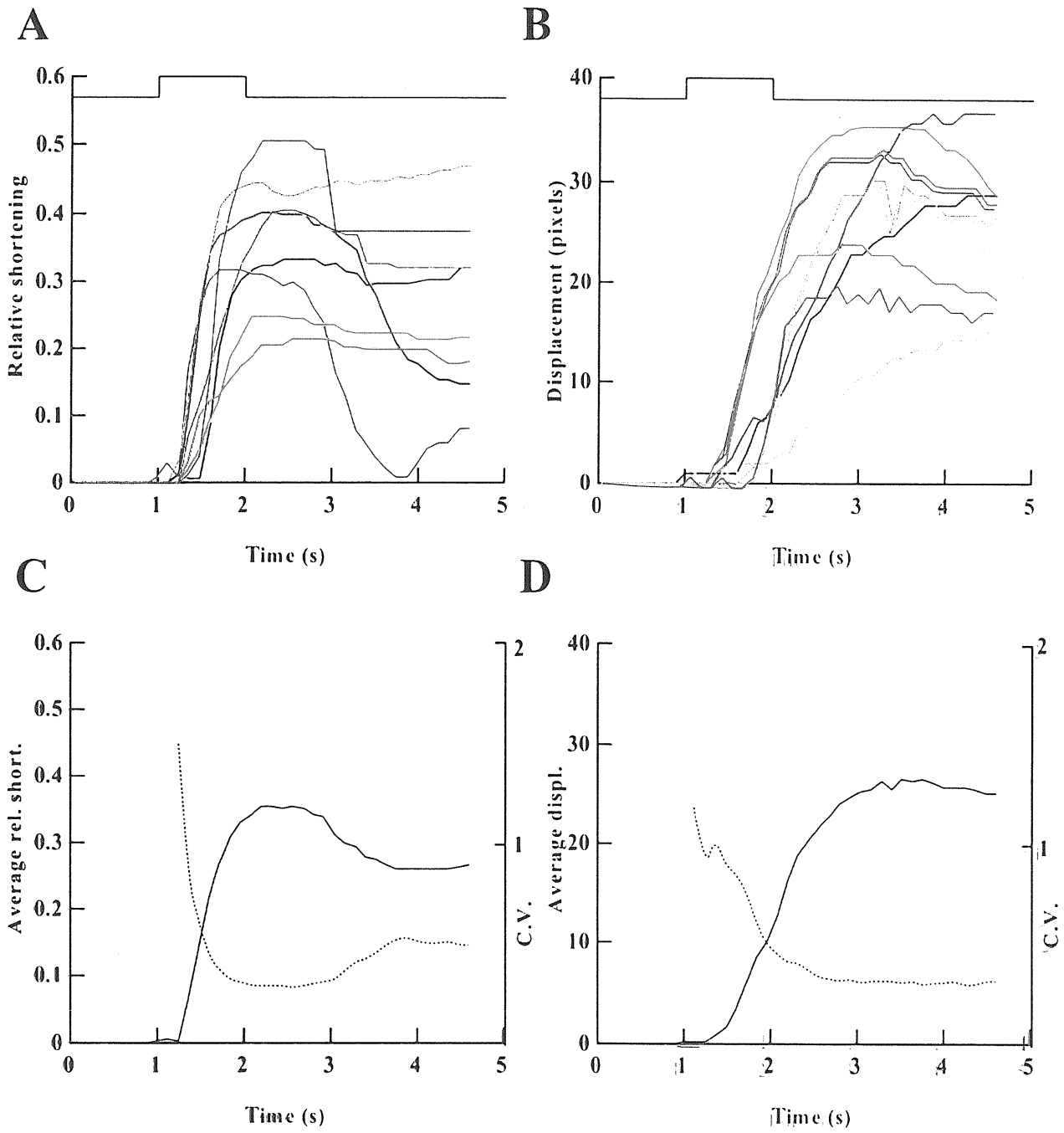

Fig. 4.1. Reproducibility of whole-body shortening. (**A**): Shortening of the anterior part of the leech, relative to the initial length (see 2.5.2), as a function of time for 8 different trials. (**B**): Total displacement in pixels of the point indicated by the dotted circle in **Fig. 2.2B**, for the same 8 trials as in (**A**). (**C**): Average relative shortening (continuous line) and its coefficient of variation (dotted line) as a function of time. Data averaged from 8 different trials. (**D**): Average total displacement of the point analyzed in (**B**) (continuous line) and its coefficient of variation (dotted line) as a function of time. Data from 8 different trials. Images were acquired at 8.3 Hz. Upper trace in (**A**) and (**B**) indicates the artifact of electrical shock, representing the noxious stimulation.

4.2.2 Electrophysiological recordings during whole body shortening

Fig. 4.2A illustrates extracellular recordings obtained with eight suction pipettes from the left and right MA, AA, DP:B1 and DP:B2 nerves of the 10th ganglion of a semi-intact leech during the noxious electric stimulation (see upper trace). This stimulation induced a vigorous electrical discharge with a delay of about 50 ms, well before the onset of the behavioural response (see inset in **Fig. 4.2**).

During whole-body shortening trains of action potentials lasting for several seconds were detected in all roots. Action potentials produced by specific motoneurons were identified, as shown on the expanded traces in **Fig. 4.2B** by analyzing their shapes and sizes in specific nerves and by comparison with intracellular recordings (see Chapter 3). Each action potential from an identified motoneuron, such as motoneurons 3, 107, 108, 109 and L on the left (L) and right (R) side of the 10th ganglion, is labelled in **Fig. 4.2B**. For instance motoneurons L_L and L_R were immediately identified because of the simultaneous presence of two large extracellular voltage signals on the DP:B1 and DP:B2 nerves (see dotted segments in **Fig. 4.2B**). All these motoneurons were activated during whole-body shortening and fired action potentials at frequencies varying between 10 and 20 Hz. The average latency of the first action potential evoked during whole-body shortening, measured from the onset of the stimulus, was 66.4 ± 43.6, 86.3 ± 33.0, 58.3 ± 7.3, 149.4 ± 196.1 and 96.2 ± 14.1 ms (n=11) for motoneurons 3, 107, 108, 109 and L respectively, in agreement with a previous analysis (Shaw and Kristan, 1995).

In contrast to the behavioural reaction, spike trains of individual motoneurons were poorly reproducible from trial to trial and did not have any obvious regularity. This poor reproducibility could be caused by a variability in the effective stimulation delivered by the metal wires sutured on the skin or by occasional failures of the neural signal to propagate from the head through the connective fibers down to the 10th ganglion.

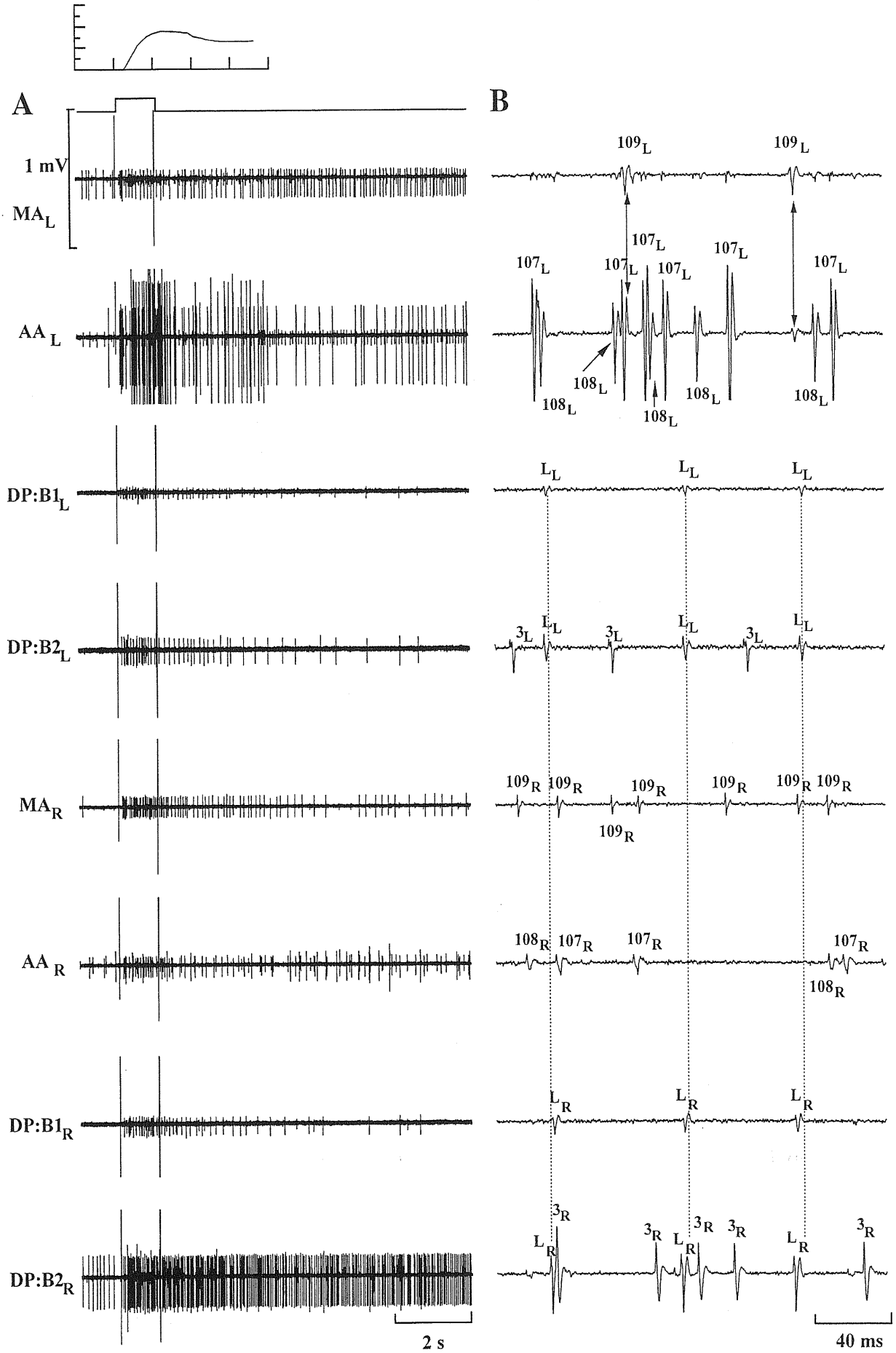
A
B
1 mV
MA L
AA L
DP:B1 L
DP:B2 L
MA R
AA R
DP:B1 R
DP:B2 R
2 s
40 ms

Fig. 4.2. Electrical recordings during whole-body shortening. (**A**): Electrical recordings obtained with eight suction pipettes from the roots of the 10th ganglion of a semi-intact leech as shown in **Fig. 2.2A**. Extracellular recordings from the medial anterior (MA), anterior anterior (AA), the B1 branch of the dorsal posterior (DP:B1), the B2 branch of the dorsal posterior (DP:B2) left (L) and right (R) nerves. The upper trace is the stimulus artifact; the inset is the average relative shortening. The stimulus was a current pulse of 1 mA lasting 1 s delivered through two wires inserted in the skin between the third and fourth segment (see **Fig. 2.2B**). (**B**): Recordings at higher sweep speed with identified neurons labelled as described in Chapter 3. Dotted and arrowed segments indicate extracellular signals associated with the (left and right) motoneuron L and with the left motoneuron 109, respectively.

A way to test these possibilities is to record the very large signals produced by the S cells from the anterior connective entering into the 10th ganglion. The S cells network is responsible for a fast signalling pathway along the ganglia chain and contributes to whole-body shortening (Shaw and Kristan, 1995 & 1999). **Fig. 4.3A** shows the average firing rate (AFR) and the coefficient of variation (CV) of the S action potentials during whole-body shortening (see Chapter 2) obtained with an en passant suction pipettes between the 9th and the 10th ganglion. The first action potential of the S cell appeared after 57.3 ms (n= 18) from the onset of the electrical stimulation (Shaw and Kristan, 1995) and had a jitter of less than 4 ms in the same preparation. As shown in **Fig. 4.3A**, during the electrical stimulation the CV of the S cell firing reached a lower value than 0.3, even when a binwidth of 50 ms was used. This result indicates that the neural signal reached the ganglion reproducibly during each trial and the variability of single neuron responses must be attributed to intrinsic firing properties.

The reproducibility of the neural response of individual motoneurons was quantified by analyzing the first order statistics of the firing of identified motoneurons. **Fig. 4.3B-F** show the AFR and the CV for the identified motoneurons on the left side from 11 different trials of the experiment shown in **Fig. 4.1** and **4.2** with a binwidth of 200 ms.

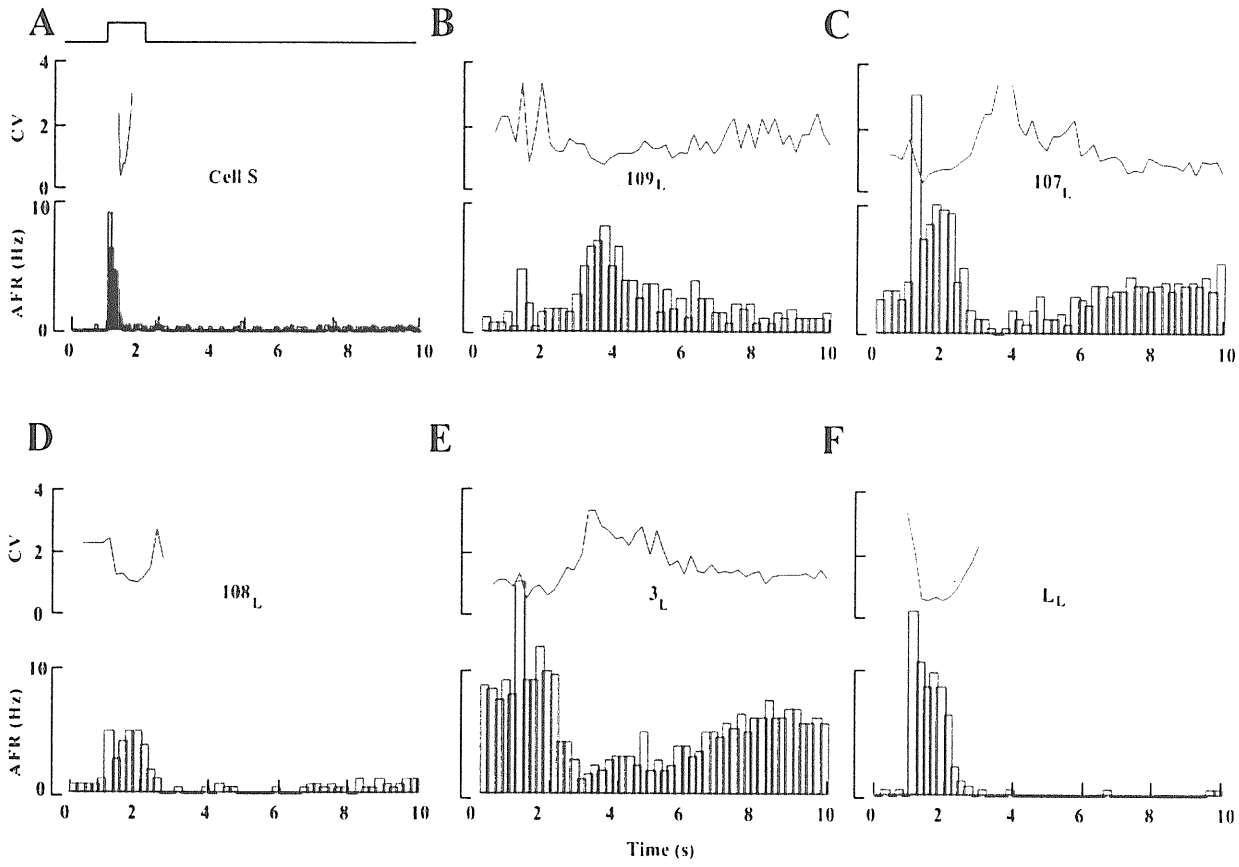

Fig. 4.3. First order properties of the S cell and identified motoneurons during whole-body shortening. (**A**): Average firing rate (AFR) and coefficient of variation (CV) of the S cell connecting the 9th and 10th ganglion during whole-body shortening obtained from 30 different trials over a binwidth of 50 ms. (**B**), (**C**), (**D**), (**E**) and (**F**): AFR (in blue) and CV (in red) of the left motoneurons 109, 107, 108, 3 and L of the 10th ganglion. Data obtained from 11 different trials of the experiment illustrated in **Fig. 4.2** over a binwidth of 200 ms.

The AFR of these motoneurons increased during electrical stimulation. After the termination of the noxious stimulation, the electrical activity of some motoneurons remained high for several seconds (motoneuron 109), but that of other motoneurons (3 and 107) was transiently depressed. The CV of all motoneurons was usually high, about 2 or larger and only during the initial activation did the CV approach a value smaller than 1. For motoneurons 3 and 107 the CV increased significantly immediately after the cessation of the electrical stimulation. Comparing the CV of the S cell with the CV of all identified motoneurons computed with the same binwidth of 50 ms, identified motoneurons showed a

larger CV than the S cell. These results suggest that the origin of the variability of motoneuron firing is within the segmental ganglion.

In another series of experiments whole-body shortening was studied while recording extracellular voltage signals from PP nerves (**Fig. 4.4A**). Also in this case an evident increase of the occurrence of action potentials was observed and as shown in **Fig. 4.4B**, it was possible to clearly identify extracellular voltage signals from the longitudinal 4, 5 and 8 motoneurons.

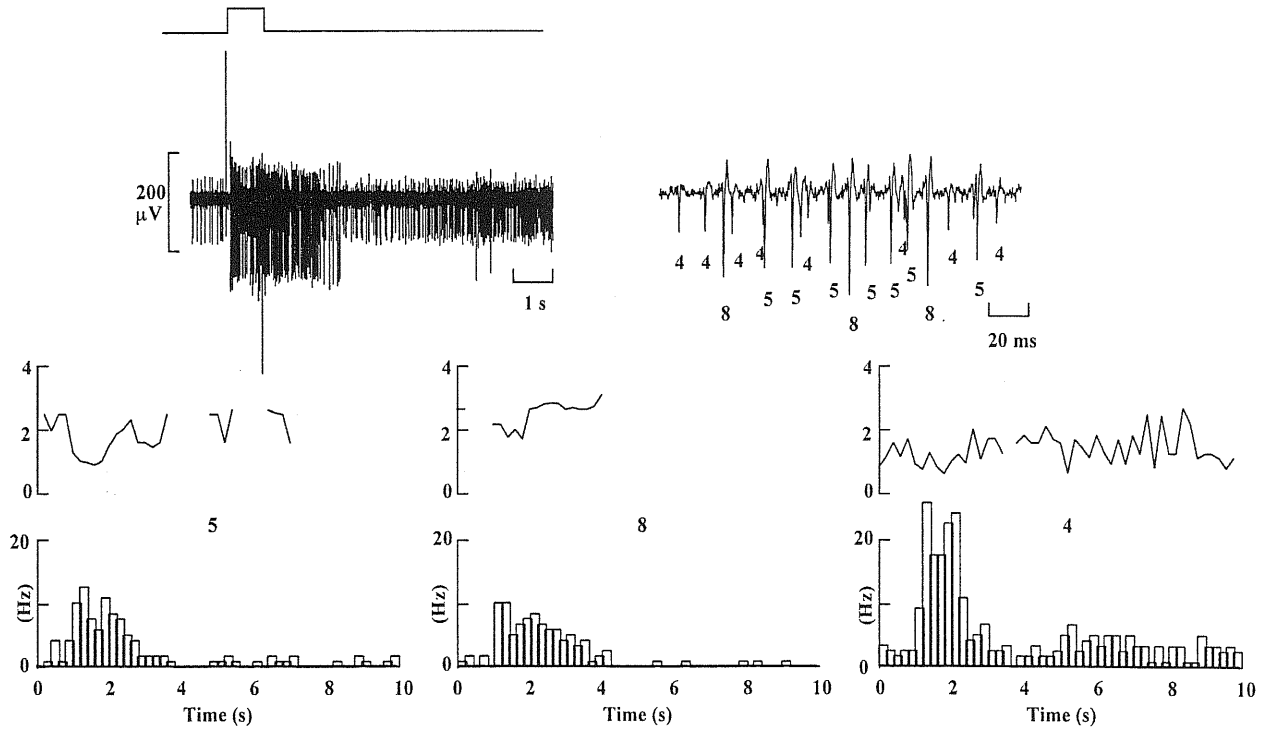

Fig. 4.4. Electrical recordings from the PP root during whole-body shortening. (**A**): suction pipette recording from the left PP root of the 10th ganglion during whole-body shortening. The upper trace is the stimulus artifact which was the same as in **Fig. 4.2.** (**B**): recordings at higher sweep speed with identified neurons labelled as described in Chapter 2. **C, D** and **E**: AFR and CV of motoneurons 8, 5 and 4 respectively.

The AFR and CV of motoneurons 8, 5 and 4 are shown in **Fig. 4.4C, D** and **E** respectively. The firing of these longitudinal motoneurons was clearly increased during

whole-body shortening and for motoneuron 5 it was transiently depressed after cessation of the noxious stimulation. Similarly to motoneurons analyzed in **Fig. 3** and **4**, the firing of action potentials in motoneurons 4, 5 and 8 was characterized by a significant variability.

By observing skin deformations induced by muscle contraction during whole-body shortening, as those shown in **Fig. 2.2B** and **C**, it was possible to evaluate the contribution of different motoneurons to the behavioural response. By using a semi-intact leech preparation, as that shown in **Fig. 2.2**, but keeping only half of the body segment connected to the 10^{th} ganglion, whole-body shortening was induced while hyperpolarizing different motoneurons, so as to inhibit the corresponding muscle contraction. When motoneuron L was strongly hyperpolarized, the skin deformation was very similar to that observed without inhibiting motoneuron L. Similar results were obtained by hyperpolarizing motoneurons 3, 107 and 108. These results indicate that whole-body shortening is not mediated primarily by motoneurons L or 3, but by the coactivation of many motoneurons.

4.3 Second order statistics of coactivated motoneurons

When different shapes of action potentials are extracted from analog recordings and assigned to identified motoneurons (see Chapter 3) it is possible to analyze their simultaneous firing. **Fig. 4.5** illustrates the occurrence of action potentials of 10 motoneurons during an episode of whole-body shortening. The total length of the episode illustrated in **Fig. 4.5** is 2.5 s, during which the noxious stimulation was delivered for 1 s (see upper trace).

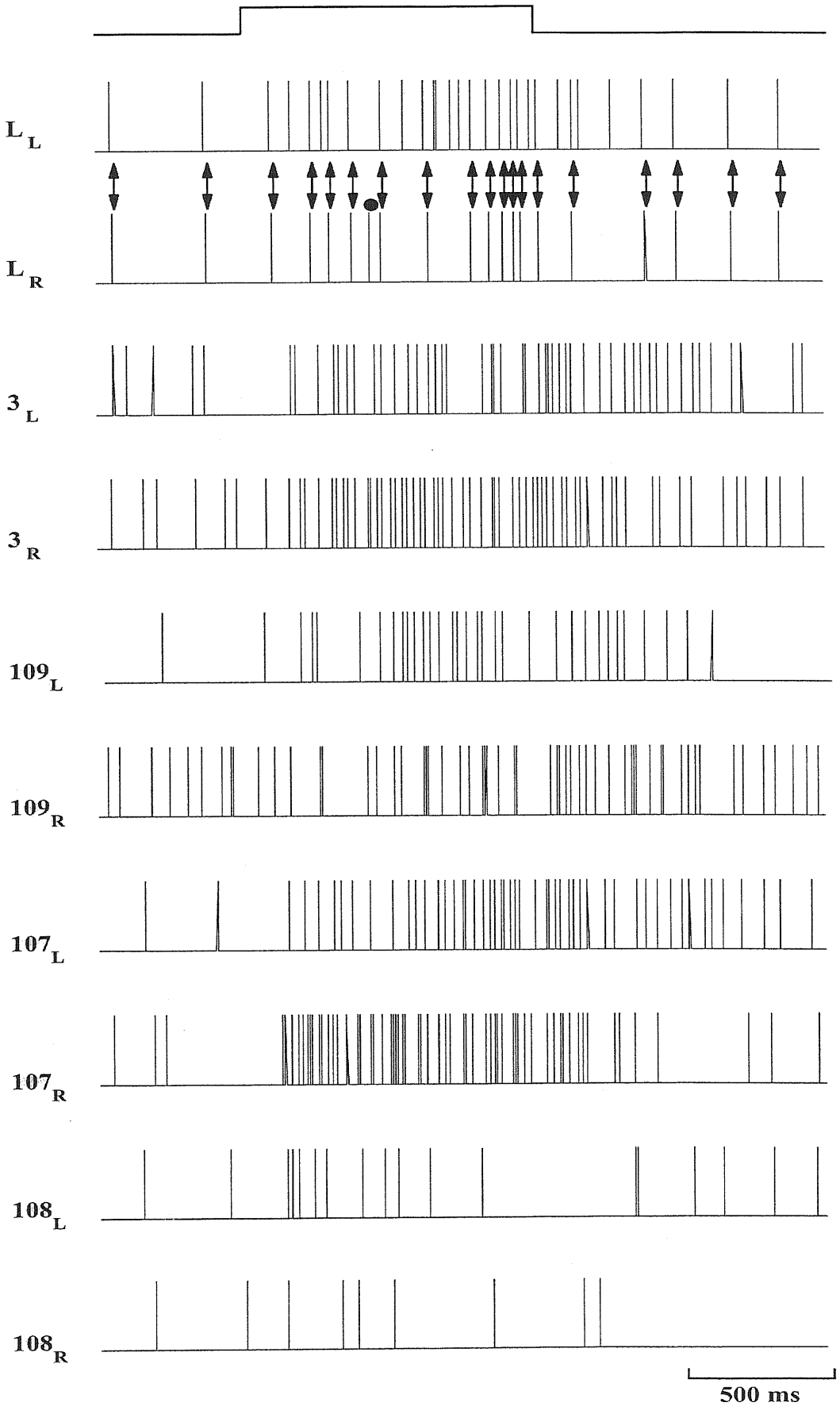
L_L
L_R
3_L
3_R
109_L
109_R
107_L
107_R
108_L
108_R
500 ms

Fig. 4.5. Firing of identified motoneurons during whole-body shortening. Each trace represents the firing of an identified motoneuron during whole-body shortening as a binary trace where an upper deflection indicates the occurrence of an action potential. The upper trace represents the timing of the current pulse of 1 mA delivered to the skin inducing whole-body shortening. From top to bottom each trace represents the firing of the left and right motoneurons L, 3, 109, 107 and 108. Only left and right L cells show significant correlation (see double arrows joining action potentials of L_L and L_R motoneurons); the black dot refers to the only uncoupled spike.

From visual inspection, it is evident that the firing of the left and right motoneurons L is highly correlated (see arrows joining almost coincident action potentials). Indeed during the time sweep considered in **Fig. 4.5** only once (see black dot) did motoneuron L_R fire an action potential not coinciding with any action potential of motoneuron L_L. This correlated firing is a consequence of the electrical coupling between L_R and L_L (Stuart, 1970; Nicholls and Purves, 1970).

The second order properties of the firing of coactivated motoneurons during whole-body shortening were analyzed by computing the crosscorrelogram for pairs of motoneurons during the time of noxious stimulation (1 s). Crosscorrelograms were computed over 32 different trials for a total time of 32 s. As shown in **Fig. 4.6A** the crosscorrelograms of the right and left motoneurons L were highly peaked, indicating a strong correlation of their electrical activity. In contrast, the crosscorrelograms of all other pairs of motoneurons in the same ganglion (**B – G**) were flat, indicating a poor correlation of their firing. A poor correlation was also observed among motoneurons of two adjacent ganglia, for example between the left motoneurons 107 and 108 of the 10^{th} and 11^{th} ganglion (see **Fig. 4.5H**), respectively.

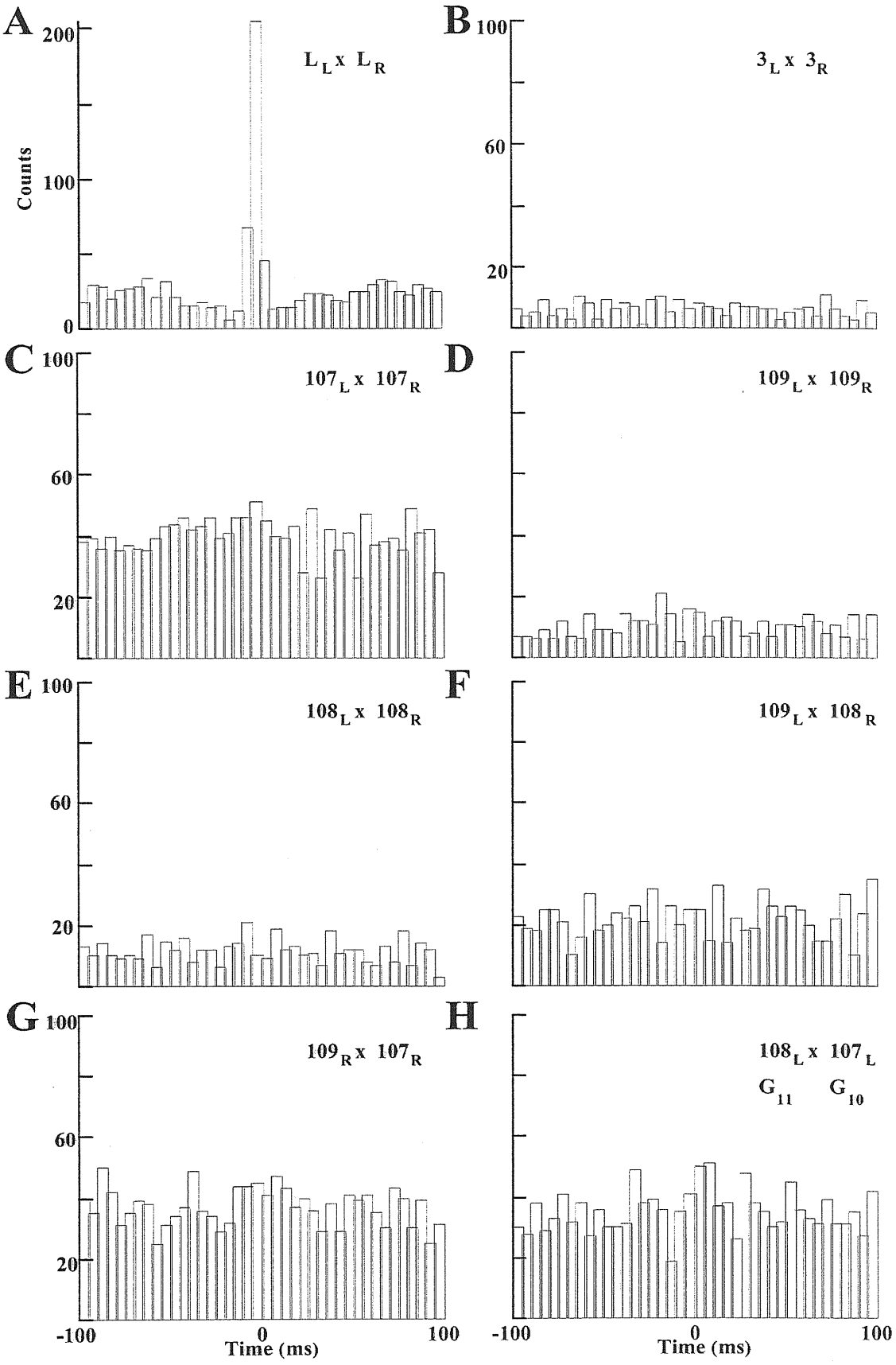
A
B
C
D
E
F
G
H
Counts
200
100
0
100
60
20
L_L x L_R
3_L x 3_R
107_L x 107_R
109_L x 109_R
108_L x 108_R
109_L x 108_R
109_R x 107_R
108_L x 107_L
G_{11} G_{10}
-100
0
100
Time (ms)

Fig. 4.6. Second order statistics of motoneurons in the same ganglion during global shortening. Crosscorrelation of identified motoneurons during whole-body shortening. Data collected during the application of a current pulse of 1 mA lasting for 1 s and over 35 different trials repeated every 3 minutes. Each panel represents the crosscorrelogram of the firing of motoneurons indicated in the right upper corner. All motoneurons in panels (**A**) –(**G**) are from the 10^{th} ganglion. Data in panel (**H**) refer to two motoneurons from the 10^{th} and 11^{th} ganglia.

4.4 Discussion

The data presented here describe new properties of the firing of action potentials of motoneurons coactivated during an escape reaction caused by a noxious stimulation. This fundamental reaction was studied in the leech because all its motoneurons have been identified and extensively studied (Stuart, 1970; Ort et al., 1974; Sawada et al., 1976; Stent et al., 1978; Blackshaw, 1981a; Muller et al., 1981; Norris & Calabrese, 1987; Baader, 1997). The results here presented are similar to those obtained in the *Aplysia* when the siphon was touched (Tsau et al., 1994; Wu et al., 1994) and are reminiscent of motoneuron firing patterns often observed in the mammalian spinal cord (Windhorst, 1990). Therefore they may help in understanding basic properties of distributed processing and neural computation.

Whole-body shortening starts within 200-300 ms from the onset of the electric stimulation (Shaw and Kristan, 1995; see also **Fig. 4.1**) producing a change of about 30% in the total length of the animal. From our results it is evident that the posterior end of the animal starts moving about 200 ms after the head, a delay comparable with the time occurring to the S cell network to conduct an impulse along the entire length of the body (Shaw and Kristan, 1995; Baader and Bächtold, 1997). Mechanical feedback may also play

a role in the transmission of excitation, given the high sensitivity of stretch receptors (Blackshaw, 1993); on the other hand, electrical feedback between adjacent ganglia is unlikely to be significant in this context, since the activity of motoneurons is uncorrelated. The relaxation phase of the shortening reaction is much longer than the contraction and less reproducible, a result compatible with leech muscle properties, which tends to remain contracted unless serotonin accelerates relaxation, since the inhibitory motoneurons just countercact the action of the excitatory ones during the contraction (Mason & Kristan, 1982; Szczupak & Kristan, 1995).

The present analysis shows that this escape reaction is mediated by the coactivation of longitudinal muscles by motoneurons L and 3, 4 and 108 as already reported (Shaw and Kristan, 1995) , but also by other motoneurons such as 5, 8, 107 and 109 and probably also by other cells which have not been identified in the present analysis. Two other observations suggest that whole-body shortening is produced by the coactivation of different motoneurons in the same ganglion. First, when specific motoneurons such as motoneurons L or 3, 107 and 108 were strongly hyperpolarized in order to inhibit their firing, the deformation in a piece of skin innervated by only one ganglion during whole-body shortening was the same as that measured without hyperpolarizing these motoneurons. Therefore whole-body shortening does not seem to be mediated by the activation of just one or two motoneurons in each ganglion. Second, during whole-body shortening (see **Fig. 4.2**) these motoneurons fire action potentials at a rate of about 10-20 Hz, so that they produce at most 4 or 5 action potentials before the onset of the behavioural response. Under these conditions individual motoneurons induce only a small muscle contraction (Mason and Kristan, 1982) and the rapid and large muscle contraction underlying whole-body shortening can only be achieved by the recruitment and coactivation of many motoneurons, as the present analysis indicates. In each leech ganglion there are about 28 known pairs of motoneurons (Blackshaw, 1981; Ort et al.,

1974; Stuart, 1970; Sawada et al., 1976; Stent et al., 1978) and therefore during whole-body shortening a significant fraction of all the leech muscles are activated. This result in the leech is supported by similar findings in the *Aplysia* (Tsau et al., 1994; Hickie et al., 1997): when the siphon receives a mechanical stimuli probably hundreds of neurons are involved, the reaction seems a largely distributed process, even at the level of synapses between sensory neurons and motoneurons. A distributed processing seems to underlie also the escape reaction in the cockroach, a more complex invertebrate (Camhi, 1988).

As shown in **Fig. 4.5 and 4.6** the global firing of coactivated motoneurons does not have any clear and statistically significant pattern. Indeed the pairwise crosscorrelogram of the electrical activity of these motoneurons is flat (see **Fig. 4.6**) except the one between the left and right motoneurons L. These motoneurons are tightly coupled by electrical junctions (Stuart, 1970; Nicholls and Purves, 1970) in each leech ganglion and electrical coupling is well known to be a powerful synchronizing mechanism (Grattarola and Torre, 1977; Bouskila and Dudek, 1993; Michelson and Wong, 1994; Traub, 1995; Bernardo, 1997; Mann-Metzer and Yarom, 1999). Motoneurons coactivated during whole-body shortening are primarily activated by the S cell network (Burrell et al, 1999 Soc. for Neuroscience abstracts) and by another parallel pathway of as yet unidentified interneurons (Shaw and Kristan, 1999). These multiple synapses are likely to have some degree of unreliability like most chemical synapses (Allen and Stevens, 1994; Goda and Sudhof, 1997; Larkman et al., 1997; Lisman, 1997; Markram et al., 1997; Zador, 1998) which could result in an almost complete loss of correlated activity (Pinato et al., 2000).

Escape reactions are vital for the animal survival and must be reliable and efficient. Indeed there are at least two mechanisms for which statistical independence among coactivated neurons is useful. It is not difficult to understand how unreliable and uncorrelated spike trains, such as those illustrated in **Fig. 4.3 and 4.6**, can lead to a reproducible global behaviour. Whole-body shortening is mediated by the electrical

activity of a large ensemble of interneurons and motoneurons and it is well known that averaging and/or pooling uncorrelated random variables reduces variability (see Appendix). Indeed when the electrical activity of an ensemble of motoneurons underlying whole-body shortening is considered, the CV of the total electrical activity is significantly smaller. As shown in **Fig. 4.7** the CV of the ensemble activity (blue line) is quite small, always less than 0.5 during the contraction phase, and is significantly smaller than the CV of individual motoneurons (red lines). The CV of the pooled electrical activity is consistent with the CV of the behavioural response shown in **Fig. 4.1**.

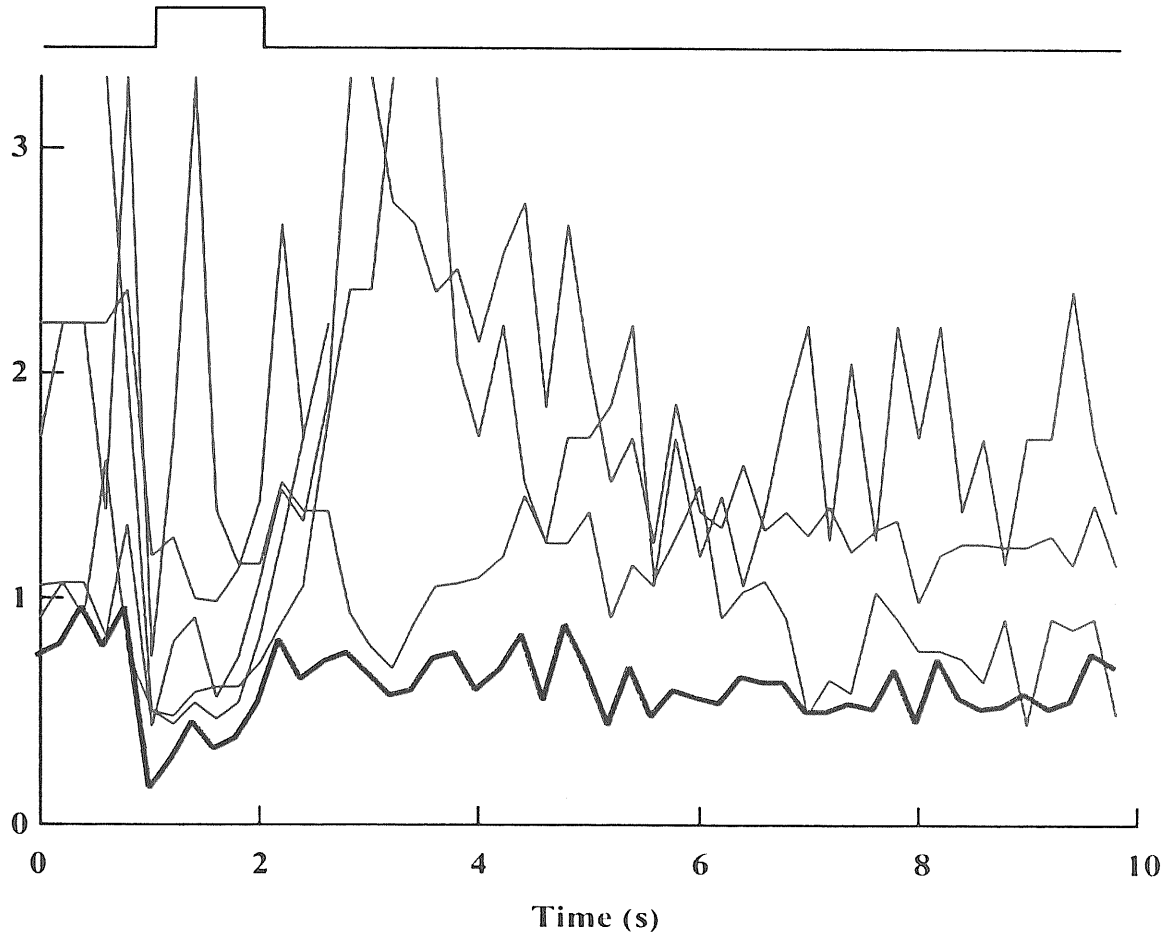

Fig. 4.7. Coefficient of variation of an ensemble of motoneurons underlying whole-body shortening. Blue line is the CV of the ensemble of left and right motoneurons L, 3, 107, 108, 109 from the 10th ganglion. Red lines are the CV of some individual motoneurons. Same data as those shown in **Fig. 4.3**.

Effective motor commands must produce smooth movements, which are unlikely to be caused by highly correlated motoneurons firing. Indeed a possible action of Renshaw interneurons in the spinal cord is to decorrelate the firing patterns of motoneurons (Windhorst, 1996), thus avoiding synchrony which can lead to tremor and jerk movements (Allum et al., 1978; Dietz et al., 1976; Schalow & Zach, 1996). Therefore statistical independence of coactivated motoneurons may be necessary to ensure a smooth motor output and an effective escape reaction. Inhibitory interneurons also play a role in the desynchronization of cat visual cortex, in response to sudden stimuli (Kruse & Eckhorn, 1996).

Statistical independence of coactivated neurons has been observed in several other cases of distributed neuronal processing. A very small correlation between neurons sharing the same stimulation has also been observed among the *Aplysia* neurons when the siphon was touched (Tsau et al., 1994), where only 0.3% of neuron pairs exhibited a significant degree of correlation on a time scale of tens of milliseconds, while on a time scale of seconds some degree of correlation is usually present (Arisi & Torre, unpublished data; Tsau et al., 1994). Statistical independence between coactivated neurons has also been observed in neuronal cultures composed by cortical neurons from neonatal rats (Pinato et al., 1999). In the vertebrate retina, sharp crosscorrelograms of the firing of coactivated neurons were observed only between electrically coupled neurons, while pairs of neurons connected by chemical synapses had a much smaller degree of correlation (Brivanlou et al., 1998). These results suggest a new and basic property of distributed processing, i.e. when a computation or an action is mediated by a large ensemble of neurons, statistical independence among coactivated neurons must be expected. This may be an important and beneficial feature of neural computation.

Conclusions and perspectives

In order to understand the nature of neural computation in the leech CNS, I developed a method to identify action potentials produced by specific motoneurons from extracellular voltage recordings obtained by pipettes sucking fine root branches. A good statistical sampling was granted by the long duration of the used preparations; the experimental measures are insensitive to mechanical artifacts, due to the high mechanical stability of the pipette-nerve seal. Software for extracellular spikes clustering and identification was entirely written in our lab.

Using eight extracellular suction pipettes and one or two intracellular conventional microelectrodes, I studied the nervous activity underlying the whole-body shortening, a vital escape reaction. Many extracellular action potentials were identified, indicating that several motoneurons were coactivated, many more than previously reported (Wittenberg & Kristan, 1992a; Shaw & Kristan, 1995). Therefore neural computation appears to be distributed.

Activated motoneurons show a large variability in their electrical response, while the network computation must produce a reliable behavioural response. Second order statistics between the firing motoneurons show they are not correlated. These two observations suggest that statistical independence of coactivated motoneurons may guarantee a motion smoothness, which could be impaired by a highly correlated firing, as in the case of synchronization. In addition simple mathematical arguments indicate that pooling uncorrelated random variables reduces variability. We propose that the network pools the activity of statistical independent motoneurons and, as a consequence, the ensemble

nervous response shows a very low variability, resulting in a reproducible behavioural reaction.

In the near future we will compare the firing properties observed during whole-body shortening with those underlying other typical leech behaviours. Statistical properties of motoneurons involved in local bending and the associated local shortening are now being investigated: preliminary results suggest that they are very similar to those found for whole-body shortening and illustrated in this thesis. The whole-body shortening and the swimming behaviours will be induced in the same preparation so as to study how the firing properties of motoneurons change in different behaviours, in particular we want to address these issues: are the motoneurons still uncorrelated or are they synchronized by the oscillating circuits? is the computation still distributed? Even more interesting would be to compare these results with the degree of statistical independence among mammalian motoneurons during known locomotory patterns of activity. There are hints that decorrelation may play a crucial role also among mammals in the generation of smooth movements (Windhorst, 1996; Maltenfort et al., 1998).

New developments are also feasible in the field of neuron identification from extracellular electrical recordings. Our software can be further developed for completely automatic spike clustering and multi-channel twin signals detection, either on the base of a dynamic template matching with signals evoked by intracellular electrodes, or by an algorithm able to detect and follow the modification of extracellular spike shapes during the experiment.

A second step forward is the analysis of neural processing by optical methods. A very promising technique to study the leech neural circuits is the use of voltage sensitive dyes to monitor the activity of interneurons, which are not accessible by extracellular recordings (Cacciatore et al., 1999). A different technique is being applied in our laboratory to analyze the evoked muscular reactions. In a semi-intact preparation each single motoneuron can be

excited and the reaction induced on the skin may be recorded by video cameras. These digitized images of muscle reaction can be analyzed by algorithms based on the optical flow (Aggarwal and Nandhakumar, 1988), to obtain a two-dimensional vectorial field describing the movement of each point on the skin. These fields could be collected in a library of video templates of the motoneuron effects on body wall muscles. Thus an arbitrary movement of the animal may in principle be decomposed as a linear combination of these video templates. This method allows to investigate the neuronal output in semi-intact preparations and even in intact animals, during any motor behaviour. Preliminary results obtained in our lab by this procedure are very encouraging.

Appendix

Role of statistical independence in neural computation

A.1 Origin of statistical independence

Recent reports have shown that the mechanism of action potential generation is very reliable (Mainen and Sejnowski, 1995), i.e. a suitable stimulation directly applied to the neuron can evoke spike trains with very reproducible patterns, while synapses exhibit in general high variability (Allen and Stevens, 1994; Larkman et al., 1997; Markram et al., 1997).

In the experiments described in my thesis the stimulus consisted in one or more action potentials induced in a single mechanosensory neuron (see **Fig. 3.9**), or in a noxious current applied to skin of the animal (see **Fig. 4.2**) exciting several mechanosensory neurons at the same time. In both cases, the mechanosensory cells activate many different interneurons and motoneurons through chemical and electrical synapses, thus resulting in a significant spatial and temporal variability. The large variability and the statistical independence of evoked action potentials here observed are likely to be due to the fact that the signal has to cross unreliable synapses, where action potentials have a low probability of crossing the synapse (Allen and Stevens, 1994), as often observed in the central nervous system (Zador, 1998; Hardingham and Larkman, 1998).

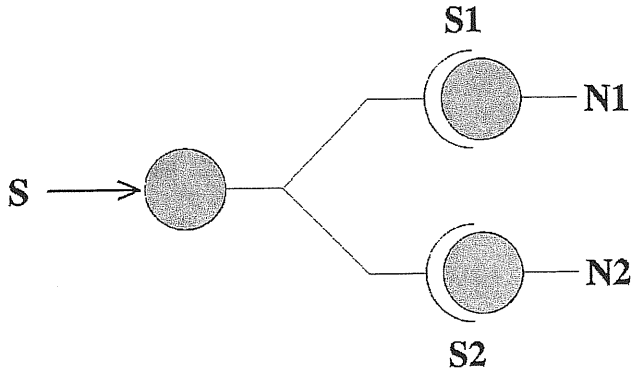

Fig. A.1. Proposed origin of statistical independence. A simple scheme accounting for the variability of the electrical activity in a network. Synaptic release at the two terminals S1 and S2 of the same presynaptic neuron is statistically independent. (*From: Pinato et al., 1999*).

Let us consider a presynaptic neuron (**Fig. A.1**) projecting onto two different neurons N1 and N2, through chemical synapses S1 and S2 respectively. When an action potential in the presynaptic neuron invades the synaptic terminals, the release at the two synapses S1 and S2 is statistically independent, because S1 and S2 are physically distant and synaptic transmission is independent. Therefore failure and success in evoking a postsynaptic action potential in the two postsynaptic neurons are statistically independent. The scheme in **Fig. A.1** shows that action potentials of neurons activated by the same presynaptic neuron are statistically independent during their activation, i.e. their instantaneous firing probability $P_i(t)$ satisfies the relation $P_{ij}(t) = P_i(t) * P_j(t)$.

The scheme of electrical excitation represented in **Fig. A.1** is mediated by excitatory synapses, however excitation may also be mediated by disinhibition. This behavior is likely to occur in the majority of neuronal networks with chemical synapses.

A.2 Variability and reliability

As the recordings from the leech ganglion (see **Fig. 3.9** and **4.2**) show, applying a stimulation the network results in an evoked pattern of activity which is distributed among a large number of neurons that individually respond in a not reproducible manner across the different trials. If a consistent output has to be produced, as the behavioural observations confirm (Lewis and Kristan, 1998a and 1998b), then the activity of groups of neurons has to be integrated. It will be demonstrated that the variability and the statistical independence in a distributed network can play a functional role to obtain a reproducible integrated response. This integration can be computed in different ways, depending on how the outputs of the different neurons are combined in the network.

A simple measure which quantifies the variability of a single neuron in a given time window is the coefficient of variation (*CV*). If $x_i(r,s,t)$ is the number of spikes fired by neuron N_i during time window $(t,t+\Delta t)$ in response to trial r of stimulation s, the coefficient of variation $CV_i(s,t)$ can be defined as:

$$CV_i(s,t) = \frac{\sigma_i(s,t)}{AFR_i(s,t)}$$

where s is the applied stimulus, $AFR_i(s,t) = \frac{1}{R}\sum_r x_i(r,s,t)$ is the mean number of spikes (over the R trials of the same stimulation s) fired by neuron N_i in the time window $(t,t+\Delta t)$, and $\sigma_i(s,t) = \frac{1}{R}\sum_r \left(x_i(r,s,t) - AFR_i(s,t)\right)^2$ is the standard deviation.

This quantity must be compared to the coefficient of variation of the overall process. Two biologically plausible ways to achieve this are averaging and pooling the activities of single neurons (Pinato et al., 1999).

Averaging. Suppose that the firing rate of each neuron N_i in response to stimulus s can be modeled as the realization of a stochastic process $x_i(s,t)$. Suppose that the network performs a sum of the neuronal activity of n distinct neurons $N_1 \ldots N_n$, converging onto a common target neuron and providing the final output $X(s,t)$, a stochastic process which can be written as

$$X(s,t) = x_1(s,t) + x_2(s,t) + \ldots + x_n(s,t) \qquad \text{(A.1)}$$

The realizations $X(r,s,t)$ of this stochastic process are the spike counts (summed over all neurons) in the interval $(t, t+\Delta t)$ after trial r of stimulation s is applied: $X(r,s,t) = \sum_i x_i(r,s,t)$ where $x_i(r,s,t)$ is the activity of neuron N_i. The global coefficient of variation is simply defined as the coefficient of variation of $X(s,t)$:

$$CV_X(s,t) = \frac{\sigma_X(s,t)}{AFR_X(s,t)} \qquad \text{(A.2)}$$

where $AFR_X(s,t) = \sum_i AFR_i(s,t)$ is the mean firing rate of $X(r,s,t)$, and $\sigma_X(s,t) = \sqrt{\frac{1}{R}\sum_{r=1}^{R}\left(X(r,s,t) - AFR_X(s,t)\right)^2}$ is its standard deviation, where R is still the number of trials.

Pooling. In the case of pooling, the stochastic processes $x_i(s,t)$ are combined as components of the same vectorial stochastic process:

$$\Xi(s,t) = (x_1(s,t), x_2(s,t) \ldots x_n(s,t)) \qquad \text{(A.3)}$$

In this case, the realizations of this stochastic processes consist of the outputs $x_i(r,s,t)$ of the isolated neurons N_i considered as components of a multivariate variable $X(r,s,t) = (x_1(r,s,t), x_2(r,s,t), \ldots x_n(r,s,t))$. Indicating as usual the average firing rate for neuron N_i as $AFR_i(s,t) = \frac{1}{R}\sum_r x_i(r,s,t)$, the coefficient of variation of the pooled output can be defined as

$$CV_{POOL}(s,t) = \frac{\sqrt{\sum_{i,j}\left|\Gamma_{i,j}(s,t)\right|}}{\sum_i AFR_i(s,t)} \qquad \text{(A.4)}$$

where $\sum_{i,j}\left|\Gamma_{i,j}(s,t)\right|$ is the sum of the absolute value of all the elements of the covariance matrix $\Gamma(s,t)$, defined as

$$\Gamma_{i,j}(s,t) = \frac{1}{R}\sum_{r=1}^{R}\left(x_i(r,s,t) - AFR_i(s,t)\right)\left(x_j(r,s,t) - AFR_j(s,t)\right)$$

Notice that the diagonal elements $\Gamma_{i,i}(s,t)$ of $\Gamma(s,t)$ are simply the variances $\sigma_i^{\,2}(s,t)$ of the firing rates $x_i(r,s,t)$ of neuron N_i. Also observe that $CV_X(s,t)$ can be written in terms of the elements $\Gamma_{i,i}(s,t)$ of the covariance matrix, giving $CV_x(s,t) = \sqrt{\sum_{i,j}\Gamma_{i,j}(s,t)}\Big/\sum_i AFR_i(s,t)$.

In Chapter 4 it has been shown how the electrical activity of the different neurons in the leech ganglion is to a large degree statistically independent, during whole-body shortening. It will now be shown with theoretical considerations how statistical independence allows to decrease variability in the electrical response of a network, for both the case where the outputs of different neurons is summed/averaged (Consequence 1) and the case where the outputs of different neurons are pooled (Consequence 2).

Consequence 1. If $x_i(s,t)$ $(i=1, \ldots n)$ are statistically independent processes, and

$$X(s,t) = x_1(s,t) + x_2(s,t) + \ldots + x_n(s,t),$$

then the variance $\sigma_X^{\,2}(t)$ of $X(t)$ is simply the sum of the variances of the individual processes (Papoulis, 1984):

$$\sigma_X^{\,2}(s,t) = \sum_i \sigma_i^{\,2}(s,t)$$

and the coefficient of variation of $X(t)$ (Eq. A.2) becomes:

$$CV_X(s,t) = \frac{\sqrt{\sum_i \sigma_i^2(s,t)}}{\sum_i AFR_i(s,t)} \qquad \text{(A.5)}$$

If $AFR_i(s,t) = AFR(s,t)$ and $\sigma_i(s,t) = \sigma(s,t)$ for all neurons N_i, and $CV(s,t) = \sigma(s,t)/AFR(s,t)$ is the coefficient of variation of the individual processes, then

$$CV_X(s,t) = \frac{\sqrt{N\sigma^2(s,t)}}{N \cdot AFR(s,t)} = \frac{1}{\sqrt{N}} CV(s,t)$$

which goes to 0 for very large N.

Consequence 1 states that by summing the individual responses of the different neurons a response is obtained which is asymptotically very stable, if the individual responses are statistically independent. Observe that if, on the other hand, the stochastic processes $x_i(s,t)$ are highly correlated, e.g.

$$x_i(s,t) = x(s,t) \quad \text{for any} \quad i = 1,...N$$

variances will not add linearly, but as:

$$\sigma_X^2(s,t) = N^2\sigma^2(s,t)$$

and the coefficient of variation will be equal to the individual coefficient of variation:

$$CV_X(s,t) = CV(s,t)$$

regardless of the value of N.

Consequence 2. If $x_i(s,t)$ $(i=1, \ldots n)$ are statistically independent processes, and

$$\Xi(s,t) = (x_1(s,t), x_2(s,t) \ldots x_n(s,t)),$$

then the covariance matrix $\Gamma(s,t)$ of the stochastic process $\Xi(s,t)$ is diagonal:

$$\Gamma(s,t) = \text{diag}(\Gamma_1^2(s,t), \Gamma_2^2(s,t), \ldots \Gamma_n^2(s,t))$$

and the coefficient of variation $CV_{POOL}(s,t)$ of Eq. (A.4) becomes

$$CV_{POOL}(s,t) = \frac{\sqrt{\sum_i \sigma_i^2(s,t)}}{\sum_i AFR_i(s,t)} \qquad \text{(A.6)}$$

which is exactly the same as Eq. (A.5): therefore $CV_X(s,t) = CV_{POOL}(s,t)$ for statistically independent processes; observe also that the sum of the variances $\sum_i \sigma_i^2(s,t)$ is simply the trace of $\Gamma(s,t)$. As a consequence, also in this case, if all the processes $\mathbf{x}_i(s,t)$ have the same mean $AFR_i(s,t)$, the same variance $\sigma(s,t)$ and therefore the same coefficient of variation $CV(s,t) = \sigma(s,t)/AFR(s,t)$, $CV_{POOL}(s,t)$ asymptotically goes to 0 as $O\left(1/\sqrt{N}\right)$ as N increases:

$$CV_X(s,t) = \frac{1}{\sqrt{N}} CV(s,t).$$

Consequence 2 states that by pooling the individual responses of different neurons a response is obtained which is asymptotically very reproducible, if the individual responses are statistically independent. If, on the contrary, the stochastic processes $x_i(s,t)$ are highly correlated the global coefficient of variation will not necessarily go to zero. If, for example,

$$x_i(s,t) = x(s,t), \qquad i = 1,...N$$

then

$$\sum_{i,j} \left|\Gamma_{i,j}(s,t)\right| = N^2 \sigma^2(s,t)$$

and the coefficient of variation will be equal as before to the individual coefficient of variation:

$$CV_X(s,t) = CV(s,t)$$

regardless of the value of N.

Finally, observe that it is always $CV_X(s,t) \le CV_{POOL}(s,t)$, since $\Gamma_{i,i}(s,t) \le \left|\Gamma_{i,i}(s,t)\right|$; also, indicating as $CV_{EXP}(s,t)$ the value expected for statistically independent variables (see Eq. A.5 and A.6), we have $CV_{EXP}(s,t) \le CV_{POOL}(s,t)$, since $\sum_{i \ne j} \left|\Gamma_{i,j}(s,t)\right| \ge 0$.

In order to confirm these theoretical considerations, **Fig. A.2** illustrates the behavior of the individual coefficients of variation as a function of time and compares them to the global coefficient of variation of the whole network. The global coefficient of variation is computed in the two ways specified by Eq. A.2 and Eq. A.4. It immediately appears that in these results the global coefficients of variation $CV_X(s,t)$ and $CV_{POOL}(s,t)$ are lower than the coefficients of variation $CV_i(s,t)$ of the individual neurons, as expected for statistically independent variables.

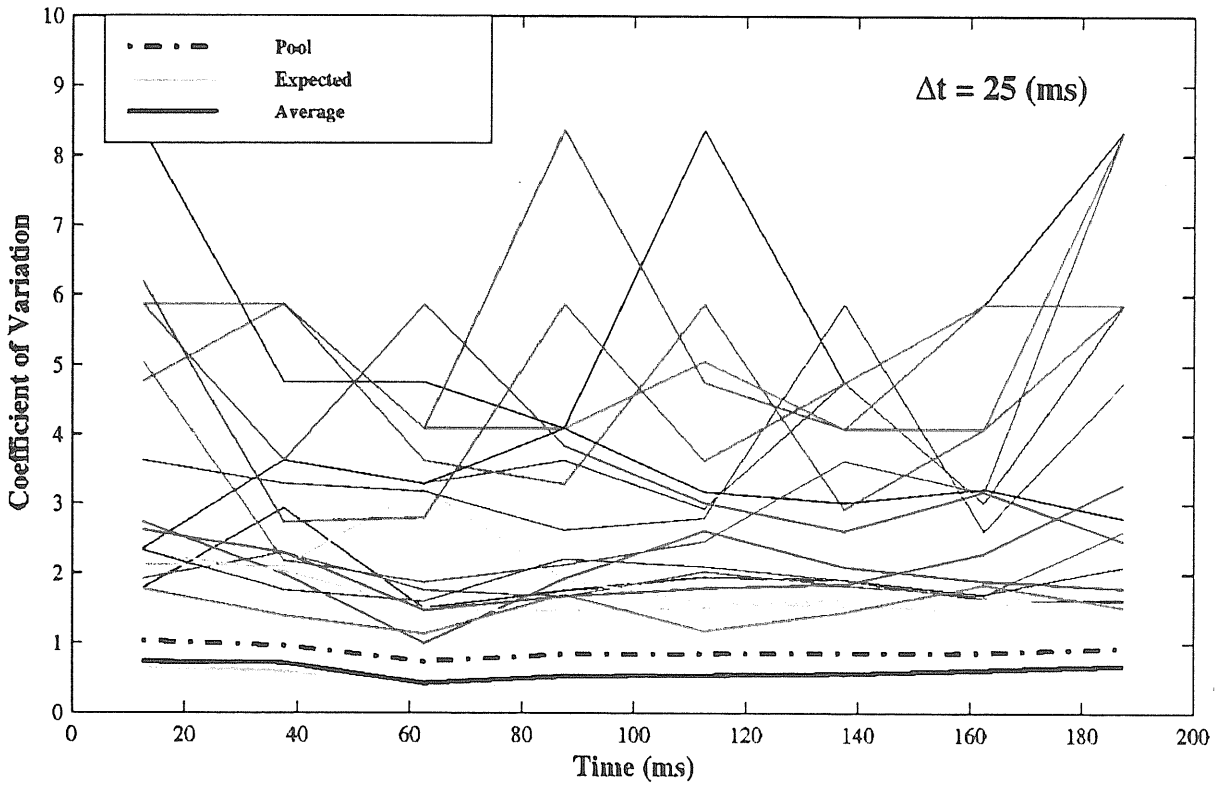

Fig. A.2. Coefficient of variation (CV) as a function time of the individual neurons compared to the CV (as a function of time) of the overall activity of the neuronal assembly in the leech ganglion. CV of different neurons whose activity was isolated in the recordings from suction pipettes (colored lines), compared with the global coefficients of variation $CV_X(s,t)$ ('Average', black line), $CV_{POOL}(s,t)$ ('Pool', black dotted line) and with $CV_{EXP}(s,t)$ ('Expected', gray line), which is the expected value of $CV_X(s,t)$ and $CV_{POOL}(s,t)$ (see Eq. A.5 and A.6) for statistically independent variables. Each coefficient of variation was computed every time window of 25 ms. (*From: Pinato et al., 2000*).

The value of the different coefficients of variation has been compared with the value of $CV_X(s,t)$ and $CV_{POOL}(s,t)$ which is expected for statistically independent variables, that is, with $CV_{EXP}(s,t) = \frac{\sqrt{\sum_i \sigma_i^2(s,t)}}{\sum_i AFR_i(s,t)}$ (see Eq. A.5 and A.6).

These results about the coefficient of variation are to be compared with the coefficient of variation computed for the case of spontaneous activity. For the leech, it was found that the coefficient of variation was in the order of $1/\sqrt{AFR}$ where AFR is the average firing rate, as predicted for a Poisson stochastic process.

I have therefore demonstrated that the statistical independence here described does not limit the performance of the nervous system. The same analysis was performed on a group of identified motoneurons. The CV of the evoked electrical activity of three motoneurons involved in bending reactions, i.e. the two DE motoneurons and the controlateral VI (colored lines in **Fig. A.3**), was compared with the CV of the pooled activity of these three motoneurons (solid black line in **Fig. A.3**) and the CV of the pooled activity of all neurons with action potentials recorded from the roots (dashed black line in **Fig. A.3**). Pooling the electrical activity among only three neurons (solid line without symbols) significantly reduced variability which was almost eliminated when a much larger neuronal population was considered (dashed line). This result, observed in all examined ganglia, provides an important key to understand information processing and neural coding in the leech nervous system.

Because sensory motor reactions and behavioral responses involve the simultaneous activation of many neurons, the large variability of the electrical activity seen in individual neurons (see **Fig. 4.3**) is reduced and almost eliminated when the electrical activity is pooled among a population of neurons (**Fig. A.2** and **A.3**).

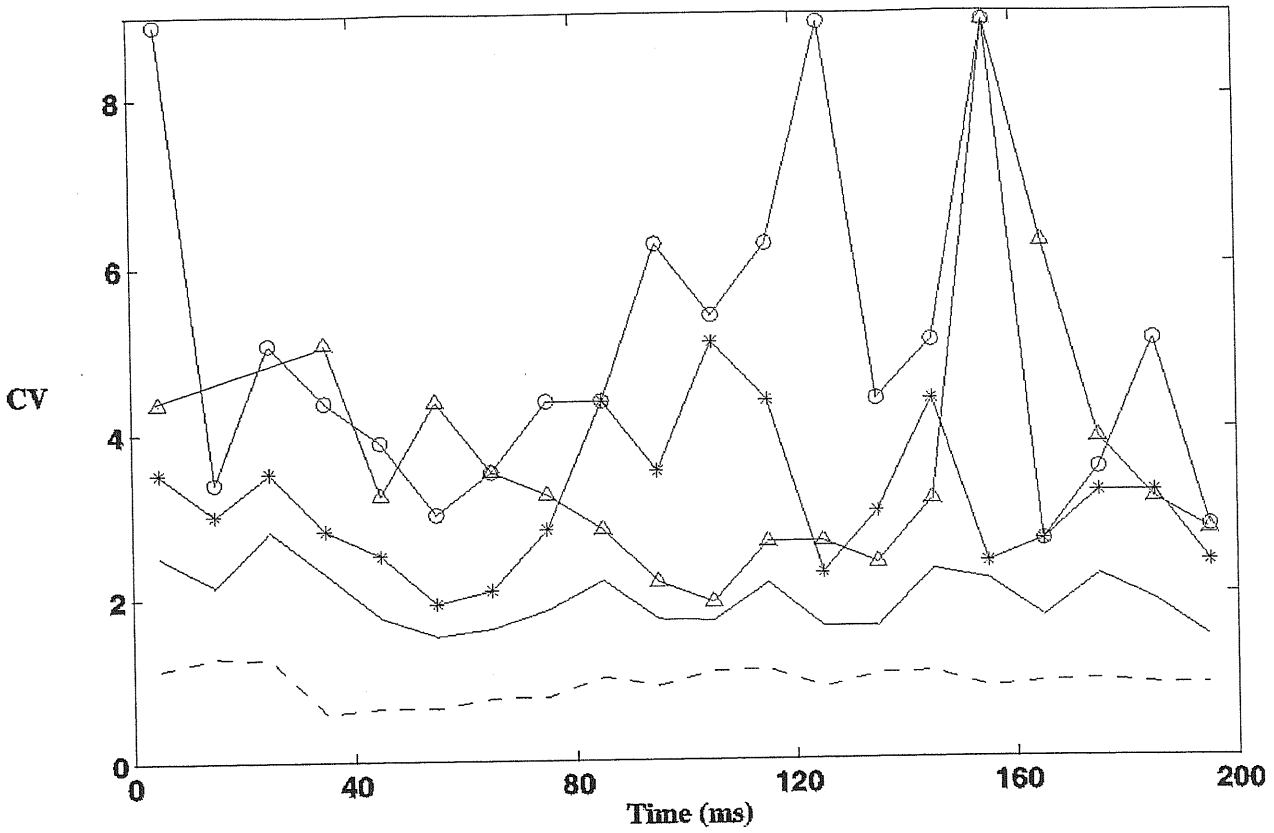

Fig. A.3. Coefficient of variation as a function time of the individual identified motoneurons DE(L), DE(R) and VI(L) (lines with symbols) compared to the coefficient of variation of pooled activity of DE(L), DE(R) and VI(L) motoneurons (solid line without symbols) and the pooled electrical activity from all neurons recorded from the roots (dashed line). The P_d(R) cell was stimulated with one action potential. Data obtained from 80 different trials of the same stimulation. (*From: Pinato et al., 1999*).

Reliability and reproducibility of important behavioral reactions of the leech, such as whole-body shortening (see Chapter 4), local bending (Lewis and Kristan, 1998a & 1998b), swimming (Brodfuehrer et al., 1995a) and crawling (Baader and Kristan, 1995), may originate from the neural mechanism here described, i.e. statistical independence among coactivated neurons. It is useful to observe that statistical independence and poor correlation among coactivated neurons will not be observed in a neuronal network with reliable synapses. In this case action potentials cross synapses, the electrical activity is reproducible and the firing of coactivated neurons is correlated. For instance if neuron N_i makes a strong electrical synapse with neuron N_j, each time neuron N_i fires, an action potential is also observed in neuron N_j and $P_i = P_j = P_{ij}$, as observed with the two L

motoneurons in each leech ganglion, which are strongly coupled (see **Fig. 4.6**). When synapses are unreliable significant spatio-temporal fluctuations are observed and coactivated neurons exhibit statistical independence. In neuronal networks with unreliable synapses, reliability can be recovered by pooling the electrical activity among coactivated neurons. This mechanism, here described in the leech ganglion, may be a common feature of computation in neural networks.

References

Aggarwal J.K. & Nandhakumar N. (1988). On the computation of motion from sequences of images - A review. Proc IEEE **76**(8) 917-935.

Allen C. & Stevens C.S. (1994). An evaluation of causes for unreliability of synaptic transmission. Proc Natl Acad Sci USA **91**(22) 10380-10383.

Allum J.H., Dietz V. & Freund H.J. (1978). Neuronal mechanisms underlying physiological tremor. J Neurophysiol **41**(3) 557-571.

Baader A.P. & Kristan W.B. Jr (1992). Monitoring neuronal activity during discrete behaviours: a crawling, swimming and shortening device for tethered leeches. J Neurosci Methods **43**, 215-223.

Baader A.P. & Kristan W.B. Jr (1995). Parallel pathways coordinate crawling in the medicinal leech Hirudo Medicinalis. J Com Physiol [A] **176**, 715-726.

Baader A.P. (1997). Interneuronal and motor patterns during crawling behavior of semi-intact leeches. J Exp Biol **200**(9), 1369-1381.

Baader A.P. & Bächtold D. (1997). Temporal correlation between neuronal tail ganglion activity and locomotion in the leech, Hirudo Medicinalis. Invert Neurosci **2**, 245-251.

Bernardo L.S. (1997). Recruitment of GABAergic inhibition and synchronization of inhibitory interneurons in rat neocortex. J Neurophysiol **77**, 3134-3144

Blackshaw S.E. (1981a). Sensory cells and motorneurons. from: Muller K.J., Nicholls J.G. & Stent G.S. *Neurobiology of the leech.* Cold Spring Harbour Laboratory, 51-78.

Blackshaw S.E. (1981b). Morphology and distribution of touch cell terminals in the skin of the leech. J Physiol **320**, 219-228.

Blackshaw S.E., Nicholls J.G. & Parnas I. (1982). Physiological responses, receptive fields and terminal arborizations of nociceptive cells in the leech. J Physiol (Lond) **326**:251-60.

Blackshaw S.E. (1993). Stretch receptors and body wall muscles in leeches. Comp Biochem Physiol **105A**(4), 643-652.

Blackshaw S.E. & Nicholls J.G (1995). Neurobiology and development of the leech. J Neurobiol **27**(3), 267-276.

Boulis N.M. & Sahley C.L. (1988). A behavioural analysis of habituation and sensitization of shortening in the semi-intact leech. J Neurosci **8**, 4621-4627.

Bouskila Y. & Dudek F.E. (1993). Neuronal synchronization without calcium-dependent synaptic transmission in the hypothalamus. Proc Natl Acad Sci USA **90**, 3207-3210.

Breckenridge L.J., Wilson R.J., Connolly P., Curtis A.S., Dow J.A., Blackshaw S.E. & Wilkinson C.D. (1995). Advantages of using microfabricated extracellular electrodes for in vitro neuronal recording. J Neurosci Res **42**(2), 266-276.

Brodfuehrer P.D. & Friesen W.O. (1986). Initiation of swimming activity by trigger neurons in the leech ganglion, I. Output connections of Tr1 and Tr2. J Comp Physiol [A] **159**, 489-502

Brodfuehrer P.D., Debski A., O'Gara B. & Friesen W.O. (1995a) Neuronal control of leech swimming. J Neurobiol **27**(3), 403-418.

Brodfuehrer P.D., Parker H.J., Burns A. & Melissa B. (1995b). Regulation of the segmental swim-generationg system by a pair of identified interneurons in the leech head ganglion. J Neurophysiol **73**(3), 983-992.

Brivanlou, I.H., Warland D.K. & Meister M. (1998). Mechanisms of concerted firing among retinal ganglion cells. Neuron **2 0**, 527-539.

Caccaciatore T.W., Brodfuehrer P.D., Gonzalez J.E., Jiang T., Adams S.R., Tsien R.Y., Kristan W.B. Jr & Kleinfeld D. (1999). Identification of neural circuits by imaging coherent electrical activity with FRET-based dyes. Neuron **23**, 449-459.

Cacciatore T.W., Rosenshteyn R. & Kristan W.B. Jr (2000). Kinematics and modelling of leech crawling: evidence for an oscillatory behaviour produced by propagating waves of excitation. J Neurosci **20**(4), 1643-1655.

Calabrese R.L. (1977). The neural control of alternate heartbeat coordination states in the leech, Hirudo medicinalis. J Comp Physiol **122**, 111-143.

Calabrese R.L., Nadim F. & Olsen O.H. (1995). Heartbeat control in the medicinal leech: a model system for understanding the origin, coordination and modulation of rhythmic motor patterns. J Neurobiol, **27**(3), 390-402.

Camhi J.M. (1988). Escape behavior in the cockroach: distributed neural processing. Experientia **44**(5), 401-408.

Canepari M, Campani M., Spadavecchia L. & Torre V. (1996). CCD imaging of the electrical activity in the leech nervous system. Eur Biophys J **24**, 359-370.

Carretta M. (1988). The Retzius cells in the leech: a review of their properties and synaptic connections. Comp Biochem Physiol **91A**(3), 405-413.

Carlton V. & McVean A. (1995). The role of touch, pressure and nociceprive mechanoreceptors of the leech in unrestrained behaviour. J Comp Physiol [A] **177**, 781-791.

Clemens S., Combes D., Meyrand P. & Simmers J. (1998a). Long-term expression of two interacting motor pattern-generating networks in the stomatogastric system of freely behaving lobster. J Neurophysiol **79**, 1396-1408.

Clemens S., Massabuau J.C., Legeay A., Meyrand P. & Simmers J. (1998b). In vivo modulation of interacting central pattern genrators in lobster stomatogastric ganglion: influenche of feeding and partial pressure of oxygene. J Neurosci **18**(7), 2788-2799.

Cottrell G.A. & Bewick G.S. (1989) Novel peripheral neurotransmitters in invertebrates. Pharmacol Ther **41**(3), 411-442.

Csicsvari J., Hirase H., Czurko A. & Buzsaki G. (1998). Reliability and state dependence of pyramidal cell-interneuron synapses in the hippocampus: and ensemble approach in the behaving rat. Neuron, **21**, 179-189.

Deitmer J.W. & Kristan W.B. Jr (1999). Glial responses during evoked behaviors in the leech. **26**(2) 186-189.

Dietz V., Bischofberger E., Wita C. & Freund H.J. (1976). Correlation between the dischanges of two simultaneously recorded motor units and physiological tremor. Electroencephalogr Clin Neurophysiol **40**(1) 97-105.

Friesen W.O. (1981). Physiology of water motion detection in the medicinal leech. J Exp Biol **92**, 255-275.

Frost W.N. & Kandel E.R. (1995). Structure of the network mediating siphon-elicited siphon mediated withdrawal in Aplysia. J Neurophysiol **73**(6), 2413-2427.

Gardner C.R. & Walker R.J. (1982). The roles of putative neurotransmitters and neuromodulators in annelids and related invertebrates. Prog Neurobiol **18**(2-3), 81-120.

Gascoigne L. & McVean A. (1991). Neuromodulatory effects of acetylcholine and serotonin on the sensitivity of leech mechanoreceptors. Comp Biochem Physiol **99**C(3), 369-374.

Gothard K.M., Skaggs W.E., Moore K.M. & McNaughton B.L. (1996). Binding of hippocampal CA1 neural activity to multiple reference frames in a landmark-based navigation task. J Neurosci **16**(2), 823-835.

Giachetti A. & Torre V. (1996). The Use of Optical Flow for the Analysis of Non-Rigid Motions. Int J Comp Vision **18**(3) 255-279.

Goda Y., Südhof T.C. (1997). Calcium regulation of neurotransmitter release: reliably unreliable? Curr Opin Cell Biol **9**(4), 513-518.

Golden M.A., Quinn J.J. & Partington M.T. (1995). Leech therapy in digital replantation. AORN J 62(3), 364-366, 369, 371-372.

Grattarola M. & Torre V. (1977). Necessary and sufficient conditions for synchronization of non-linear oscillators with a given class of coupling. IEEE Trans On CAS **24**, 209-215.

Granzow B., Friesen W.O. & Kristan W.B. Jr (1985). Physiological and morphological analysis of synaptic transmission between leech motor neurons. J Neurosci **8**(5), 2035-2050.

Gu X. (1991). Effect of conduction block at axon bifurcations on synaptic transmission to different postsynaptic neurons in the leech. J Physiol **441**, 755-778.

Hardingham N.R. & Larkman A.U. (1998). The reliability of excitatory synaptic transmission in slices of rat visual cortex in vitro is temperature dependent. J Physiol **507**(1), 249-256.

Hashemzadeh-Gargari H. & Friesen W.O. (1989). Modulation of swimming activity in the medicinal leech by serotonin and octopamine. Comp Biochem Physiol, **94C**(1), 295-302.

Haycraft J.B. (1884). On the a ction of a secretion obtained from the medicinal leech on the coagulation of blood. Proc Roy Soc **36**, 478-487.

Helmholtz H. Uber Integrale der hydrodynamischen Gleichungen welche den Wirbelwegungen entsprechen. Crelles J, **55**:25.

Hickie C., Cohen L.B. & Balaban P.M. (1997).The synapse between LE sensory neurons and gill motoneurons makes only a small contribution to the Aplysia gill-withdrawal reflex. Eur J Neurosci **9**(4), 627-636.

Iscla I., Arini P.D., Szczupak L. (1999). Differential channeling of sensory stimuli onto a motor neuron in the leech. J Comp Physiol [A] **184**(2) 233-241.

Jansen J.K.S. & Nicholls J.G. (1972). Regeneration and changes in synaptic connections between individual nerve cells in the central nervous system of the leech. Proc Nat Acad Sci USA **69**(3), 663-639.

Jellies J., Johansen K.M. & Johansen J. (1995). Peripheral neurons depend on CNS-derived guidance cues for proper navigation during leech development. Dev Biol **171**, 471-482.

Kristan W.B. (1982). Sensory And Motor Neurones Responsible For The Local Bending Response in Leeches, J Exp Biol **96**, 161-180.

Kristan W.B. Jr & Nusbaum M.P. (1982). The dual role of serotonin in leech swimming. J Physiol (Paris) **78**(8) 743-747

Kruse W. & Eckhorn R. (1996). Inhibition of sustained gamma oscillations (35-80 Hz) by fast transient responses in cat visual cortex. Proc Nat Acad Sci USA **93**, 6112-6117.

Kuffler S.W. & Potter D.D. (1964). Glia in the leech nervous system: physiological properties and neuron-glia relationships. J Neurophysiol **27**, 290-320.

Kuffler S.W. & Nicholls J.G. (1966). The physiology of neuroglial cells. Ergeb Physiol Biol Chem Exp Pharmakol **57**, 1-90.

Larkman A.U., Jack J.J.B. & Stratford K.J. (1997). Assessment of the reliability of amplitude histograms from excitatory synapses in rat hippocampal CA1 in vitro. J Physiol **505**(2), 443-456.

Laurent G., Wehr M. & Davidowitz H. (1996). Temporal representations of odours in an olfactory network. J Neurosci **16**(12), 3837-3847.

Lewis J.E. & Kristan W.B. Jr (1998a). Representation of touch location by a population of leech sensory neuro. J Neurophysiol **80**(5) 2584-2592.

Lewis J.E. & Kristan W.B. Jr (1998b). A neuronal network for computing population vectors in the leech. Nature **391**, 76-79.

Lewis J.E. & Kristan W.B. Jr (1998c). Quantitative analysis of a directed behaviour in the medicinal leech. J Neurosci **18**(4), 1571-1582.

Lisman J.E. (1997). Bursts as a unit of neural information: making unreliable synapses reliable. Trends Neurosci **20**(1) 38-43.

Lockery S.R., Wittemberg G., Kristan W.B. Jr, Cottrell Jr & Cottrell G.W. (1989). Function of identified interneurons in the leech elucidated using neural networks trained by back propagation. Nature, **340**, 468-471.

Lopez-Aguado L., Ibarz J.M. & Herreras O. (2000). Modulation of dendritic axon currents decreases the reliability of population spikes. J Neurophysiol **83**(2), 1108-1114.

Macagno, E.R. (1981). Number and distribution of neurons in leech segmental ganglia Journal of Comparative Neurology **190**, 283-302.

MacLeod K. & Laurent G. (1996). Distinct mechanisms for synchronization and temporal patterning of odour encoding neural assemblies. Science **274**, 976-979.

Magni F. & Pellegrino M. (1978). Neural mechanisms underlying the segmental and generalized chord shortening reflexes in the leech. J Comp Physiol **124**, 339-351.

Maltenfort M.G., Heckman C.J. & Rymer W.Z. (1998). Decorrelating actions of Renshaw interneurons on the firing of spinal motoneurons within a motor nucleus: a simulation study. J Neurophysiol, **80**(1), 309-23.

Mann-Metzer P. & Yarom Y. (1999) Electrotonic coupling interacts with intrinsic properties to generate synchronized activity in cerebellar networks of inhibitory interneurons. J Neurosci 1999 **19**(9), 3298-3306.

Mar A. & Drapeau P. (1996). Modulation of conduction block in leech mechanosensory neurons. J Neurosci **16**(14), 4335-4343.

Markram H.L., Frotscher M., Roth A. & Sakmann B. (1997). Physiology and anatomy of synaptic connections between thick tufted pyramidal neurones in the developing rat neocortex. J Phisiol **500**, 409-440.

Martindale M.Q. & Shankland M. (1990). Intrinsic segmental identity of segmental founder of the leech embryo. Nature 347, 672-674.

Mason A. & Kristan W.B. Jr (1982). Neuronal excitation, inhibition and modulation of leech longitudinal muscle. J Comp Physiol **146**, 527-536.

Meinen Z.F. & Sejnowski T.J. (1995). Reliability of spike timing in neocortical neurons. Science **268**, 1503-1506.

Melinek R. & Muller K.J. (1996). Acton potential initiation site depends on neuronal excitation. J Neurosci **16**(8), 2585-2591.

Michelson H.B. & Wong R.K.S. (1994). Synchronization of inhibitory neurons in the guinea pig hippocampus in vitro. J Physiol **477**, 35-45.

Modney B.K., Sahley C.L. & Muller K.J. (1997). Regeneration of a central synapse restores nonassociative learning. J Neurosci **17**(16), 6478-6842.

Morton D.W. & Chiel H.J. (1994). Neural architectures for adapting behaviours. TINS **17**(10), 413-420.

Muller K.J. (1981a). Synapses and synaptic transmission. from: Muller K.J., Nicholls J.G. & Stent G.S. *Neurobiology of the leech.* Cold Spring Harbour Laboratory, 79-111.

Muller K.J., Nicholls J.G. & Stent, G.S. (1981b). The nervous system of the leech: a laboratory manual. from: Muller K.J., Nicholls J.G. & Stent G.S. *Neurobiology of the leech.* Cold Spring Harbour Laboratory, 249-276.

Muller K.J., Nicholls J.G. & Stent G.S. (1981c). An atlas of neurons in the leech Hirudo medicinalis. from: Muller K.J., Nicholls J.G. & Stent G.S. *Neurobiology of the leech.* Cold Spring Harbour Laboratory, 277-288.

Nicholls, J.G. & Baylor, D.A. (1968). Specific modalities and receptive fields of sensory neurones in CNS of the leech. J Neurophysiol **31**, 740-756.

Nicholls, J.G.& Purves D. (1970). Monosynaptic chemical and electrical connections between sensory and motor cells in the central nervous system of the leech. J Physiol **209**, 647-667.

Nicholls J.G., Martin A.R., Wallace B.G. (1992).From Neuron to Brain. Sinauer Associates Inc., USA.

Norris B.J. & Calabrese R.L. (1987). Identification of motoneurons that contain FMRFamidelike peptide and the effect of FMRFamide on longitudinal muscle in the medicinal leech, Hirudo Medicinalis. J Comp Neurol **266**, 95-111.

O'Gara B.A. & Friesen W.O. (1995). Termination of leech swimming activity by a previously identified swim trigger neuron. J Comp Physiol [A] **177**, 627-636.

O'Gara B.A., Illuzzi F.A., Chung M., Portnoy A.D., Fraga K. & Frieman V.B. (1999). Serotonin induces four pharmacologically separable contractile responses in the pharinx of the leech Hirudo Medicinalis. Gen Pharmacol **32**(6) 669-681.

O'Keefe J. & Burgess N. (1996). Geometric determinants of the place fields of hippocampal neurons. Nature **381**, 425-428.

Ort, C.A., Kristan, W.B. Jr & Stent G.S.(1974). Neuronal control of swimming in the medicinal leech II. Identification and connections of motor neurons. J Comp Physiol **94**, 121-154.

Otmakhov N., Shirke A.M. & Malinow R. (1993). Measuring the impact of probabilistic transmisson on neuronal output. Neuron **10**, 1101-1111.

Pastor J., SoriaB. & Belmonte C. (1996). Properties of nociceptive neurons of the leech segmental ganglion. J Neurophysiol, **75**(6), 2268-2279.

Payton B. (1981a). History of medicinal leeching and early medical references. from: Muller K.J., Nicholls J.G. & Stent G.S. *Neurobiology of the leech.* Cold Spring Harbour Laboratory, 27-34.

Papoulis A. (1984). Probability, random variables and stochastic processes. McGraw-Hill, New York

Payton B. (1981b). Structure of the nervous system of the leech. from: Muller K.J., Nicholls J.G. & Stent G.S. *Neurobiology of the leech.* Cold Spring Harbour Laboratory, 35-50.

Pearce R.A. & Friesen W.O. (1985a). Intersegmental coordination of the leech swimming rythm: I. Roles of cycle period gradient and coupling strength. J Neurophysiol **54**(6), 1444-1459.

Pearce R.A. & Friesen W.O. (1985b). Intersegmental coordination of the leech swimming rythm: II. Comparison of long and short chains of ganglia. J Neurophysiol **54**(6), 1460-1472.

Peterson E.L. (1985a). Visual interneurons in the leech brain.I. Lateral visual cells in the subesophageal ganglion. J Comp Physiol [A] **156**, 697-706.

Peterson E.L. (1985b). Visual interneurons in the leech brain.II. The anterior visual cells of the supraesophageal ganglion. J Comp Physiol [A] **156**, 707-717.

Pinato G., Parodi P., Bisso A., Macri D., Kawana A., Jimbo Y. & Torre V. (1999). Properties of the evoked spatio-temporal electrical activity in neuronal assemblies. Rev Neurosci **10**, 279-290.

Pinato G., Battiston S. & Torre V. (2000). Statistical independence and neural computation in the leech ganglia. Biol Cybern (in press).

Pinato G. & Torre V. (2000). Coding and adaptation during mechanical stimulation in the leech nervous system. J Physiol (submitted).

Quirk G.J., Muller R.U. & Kubie J.L. (1990). The firing of hippocampal place cells in the dark depends on the rat's recent experience. J Neurosci **10**(6), 2008-2017.

Quirk M.C., Wilson M.A. (1999). Interaction between spike waveform classification and temporal sequence detection. J Neurosci Methods **94**(1), 41-52.

Reich D.S., Jonathan D.V., Knight B.W., Ozaki T. & Kaplan E. (1977). Response variability and timing precision of neuronal spike trains in vivo. J Neurophysiol **77**, 2836-2841.

Retzius G. (1891). Zur kenntniss des centralen Nervensystems der Wurmer. *Biologische Untersuchungen*, Neue Folge II, 1-28. Samson and Wallin, Stockolm.

Reynolds S., French K., Baader A. & Kristan W. (1998). Development Of Spontaneous And Evoked Behaviors In The Medicinal Leech, Journal Comp. Neurology. **402**(2) 168-180.

Rozsa K.S. (1995). Two types of reorganization in multifunctional neural networks of Helix Pomatia L. Acata Biol Hung 46(2-4), 247-262.

Sahley C.L., Modney B.K., Boulis M.B. & Muller K.J. (1994a). The S cell: an interneuron essential for sensitization and full dishabituation of leech shortening. J Neurosci **14**(11), 6715-6721.

Sahley C.L., Boulis M.B. & Schurman B. (1994b). Associative learning modifies the shortening reflex in the semi-intact leech Hirudo medicinalis: effects of pairing, predictability and CS preexposure. Behav Neurosci **108**(2), 340-346.

Sawada M., Wilkinson J.M., MacAdoo D.J., Coggeshall R.E. (1976). The identification of two inhibitory cells in each segmental ganglion of the leech and studies on the ionic mechanism of the inhibitory junctional potentials produced by these cells. J Neurobiol **7**(5), 435-45.

Sawyer R.T. (1981). Leech biology and behaviour. from: Muller K.J., Nicholls J.G. & Stent G.S. *Neurobiology of the leech.* Cold Spring Harbour Laboratory, 7-26.

Schalow G. & Zach G.A. (1996). External loops of human premotor spinal oscillators identified by simultaneous measurements of interspike intervals and phase relations. Gen Physiol Biophys **15** Suppl 1, 95-119.

Schmidt J. & Deitmer J.W. (1996). Photoinactivation of the giant neuropil glial cells in the leech Hirudo Medicinalis: effects on neuronal activity and synaptic transmission. J Neurophysiol **76**(5), 2861-2871.

Shain D.H., Ramirez-Weber Joyce-Hsu F.A. & Weisblat D.A. (1998). Gangliogenesis in leech: morphogenetic processes leading to segmentation in the central nervous system. Dev Genes Evol **208**, 28-36.

Shaw B. K. & Kristan W.B. Jr (1995). The whole-body shortening reflex of the medicinal leech: motor pattern, sensory basis, and interneuronal pathways. J Comp Physiol [A] **177**(6) 667-681.

Shaw B. K. & W.B. Kristan Jr (1997). The neuronal basis of the behavioral choice between swimming and shortening in the leech: control is not selectively exercised at higher circuit levels. J Neurosci **17**(2) 786-95.

Shaw B. K. & Kristan W.B. Jr (1999). Relative roles of the S cell network and parallel interneuronal pathways in the whole-body shortening reflex of the Medicinal leech. J Neurophysiol **82**, 1114-1123.

Snider R.K. & Bonds A.B. (1998). Classification of non-stationary neural signals. J Neurosci Methods **84**(1-2), 155-166.

Stent G.S., Kristan W.B. Jr, Friesen W.O., Ort C.A., Poon M. & Calabrese R.L. (1978). Neuronal generation of the leech swimming movement. Science **200**, 1348-1357.

Stopfer M., Bhagavan S., Smith B.H. & Laurent G. (1997). Impaired odour discrimination on desynchronization of odour-encoding neural assemblies. Nature **390**, 70-74.

Stuart A.E. (1970). Physiological and morphological properties of motoneurones in the central nervous system of the leech. J Physiol (Lond) **209**(3) 627-646.

Szczupak L. & Kristan W.B. Jr (1995). Widespread mechanosensory activation of the serotonergic system of the medicinal leech. J Neurophysiol, **74**(6), 2614-2624.

Tai M.H., Rheuben M.B., Autio D.M. & Zipser B. (1996). Leech photoreceptor project their galactin-containing processes into the optic neuropil where they contact AP cells. J Comp Neurol **371**:235, 235-248.

Thorogood M.S.E. & Brodfuehrer P.D. (1995). The role of glutamate in swim initiation in the medicinal leech. Invert Neurosci **1**, 223-233.

Traub R.D. (1995). Model of synchronized population bursts in electrically coupled interneurons containing active dendritic conductances. J Comp Neurosci **2**, 283-289.

Tsau Y., Wu J.Y., Hopp H.P., Cohen L.B., Schiminovich D. & Falk C.X. (1994). Distributed aspects of the response to siphon touch in Aplysia: spread of stimulus information and cross-correlation analysis. J Neurosci **14**(7), 4167-4184.

Varona P., Ibarz J.M., LOpez-Aguado L. & Herreras O. (2000). Macroscopic and subcellular factors shaping population spikes. J Neurophysiol **83**(4), 2192-2208.

Wallace B.G. (1981). Neurotransmitter chemistry. from: Muller K.J., Nicholls J.G. & Stent G.S. *Neurobiology of the leech.* Cold Spring Harbour Laboratory, 147-172.

Wehr M. & Laurent G. (1996). Odour encoding by temporal sequences of firing in oscillating neural assemblies. Nature **384**, 162-166.

Wenning A., Bazin B.& Zerbst-boroffka I. (1982). Primary urine formation during diuresis in the leech Hirudo Medicinalis. J Comp Physiol B, **146**: 75-79.

Wilkinson J.M. & Coggeshall R.E. (1975). Axonal numbers and sizes in the connectives and peripheral nerves of the leech. J Comp Neur **162**, 387-396.

Willard A.L. (1981). Effects of serotonin on the generation of the motor program for swimming by the medicinal leech. J Neurosci **1**(9), 936-944.

Wilson M.A. & McNaughton B.L. (1993). Dynamics of the hippocampal ensemble code for space. Science **261,** 1055-1058.

Wilson R.J., Breckenridge L., Blackshaw S.E., Connolly P., Dow J.A., Curtis A.S. & Wilkinson C.D. (1994). Simultaneous multisite recordings and stimulation of single isolated leech neurons using planar extracellular electrode arrays. J Neurosci Methods **53**(1), 101-110.

Windhorst, U. (1990). Activation of Renshaw cells. Prog Neurobiol **35**, 135-179.

Windhorst, U. (1996). On the role of recurrent inhibitory feedback in motor control. Prog Neurobiol **49**, 517-587.

Wittenberg, G. & Kristan W.B. Jr (1992a). Analysis and modelling of the Multisegmental Coordination of Shortening Behaviour in the Medical Leech. I. Motor Output Pattern. J Neurophysiol **68**(5), 1683-1692.

Wittenberg, G. & Kristan W.B. Jr (1992b). Analysis and modelling of the Multisegmental Coordination of Shortening Behaviour in the Medical Leech. II. Role of identified interneurons. J Neurophysiol **68**(5), 1693-1707.

Wu J.Y., Cohen L.B. & Falk C.X. (1994). Neuronal activity during different behaviors in Aplysia: a distributed organization? Science **263**:5148, 820-823.

Yau, K.W. (1976a) Physiological properties and receptive fields of mechanosensory neurones in the head ganglion of the leech. Journal of Physiology **263**(3), 489-512.

Yau K.W. (1976b). Receptive fields, geometry and conduction block of sensory neurones in the central nervous system of the leech. Journal of Physiology **263**(3), 513-538.

Yu X., Nguyen B & Friesen W.O. (1999). Sensory feedback can coordinate the swimming activity of the leech. J Neurosci **19**(11), 4634-4643.

Zador A.J. (1998). Impact of Impact of synaptic unreliability on the information transmitted by spiking neurons. J Neurophysiol **79**(3), 1219-1229.

Zipser B. & McKay R. (1981). Monoclonal antibodies distinguish identifiable neurones in the leech. Nature **289**:5798, 549-554.